Report
P-16-27
May 2017

Forsmark site investigations

Difference flow logging in borehole KFM24

Eemeli Hurmerinta

SVENSK KÄRNBRÄNSLEHANTERING AB

SWEDISH NUCLEAR FUEL
AND WASTE MANAGEMENT CO

Box 3091, SE-169 03 Solna
Phone +46 8 459 84 00
skb.se

SVENSK KÄRNBRÄNSLEHANTERING

ISSN 1651-4416
SKB P-16-27
ID 1567669
May 2017

Forsmark site investigations

Difference flow logging in borehole KFM24

Eemeli Hurmerinta, Pöyry Finland Oy

Keywords: Forsmark, Hydrogeology, Hydraulic tests, Difference Flow measurements, KFM24, AP SFK-16-015, SFK.

This report concerns a study which was conducted for Svensk Kärnbränslehantering AB (SKB). The conclusions and viewpoints presented in the report are those of the author. SKB may draw modified conclusions, based on additional literature sources and/or expert opinions.

Data in SKB's database can be changed for different reasons. Minor changes in SKB's database will not necessarily result in a revised report. Data revisions may also be presented as supplements, available at www.skb.se.

A pdf version of this document can be downloaded from www.skb.se.

Abstract

This report presents the main principles of the methods as well as the results of measurements carried out in borehole KFM24 at Forsmark, Sweden, in August 2016.

The Posiva Flow Log, Difference Flow Method (PFL DIFF) uses a flowmeter that incorporates a flow guide and can be used for relatively quick determinations of hydraulic conductivity and hydraulic head of fractures/fracture zones in boreholes.

The first flow logging measurements were done with a 5 m test section by moving the measurement tool in 0.5 m steps. This method was used to flow log the entire measurable part of the borehole in undisturbed as well as in pumped conditions. The flow measurements in pumped conditions were repeated using a 1 m long test section, with 0.1 m steps.

A high-resolution absolute pressure sensor was used to measure the absolute total pressure along the borehole. These measurements were carried out together with the flow measurements.

The flow along the borehole was measured below the casing tube during undisturbed conditions to detect the leakage of the casing tube.

The electrical conductivity (EC) and temperature of borehole water were also measured. The EC measurements were used to study the occurrence of saline water in the borehole in undisturbed as well as pumped conditions. The EC of fracture-specific water was measured (1 m test section) for a selection of fractures.

The recovery of the groundwater level in the borehole was measured after the pumping of the borehole was stopped.

Length calibration was made based on geophysical data from AP SFK-16-019 Geophysical logging in KFM24. The length was corrected by synchronizing the single-point resistance (SPR) measurements to length corrected geophysics resistance measurement.

Sammanfattning

Denna rapport presenterar huvudprinciperna för metoden och resultat av mätningar utförda i borrhål KFM24 i Forsmark, Sverige, i augusti 2016.

Posiva Flow Log, Differensflödesloggning (PFL DIFF) är en snabb metod för bestämning av transmissiviteten och hydraulisk tryckhöjd i borrhålssektioner och sprickor/sprickzoner i kärnborrhål.

Flödet till eller från en 5 m lång testsektion (som successivt förflyttades med 0,5 m) mättes i borrhålet under såväl naturliga förhållanden som vid pumpning. Flödesmätningarna upprepades under pumpning med en 1 m lång testsektion som successivt förflyttades i steg om 0,1 m.

En högupplösande absoluttryckgivare användes för att mäta det absoluta totala trycket längs borrhålet. Dessa mätningar utfördes tillsammans med flödesmätningarna.

Mätning av flödet längs borrhålet gjordes nedanför foderröret under naturliga betingelser för att detektera läckage av foderröret.

Elektrisk konduktivitet (EC) och temperatur på borrhålsvattnet mättes också. EC-mätningarna användes för att studera förekomsten av saltvatten i borrhålet under såväl naturliga som pumpade förhållanden. EC mättes även i ett antal utvalda sprickor i borrhålet (1 m lång testsektion).

Återhämtningen av grundvattennivån mättes efter att pumpningen i borrhålet avslutats.

Längdkalibrering gjordes med hjälp av de geofysiska data från AP SFK-16-019 Geophysical logging in KFM24. Längden korrigerades till geofysiken resistans, med användning av punktresistans (SPR) mätningar.

Contents

1 Introduction

The core drilled borehole KFM24 at Forsmark, Sweden was measured using the Posiva Flow Log, Difference Flow Method (PFL DIFF) which provides a swift, multifaceted characterization of a borehole. The borehole was measured between August 1 – August 11, 2016.

KFM24 is 550.17 m long and its inclination at the ground level is c. −83° from the horizontal plane. The length interval c. 0 m – 35 m was percussion drilled, with an inner diameter of 248 mm. Interval 35–37 m was core drilled with a diameter of 86 mm. A stainless steel support casing has been inserted into this part. The rest of the borehole was drilled with a diameter of c. 76 mm.

The location of KFM24 at Forsmark is illustrated in Figure 1-1.

The field work and the subsequent data interpretation were conducted by Pöyry Finland Oy. PFL DIFF has previously been employed in Posiva's site characterisation programme in Finland as well as at the Äspö Hard Rock Laboratory at Simpevarp, Sweden. The commissions at the latter site included measurements in the 1 700 m long cored borehole KLX02 at Laxemar together with a methodology study (Ludvigson et al. 2002). PFL DIFF has also been employed in SKB's site characterisation programme at Laxemar and Forsmark.

This document reports the results acquired by PFL DIFF in borehole KFM24. The measurements were carried out as a part of preparatory investigations and in accordance to SKB's internal controlling document AP SFK-16-015. The controlling documents for performing according to this Activity Plan are listed in Table 1-1. The list of the controlling documents excludes the assignment-specific quality plans. Both the Activity Plan and the Method Descriptions are SKB's internal controlling documents. The measurement data and the results were delivered to the SKB site characterization database SICADA and are traceable by the Activity Plan number.

Table 1-1. SKB's internal controlling documents for the activities concerning this report.

Activity Plan	**Number**	**Version**
Difference flow logging in borehole KFM24	AP SFK-16-015	2.0
Method Descriptions	**Number**	**Version**
Method Description for Difference Flow Logging	SKB MD 322.010e	2.0
Instructions for cleaning borehole equipment and certain surface equipment	SKB MD 600.004e	1.0
Instruction for length calibration in investigation of core boreholes	SKB MD 620.010e	2.0

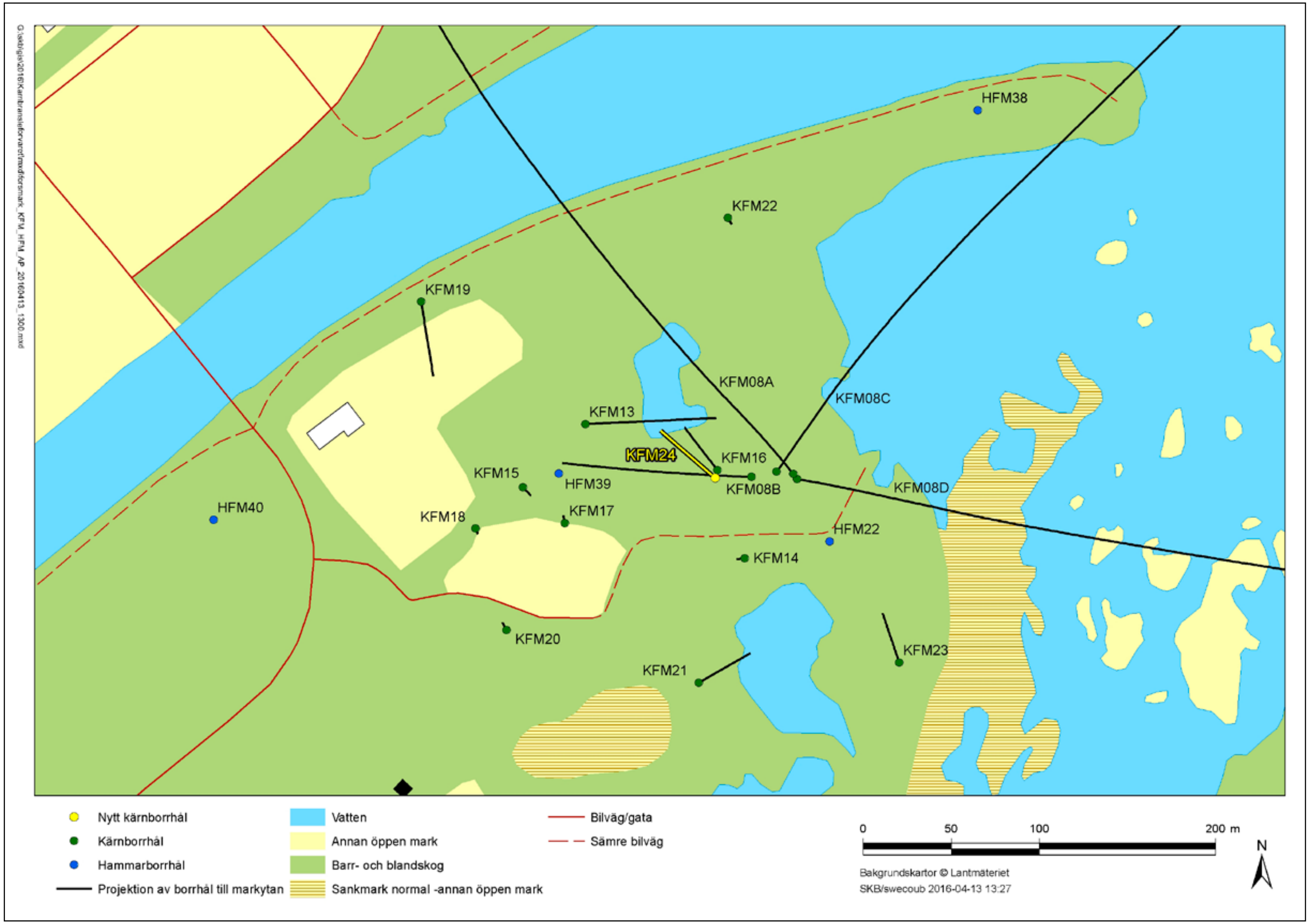

Figure 1-1. *Detailed map over the location of the borehole KFM24 and all the boreholes within the area.*

2 Objective and scope

The main objective of the PFL DIFF measurements in KFM24 was to identify water-conductive sections/fractures suitable for subsequent hydro-geochemical characterisation. Secondly, the measurements aimed at a hydro-geological characterisation, which includes the inspection of the prevailing water flow balance in the borehole and the hydraulic properties (transmissivity and undisturbed hydraulic head) of the tested sections. Based on the results of these investigations, a more detailed characterisation of flow anomalies along the borehole, e.g. an estimate of the conductive fracture frequency (CFF), may be obtained.

Besides difference flow logging, the measurement programme also included supporting measurements, performed in order to gain a better understanding of the overall hydro-geochemical conditions. These measurements included the electrical conductivity (EC) and the temperature of the borehole fluid as well as the single-point resistance of the borehole wall. The electrical conductivity of a number of selected high-transmissive fractures (the electrical conductivity of the water in the fractures) in the borehole was also measured. Furthermore, the recovery of the groundwater level after pumping the borehole was registered.

To measure the absolute pressure along the borehole, a high-resolution pressure sensor was used, and carried out simultaneous as the flow measurements. The results are used for the calculation of the hydraulic head along the borehole.

The flow along the borehole was measured below the casing tube in undisturbed conditions (without pumping) to detect possible leakages of the casing tube.

3 Principles of measurement and interpretation

3.1 Measurements

Unlike conventional borehole flowmeters, which measure the total cumulative flow rate along a borehole, the PFL DIFF probe measures the flow rate into or out of defined borehole sections. The advantage that follows from measuring the flow rate in isolated sections is improved detection of incremental changes of flow along the borehole. As these flows are generally very small, they can easily be missed when using conventional flowmeters.

Rubber sealing discs located at the top and bottom of the probe are used to isolate the flow of water in the test section from the flow in the rest of the borehole (Figure 3-1). Flow inside the test section is directed through the flow sensor. Flow along the borehole is directed around the test section by means of a bypass pipe and is discharged at either the upper or lower end of the probe. The entire structure is called flow guide.

Generally two separate measurements with two different section lengths (e.g. 5 m and 1 m) are used. The 5 m setup is usually used first to obtain a general picture of the flow anomalies. It is also good for measuring larger (less than 5 m in length) fracture zones. The 1 m section setup can separate anomalies which are close to each other. Different section lengths can also confirm that a flow anomaly is real and not caused for instance by leakage at the rubber discs.

Flow rates into or out of the test section are monitored using thermistors, which track both the dilution (cooling) of a thermal pulse and its transfer by the moving water (Öhberg and Rouhiainen 2000). The thermal dilution method is used in measuring flow rates because it is faster than the thermal pulse method, where the latter is used only to determine flow direction within a given time frame. Both methods are used simultaneously at each measurement location.

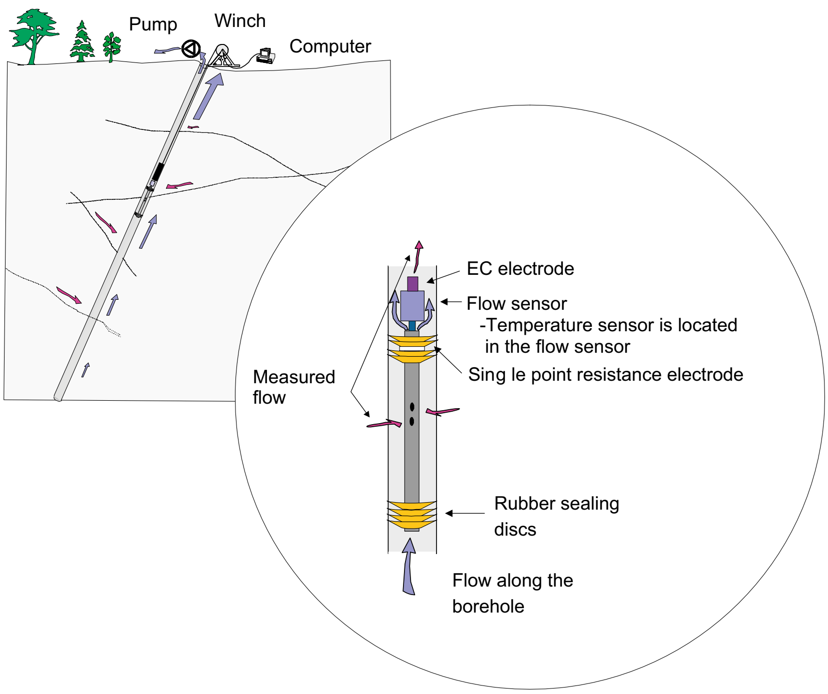

Figure 3-1. *Schematic of the probe used in the PFL DIFF.*

In addition to incremental changes in flow, the PFL DIFF probe can also be used to measure.

- The electrical conductivity (EC) of both borehole water and fracture-specific water. The electrode used in EC measurements is located at the top of the flow sensor (Figure 3-1).
- The single point resistance (SPR) of the borehole wall (grounding resistance). The SPR electrode is located between the uppermost rubber sealing discs (Figure 3-1), and is used for the high-resolution depth determination of fractures and geological structures.
- The ambient water pressure profile in the borehole. Located inside the watertight electronics assembly, the pressure sensor transducer is connected to the borehole water through a tube (Figure 3-2).
- The temperature of the water in the borehole. The temperature sensor is part of the flow sensor (Figure 3-1).

The principles behind PFL DIFF flow measurements are shown Figure 3-3. The flow sensor consists of three thermistors (Figure 3-3 a). The central thermistor, A, is used both as a heating element and to register temperature changes (Figure 3-3 b and c). The side thermistors, B1 and B2, serve as detectors of the moving thermal pulse caused by the heating of A.

Flow rate is measured by monitoring heat transients after constant power heating in thermistor A and begins by constant power (P1) heating. After the power is cut off the flow rate is measured by monitoring transient thermal dilution (Figure 3-3 c). If the measured flow rate exceeds a certain limit, another constant power heating (P2) period is started after which the flow rate is re-measured from the following heat transient.

Flows are measured when the probe is at rest. After transferring the probe to a new position, a waiting period (which can be adjusted according to the prevailing circumstances) is allowed to elapse before the heat pulse (Figure 3-3 b) is applied. The measurement period after the constant-power thermal pulse (normally 100 s each time the probe has moved a distance equal to the test section length and 10 s in every other location) can also be adjusted. The longer (100 s) measurement time is used to allow the direction of even the smallest measurable flows to be visible.

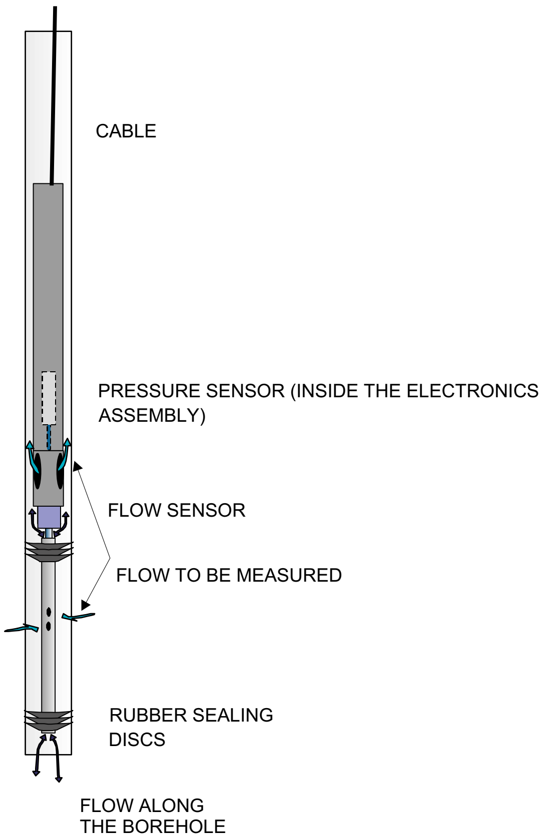

***Figure 3-2.** The absolute pressure sensor is located inside the electronics assembly and connected to the section through a tube.*

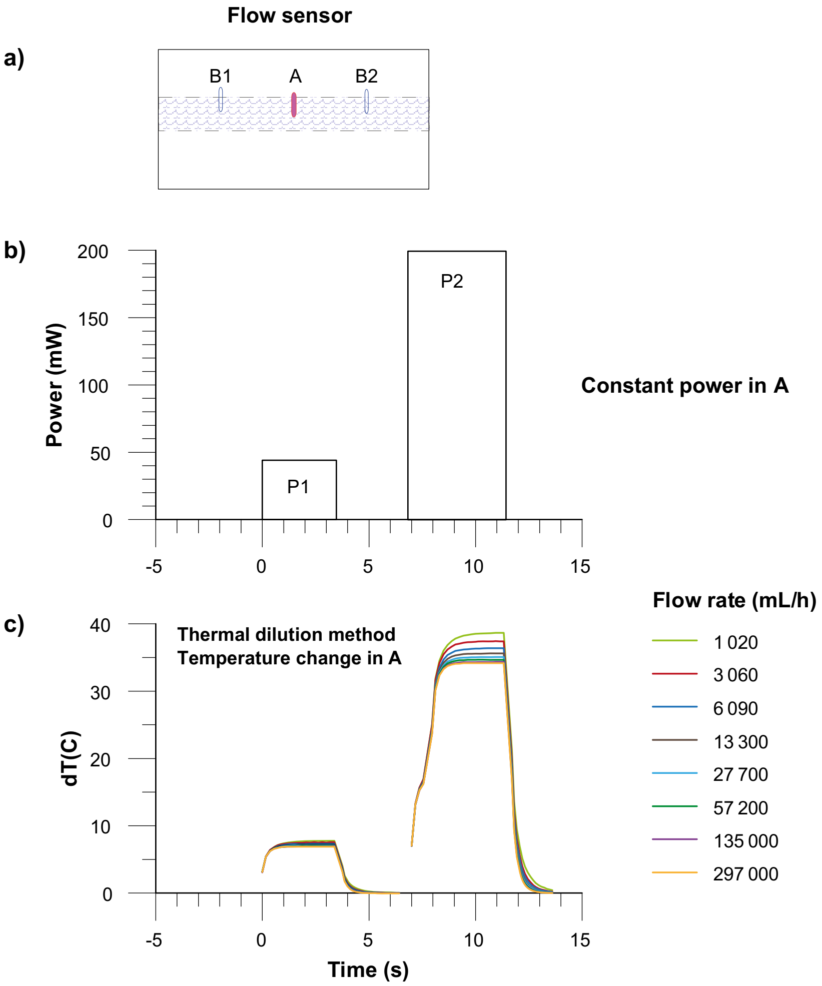

Figure 3-3. *Flow rate measurement.*

The flow rate limits are between 30 mL/h and 300 000 mL/h, where the lower limit for the thermal dilution method is the theoretical lowest measurable value. Depending on conditions in the borehole, these flow limits may not always prevail. Examples of possible disturbances are drilling debris entrained in the borehole water, bubbles of gas in the water and high flow rates (some 30 L/min, i.e. 1 800 000 mL/h or more) along the borehole. With significant disturbances, limits on practical measurements are calculated for each set of data.

3.2 Interpretation

The interpretation of data is based on Thiem's or Dupuit's formula, which describes a steady state and two-dimensional radial flow into the borehole (de Marsily 1986):

$$h_s - h = \frac{Q}{T \cdot a} \qquad 3\text{-}1$$

where

h is the hydraulic head in the vicinity of the borehole and h = hS at the radius of influence (R),

Q is the flow rate into the borehole,

T is the transmissivity of the test section.

The constant a depends on the assumed flow geometry. For cylindrical flow, the constant a is:

$$a = \frac{2\pi}{\ln(R/r_0)} \qquad 3\text{-}2$$

where

r_0 is the radius of the borehole and

R is the radius of influence, i.e. the zone inside which the effect of pumping is noticeable.

If measurements of flow rate are carried out using two levels of hydraulic head in the borehole, i.e. undisturbed and pump-induced heads, then the computational value of head when section flow is zero (h_s) and the transmissivity of the borehole sections tested can be calculated. Equation 3-1 can be reformulated in the following two ways:

$$Q_{s0} = T_s \cdot a \cdot (h_s - h_0) \qquad 3\text{-}3$$

$$Q_{s1} = T_s \cdot a\ (h_s - h_1) \qquad 3\text{-}4$$

where

h_0 and h_1 are the hydraulic heads in the borehole at the test levels,

Q_{s0} and Q_{s1} are the measured flow rates in the test section,

T_s is the transmissivity of the test section and

h_s is the undisturbed hydraulic head of the section, i.e. head when the section flow is zero.

In general, since very little is known about the flow geometry, cylindrical flow without skin effect is assumed. The measurements are conducted in steady state conditions therefore no skin effect is assumed and the calculated transmissivity is determined based on the smallest conductivity in the fracture network where the water flow is coming from or going to. Basically in case of positive skin the calculated transmissivity represents only the transmissivity close to the borehole and transmissivity of the fracture or fracture network further away from the borehole wall cannot be estimated. Cylindrical flow geometry is also justified because the borehole is at a constant head, and no strong pressure gradients along the borehole exist except at its ends.

The radial distance R to the undisturbed hydraulic head h_s is not known and must be assumed. Here a value of 500 is selected for the quotient R/r_0.

The hydraulic head and the test section transmissivity can be deduced from Equation 3-5 and 3-6:

$$h_s = \frac{h_0 - bh_1}{1-b} \qquad 3\text{-}5$$

$$T_s = \frac{1}{a}\frac{Q_{s0} - Q_{s1}}{h_1 - h_0} \qquad 3\text{-}6$$

where $b = Q_{s0}/Q_{s1}$

The transmissivity (T_f) and hydraulic head (h_f) of individual fractures can be calculated provided that the flow rates at the individual fractures are known. Similar assumptions to those employed above must be used (a steady-state cylindrical flow regime without skin zones).

$$h_f = \frac{h_0 - bh_1}{1-b} \qquad 3\text{-}7$$

$$T_f = \frac{1}{a}\frac{Q_{f0} - Q_{f1}}{h_1 - h_0}, \qquad 3\text{-}8$$

where Q_{f0} and Q_{f1} are the flow rates at a fracture and h_f and T_f are the hydraulic head (head when fracture flow is zero) and transmissivity of a fracture, respectively.

Since the actual flow geometry and any skin effects are unknown, transmissivity values should only be considered as an indication of the prevailing orders of magnitude. As the calculated hydraulic heads do not depend on geometrical properties but only on the ratio of the flows measured at different heads in the borehole, they should be less sensitive to unknown fracture geometry. A discussion of potential uncertainties in the calculation of transmissivity and hydraulic head can be found in (Ludvigson et al. 2002).

Transmissivity of the entire borehole can be evaluated in several ways using data of the pumping phase. The assumption above (cylindrical and steady state flow) leads to Dupuit's formula (de Marsily 1986):

$$T = \frac{Q}{s2\pi} \ln\left(\frac{R}{r_0}\right) \qquad 3\text{-}9$$

where

s is drawdown and

Q is the pumping rate at the end if the pumping phase.

In Moye formula (Moye 1967) it is assumed the steady state flow is cylindrical near the borehole (to distance r = L/2, where L is the section under test) and spherical further away:

$$T = \frac{Q}{s2\pi}\left[1 + ln\left(\frac{L}{2r_0}\right)\right] \qquad 3\text{-}10$$

where L is length of the test section (m), in this case water filled uncased part of the borehole.

4 Equipment specification

With the PFL DIFF method, the flow of groundwater into or out of a borehole section is monitored using a flow guide which employs rubber sealing discs to isolate any such flow from the flow of water along the borehole. This flow guide defines the test section being measured without altering the hydraulic head. Groundwater flowing into or out of the test section is guided to the flow sensor, and flow is measured using the thermal pulse and thermal dilution methods. Measured values are transferred to a computer in digital form.

Type of instrument:	PFL DIFF probe.
Borehole diameters:	56 mm, 66 mm and 76 mm (or larger).
Length of test section:	The flow guide length can be varied.
Method of flow measurement:	Thermal pulse and thermal dilution.
Range and accuracy of measurement:	See Table 4-1.
Additional measurements:	Temperature, Single point resistance, Electrical conductivity of water, Water pressure.
Winch:	Mount Sopris Wna 10, 0.55 kW, conductors, Gearhart-Owen cable head.
Depth determination	Based on a digital distance counter.
Logging computer:	PC (Windows 7).
Software	Based on MS Visual Basic.
Total power consumption:	1.5–2.5 kW depending on the type of pump employed.
Calibration of flow probe:	February 2016 (Probe FL2 and FL12).

The range and accuracy of the sensors used is shown in Table 4-1.

Table 4-1. Range and accuracy of sensors.

Sensor	Range	Accuracy
Flow	30–300 000 mL/h	± 10% curr. value
Temperature (central thermistor)	0–50 °C	0.1 °C
Temperature difference (between outer thermistors)	−2–+2 °C	0.0001 °C
Electrical conductivity of water (EC)	0.02–11 S/m	± 5% curr. value
Single point resistance (SPR)	5–500 000 Ω	± 10% curr. value
Groundwater level sensor	0–0.1 MPa	± 1% full-scale
Air pressure sensor	800–1 060 hPa	± 5 hPa
Absolute pressure sensor	0–20 MPa	± 0.01% full-scale

4.1 Electrical conductivity of water–electrode

The electrode for measuring electrical conductivity of water is located right above the flow sensor and the water going to or coming from flow sensor goes through the electrode. The electrode (Figure 4-1) was modified in 2015 by adding heat shrink tubing around the body of the electrode and by replacing the previous electrode cup with a new thinner one. The collar of the new cup also extends deeper into the flow channel and the connection between the two is sealed by an O-ring. A capillary pipe was added to the upper end of the heat shrink tubing to allow trapped air to escape when the device is lowered into a borehole. The purpose of these modifications is to guide the fracture water to flow along a pre-determined route and to prevent it from mixing with the surrounding bore-hole water in the electrode and thus to prevent possible distortion of the measured fracture specific EC value. Unmodified EC-electrode is presented in Figures Figure 4-1 and Figure 4-2 electrode with modified setup in Figure 4-3.

Figure 4-1. *EC-electrode with cup detached.*

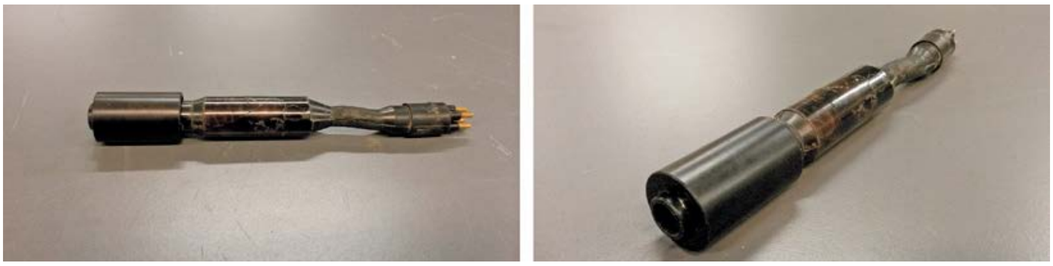

Figure 4-2. *Unmodified EC-electrode.*

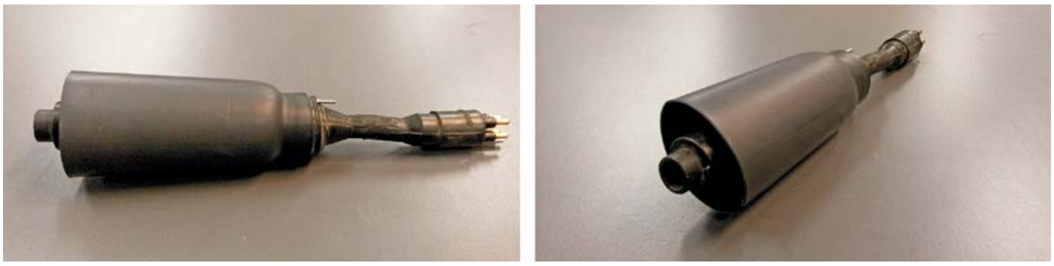

Figure 4-3. *Modified EC-electrode.*

5 Execution of measurements

5.1 General

The work commission was performed according to Activity Plan AP SFK-16-015 following the SKB Method Description 322.010e, Version 2.0 (Method description for Difference Flow Logging; Table 1-1). Prior to the measurements, the downhole tools and the measurement cable were disinfected. Time was synchronized to local Swedish time. The activity schedule of the borehole measurements is presented in Table 5-1. The items and activities in Table 5-1 are the same as in the Activity Plan.

The dummy logging (Item 6) of the borehole was done in order to assure that the measurement tools do not get stuck in the borehole. The dummy also collects solid material from the borehole wall. The solid material in the dummy is used for evaluation whether it is safe to continue with other logging tools.

The electrical conductivity (EC) and temperature of borehole water (Item 7) during undisturbed conditions were measured before flow logging.

The flow along the borehole (Item 8) was measured below the casing tube to observe leakages from the casing. Measurement was conducted during undisturbed conditions.

The flow logging during undisturbed conditions (Item 9) was carried out in the borehole with a 5 m section length and in 0.5 m length increments (step length).

The pumping was started on August 4, 2016. After 12 hours flow logging with pumping (Item 10) was conducted using the same section and step lengths as Item 9.

The flow logging was continued by measuring the borehole with a 1 m section length and a 0.1 m step length (Item 11). The fracture specific EC of the water from some selected fractures (Item 11) was performed in conjunction with flow logging with a 1 m section length.

The EC of borehole water (Item 12) was logged while the measured borehole was still pumped. After the pumping, the recovery of the groundwater level was monitored (Item 13).

Table 5-1. Flow logging and testing in KFM24. Activity schedule.

Item	Activity	Explanation	Date
6	Dummy logging	Borehole stability/risk evaluation.	2016-08-01–2016-08-02
7	Borehole fluid logging	Logging without the lower rubber discs, no pumping.	2016-08-02
8	Flow along the borehole	Flow along the borehole below the casing tube without the lower rubber discs, no pumping.	2016-08-02
9	Flow logging without pumping	Section length L_w=5 m, step length dL=0.5 m, no pumping.	2016-08-03–2016-08-04
10	Flow logging with pumping	Section length L_w=5 m, step length dL=0.5 m, with pumping. Drawdown = 10 m.	2016-08-05
11	Flow logging and fracture-EC with pumping	Section length L_w=1 m, step length dL=0.1 m, with pumping. Drawdown = 10 m.	2016-08-06–2016-08-10
12	Borehole fluid EC before pump stop	Logging without the lower rubber discs, with pumping. Drawdown = 10 m.	2016-08-10
13	Transient registration of recovery	Measurement of water level and absolute pressure in the borehole after the pumping was stopped. The measurement was continued between 2016-08-11–2016-08-24 by SKB.	2016-08-10–2016-08-11

5.2 Nonconformities

The borehole length 35–84 m was re-measured with flow logging without pumping (Item 9), because bubbles of gas from the borehole possibly caused distortion in the first measurement. The EC electrode's capillary tube was blocked by clay, and gas accumulated in the electrode causing variation to flow results. Re-measurement is seen as a small leap in the plots at the length of c. 84 m (Appendix KFM24.3.4).

The pumping rate (outflow from the borehole) was oscillating throughout the measurements. Unstable pumping was caused by the gas from the borehole combined with a small outflow. Despite the unstable pumping rate, the drawdown remained relatively constant for the whole period of pumping.

It was not physically possible to measure approximately 3.8 m from the bottom of the borehole. There are weights and a centralizer in the measurement device, which reduce the measured distance by c. 3.4 m. The rubber sealing discs in the device must also be flipped before the measurement begins. This reduces the measured distance for approximately 50 cm. It is possible that there were also fallen rocks and debris at the bottom of the borehole.

6 Results

6.1 Length calibration

An accurate length scale for the measurements is difficult to achieve in long boreholes. The main cause of inaccuracy is the stretching of the logging cable. The stretching depends on the tension on the cable, the magnitude of which in turn depends, among other things, on the inclination of the borehole and the roughness (friction properties) of the borehole wall. The cable tension is larger when the borehole is measured upwards. The cables, especially new cables, may also stretch out permanently.

6.1.1 SPR measurement

All flow measurement sequences can be length corrected by synchronising the SPR results (SPR is recorded during all the measurements except borehole EC measurements) with other resistivity measurements. In this measurement campaign, all flow measurement sequences were length corrected by synchronising the SPR results with the geophysics resistivity measurement.

Length corrections are presented in Appendix KFM24.1.13. The procedure of the length calibration is as follows.

- The SPR-measurements during flow loggings (Items 8, 9, 10 and 11) were initially length corrected in relation to the Geophysics resistivity measurement, Appendices KFM24.1.1–KFM24.1.12, black curve.
- Corrections between the lengths were obtained by linear interpolation.

The results of the length corrected SPR measurements from the entire borehole are presented in Appendix KFM24.1.1. Three SPR-curves are plotted together with the geophysics resistivity data. These measurements correspond to Items 9, 10 and 11. The measurements of vertical flow along the borehole (Item 8) were also length corrected by SPR-measurement.

The aim of the plots in Appendices KFM24.1.2–KFM24.1.12 is to verify the accuracy of the length correction. The curves in these plots represent length corrected results.

The magnitude of length correction along the borehole is presented in Appendix KFM24.1.13. The negative values of the error represent the situation where the logging cable has been extended, i.e. the cable is longer than the nominal length marked on it.

6.1.2 Estimated error in location of detected fractures

Despite the length correction described above, there can still be errors due to the following reasons.

1. The point interval in the overlapping mode flow measurements is 0.1 m. This could cause an error of ± 0.05 m. This error is random.
2. The length of the test section is not exact. The specified section length denotes the distance between the nearest upper and lower rubber sealing discs. Effectively, the section length can be larger. At the upper end of the test section there are four rubber sealing discs. The distance between them is 5 cm. This will cause rounded flow anomalies: a flow may be detected already when a fracture is situated between the upper rubber sealing discs. These phenomena can cause an error of ± 0.05 m when the short step length (0.1 m) is used.
3. SPR curves may be imperfectly synchronized. This could cause an error of ± 0.1 m.

In worst case scenario, the errors from sources 1, 2 and 3 are summed and the total estimated error to the geophysics resistivity measurement would be ± 0.2 m.

Knowing the location accurately is important when different measurements are compared, for instance flow logging and borehole TV. In that case, the situation may not be as severe as the case above, since some of the length errors are systematic and the error is nearly constant in fractures that are close to each other.

Fractures nearly parallel with the borehole may also be problematic. Fracture location may be difficult to define accurately in such cases.

6.2 Electrical conductivity and temperature

6.2.1 Electrical conductivity and temperature of borehole water

The EC of the borehole water is initially measured when the borehole is at rest, i.e. at undisturbed conditions. The measurement was performed downwards (Appendices KFM24.2.1 (linear scale) and KFM24.2.2 (logarithmic scale)), cyan curve.

The EC measurement was repeated during pumping (after a pumping period of approximately six days (Appendices KFM24.2.1 and KFM24.2.2, green curve)).

The temperature of the borehole water was measured simultaneously with the EC measurements. The EC values are temperature corrected to 25 °C to make them more comparable with other EC measurements (Heikkonen et al. 2002). The temperature results in Appendix KFM24.2.3 have the same length axis as the EC results in KFM24.2.1 and KFM24.2.2.

The length calibration of the borehole EC measurements is not as accurate as in other measurements, because SPR is not registered. The length correction is linear and based on the nearest tape marks on the cable at start and end depth.

6.2.2 Electrical conductivity of fracture-specific water

The flow direction is always from the fractures into the borehole if the borehole is pumped with a sufficiently large drawdown. This enables the determination of EC from fracture-specific water. Both EC and temperature of flowing water from the fractures were measured.

The fractures detected in the flow measurements can be measured for EC later. These fracture-specific measurements begin near the fracture which has been chosen for inspection. The probe is first moved stepwise closer to the fracture until the detected flow is larger than a predetermined limit. At this point the probe is stopped. The measurement is continued at the given position allowing the fracture-specific water to enter the section. The waiting time for the EC measurement can be automatically calculated from the measured flow rate. The aim is to flush the water volume within the test section sufficiently to gain accurate results. The water in the test section is replaced approximately three times over. After the set of stationary measurements, the tool is once again moved stepwise past the fracture. The EC is also measured during the stepwise movement before and after the set of stationary measurements.

The test section in these measurements was 1 m long and the tool was moved in 0.1 m steps. The water volume in a 1 m long test section is 3.6 L. The results are presented in Appendices KFM24.11.1–KFM24.11.5. The blue symbol represents the conductivity value when the tool was moved and the red symbol is used for the set of stationary measurements.

Lengths to the upper and lower ends of the section, fracture locations, fracture flow and the final EC values for borehole are listed in Table 6-3.

For comparison, the fracture-specific EC and temperature results are also plotted with the EC and temperature results of borehole water (Appendices KFM24.2.1–KFM24.2.3.

Table 6-3. Fracture-specific EC.

Upper end of section (m)	Lower end of section (m)	Measured fracture (m)	Flow (mL/h)	EC (S/m) at 25 °C
51.70	52.70	52.0	1700	0.75
184.68	185.68	185.0	11500	0.62
194.77	195.77	195.1	5720	0.60
398.53	399.53	398.9	1970	1.46
412.40	413.40	412.7	577	1.60

6.3 Pressure measurements

Absolute pressure was registered together with the other measurements in Items 9–11 and 13. The pressure sensor measures the sum of hydrostatic pressure in the borehole and air pressure. Air pressure was also registered separately (Appendix KFM24.10.2. The hydraulic head along the borehole at undisturbed and pumped conditions is determined in the following way. First, the monitored air pressure at the site is subtracted from the measured absolute pressure. The hydraulic head (h) at a certain elevation (z) is calculated according to the following expression:

$$h = (p_{abs}-p_b)/(\rho_{fw} \cdot g) + z \qquad 6\text{-}1$$

where

h is the hydraulic head metre above sea level (m.a.s.l.) according to the RHB 70 reference system,

p_{abs} is the absolute pressure (Pa),

p_b is the barometric (air) pressure (Pa),

ρ_{fw} is the unit density, 1000 kg/m^3

g is the standard gravity, 9.80665 m/s^2 and

z is the elevation of measurement (m.a.s.l.) according to the RHB 70 reference system.

A sensor-specific offset of 3.1 kPa is subtracted from absolute pressure results.

The calculated head distributions are presented in Appendix KFM24.10.1. Exact z-coordinates are important in hydraulic head calculation as an error in the z-coordinate leads to an equal error in the calculated head.

6.4 Flow logging

6.4.1 General comments on results

The measuring programme contained several flow logging sequences, which are numbered as Flow 1 (flow flogging without pumping with a 5 m section length, Q_0 in tables), Flow 2 (flow logging with pumping with a 5 m section length, Q_1 in section flow table) and Flow 3 (flow logging with pumping with a 1 m section length, Q_1 in fracture flow table). They are shown on the same diagram with the SPR (right hand side; Appendices KFM24.3.1–KFM24.3.27). The SPR has a lower value over fractures where flow is detected. Many other resistance anomalies result from other fractures and geological features. As the electrode of the SPR tool is located within the upper rubber sealing discs of the probe, the locations of resistance anomalies associated with leaking fractures coincide with the lower end of the flow anomalies.

The flow logging was first performed with a 5 m section length and with 0.5 m length increments. The method (overlapping flow logging) gives the length and the thickness of conductive zones with a length resolution of 0.5 m.

Under undisturbed conditions or if the borehole is not pumped using a sufficient drawdown the flow direction may be into the borehole or out from it. The direction of small flows (< 100 mL/h) cannot be detected in the normal overlapping mode (thermal dilution method). Therefore the measurement time was longer (so that the thermal pulse method could be used) at every 5 metre interval in both 5 m section measurements.

The test section length determines the width of a flow anomaly of a single fracture. If the distance between flow yielding fractures is less than the section length, the anomalies will overlap, resulting in a stepwise flow data plot. The overlapping flow logging was repeated using a 1 m long test section and 0.1 m length increments.

The position (borehole length) of the detected fractures is shown on the middle scale. They are interpreted on the basis of the flow curves and therefore represent flowing fractures. A long line represents the location of a leaking fracture; a short line denotes that the existence of a leaking fracture is uncertain. The short line is used when the flow rate is less than 30 mL/h, the flow anomalies are overlapping or unclear because of noise (see Section 6.4.4).

The coloured triangles show the magnitude and direction of the measured flows. The triangles have the same colour as the corresponding curves.

The explanations to the tables in Appendices KFM24.5.1–KFM24.5.4 and KFM24.7 are given in Appendix KFM24.4.

Result from the vertical flow along the borehole measurement without pumping, alongside with air pressure and water level, is presented in Appendix KFM24.3.28. Time-series measurement was conducted at the length of 37.5 m, just below the percussion drilled part of the borehole where the casing tube is installed. Measured vertical flow was c. 200 mL/h downwards, i.e. the casing tube, or its seams, has a leakage of c. 200 mL/h.

6.4.2 Transmissivity and hydraulic head of borehole sections

The borehole was flow logged with a 5 m section length and with 0.5 m length increments both in undisturbed conditions and during pumping.

The results of the measurements with a 5 m section length are presented in tables (Appendices KFM24.5.1–KFM24.5.4. Only the results with 5 m length increments are used. All flowing borehole sections are shown in Appendices KFM24.3.1–KFM24.3.27. Secup and Seclow in Appendices KFM24.5.1–KFM24.5.4 are the distances along the borehole from the reference level (top of the casing tube) to the upper end of the test section and to the lower end of the test section, respectively. The Secup and Seclow values for the two sequences (measurements in undisturbed conditions and during pumping) are not exactly identical, due to a minor difference in the cable stretching. The difference between these two sequences was small. Secup and Seclow given in Appendices KFM24.5.1–KFM24.5.4 are calculated as the average of these two values.

The total conductive fracture frequency (CFF) is presented graphically (Appendix 6.3).

Pressure was measured and calculated as described in Section 6.3. h_{0FW} and h_{1FW} in Appendices KFM24.5.1–KFM24.5.4 represent heads determined without and with pumping, respectively. The head in the borehole and calculated heads of borehole sections are given in RHB 70 scale.

The flow results in Appendices KFM24.5.1–KFM24.5.4 (Q_0 and Q_1), representing the flow rates derived from measurements during undisturbed conditions and under pumping, are presented side by side to make comparison easier. Flow rates are positive if the flow direction is from the bedrock into the borehole and vice versa. With the borehole at rest, eleven sections were detected as flow yielding, six of which had a flow direction from the borehole into the bedrock (negative flow). During pumping, all 27 detected flow yielding sections were directed towards the borehole (positive flow).

It is also possible to detect the existence of flow anomalies below the measurement limit (30 mL/h = $8.33 \cdot 10^{-9}$ m^3/s), even though the exact numerical values below the limit are uncertain.

The flow data is presented as a plot (Appendix KFM24.6.1). The left-hand plot in each diagram represents flow from the borehole into the bedrock for the respective test sections, while the right-hand plot represents flow from the bedrock into the borehole. If flow could not be detected (zero flow), no corresponding point will be visible on the logarithmic plots in the appendices.

The lower and upper measurement limits of the flow are also presented in the plot (Appendix KFM24.6.1) and in the tables (Appendices KFM24.5.1–KFM24.5.4). There are theoretical and practical lower limits of flow (Section 6.4.4).

The hydraulic head and transmissivity (T_D) of borehole sections can be calculated from the flow data using the method described in Chapter 3. The results are illustrated in Appendix KFM24.6.2. The hydraulic head of sections is presented in the plots if none of the two flow values at the same length is equal to zero. Transmissivity is presented if none or just one of the flows is equal to zero.

The measurement limits of transmissivity are also shown in Appendix KFM24.6.2 and in Appendices KFM24.5.1–KFM24.5.4. All the measurement limit values of transmissivity are based on the actual pressure difference in the borehole (h_{0FW} and h_{1FW} in Appendices KFM24.5.1–KFM24.5.4).

The sum of all the detected flows without pumping (Q_0) was $1.96 \cdot 10^{-8}$ m^3/s (0.07 L/h). When the leakage of the casing tube (Appendix KFM24.3.28), $5.28 \cdot 10^{-8}$ m^3/s (0.19 L/h), is subtracted from the flows, the total sum of flows from the measurement without pumping is $-3.32 \cdot 10^{-8}$ m^3/s (−0.12 L/h). This sum should normally be zero if all the flows in the borehole are not disturbed by noise or other external factors, the borehole is not pumped, the water level is constant, the salinity distribution in the borehole is stabilized and the fractures are at steady state pressure. In this case inflows and outflows were relatively well balanced.

6.4.3 Transmissivity and hydraulic head of fractures

An attempt was made to evaluate the magnitude of fracture-specific flow rates. The results for a 1 m section length and 0.1 m length increments were used for this purpose. The first step in this procedure is to identify the locations of individual flowing fractures and then evaluate their flow rates.

In cases where the fracture distance is less than one metre, it may be difficult to evaluate the flow rate. Such cases are shown in Appendix KFM24.3.12. In these cases a stepwise increase or decrease in the flow data plot equals the flow rate of a specific fracture (filled triangles in the appendices).

Since the 1 m long measurement section was not used during undisturbed conditions, the results for the 5 m section were used instead. The fracture locations are important when evaluating the flow rate under undisturbed conditions. The fracture locations are known on the basis of the 1 m section measurements. It is not a problem to evaluate the flow rate during undisturbed conditions when the distance between flowing fractures is more than 5 m. The evaluation may, however, be problematic when the distance between fractures is less than 5 m. In this case an increase or decrease of a flow anomaly at the fracture location determines the flow rate. However, this evaluation is used conservatively, i.e. only in the clearest of cases and no flow value is usually evaluated during undisturbed conditions at densely fractured parts of bedrock. If the flow for a specific fracture cannot be determined conclusively, the flow rate is marked with "–" and the value 0 is used in the transmissivity calculation (Appendix KFM24.7. The flow direction is evaluated as well. The results of the evaluation are plotted in Appendix KFM24.3, blue filled triangle.

The total amount of detected flowing fractures was 34, but only eleven of them could be defined without pumping. Eleven of these fractures could be used for head estimations and 34 were used for transmissivity estimations. The transmissivity and hydraulic head of fractures are presented in Appendices KFM24.7 and KFM24.8.

Some fracture-specific results were classified to be "uncertain". The basis for this classification is either a minor flow rate (<30 mL/h) or unclear fracture anomalies. Anomalies are considered unclear if the distance between them is less than 1 m or their nature is unclear because of noise.

Fracture-specific transmissivities were compared with transmissivities of sections in Appendix KFM24.9. All fracture-specific transmissivities within each 5 m interval were first summed together to make them comparable with measurements with a 5 m section length. The results are fairly consistent between the two types of measurements. The decrease of flow as a function of pumping time can sometimes be seen in some fractures (storage effect). The 1 m section measurements were carried out after the 5 m section measurements and therefore flow rate and transmissivity can be smaller in the 1 m section measurement results.

The flow rates and heads with pumping at the fracture lengths of 48.8, 175.3, 261.1, 284.4, 297.4, 304.8, 370.3 and 387.8 m were interpreted using values from the measurement with a 5 m section length. The roughness of the borehole wall or wider diameter of the borehole caused leakage of the rubber discs at fractures 48.8, 175.3, 261.1 and 370.3 m and therefore the flow rates were interpreted with a 5 m section length when the rough zone was entirely in between the section, i.e. when the rubber discs were not on the rough zone. The flow rates of these fractures were distorted with a 1 m section length (Appendices KFM24.3.2, KFM24.3.8, KFM24.3.13 and KFM.3.18). The roughness of the borehole wall or wider parts of the hole can also be seen as wider spikes in the SPR-curve.

The flow rates of fractures 297.4, 304.8 and 387.8 m were under the detection limit with a 1 m section length. The flows were also under the measurement limit (30 mL/h) in the measurement with a 5 m section, but clearly visible (Appendices KFM24.3.14, KFM24.3.15 and KFM24.3.19). The decrease of the flow rate can be result of the storage effect explained above. The flow rates of these fractures were marked as uncertain.

Orientation of the borehole was corrected during the drilling of KFM24 at certain lengths. These lengths are presented in Appendices KFM24.3.1–KFM24.3.27 at the SPR-axis. The borehole diameter is probably wider at these positions by length interval c. 2 m causing the PFL probe's rubber discs leaking. For example (Appendix KFM24.3.10), at the length of 203.0 m, where the orientation correction had been made, there is rubber discs leakage which can be seen as an incorrect flow anomaly. Uncertain flowing fractures at the lengths of 284.4 m and 414.5 m are in the zone where the drilling orientation has been made, but the flow anomalies with a 5 m section length indicates that the flow is actual fracture flow, not the flow caused by the leakage of the rubber discs.

The flowing fractures at the lengths of 214.4 m and 232.4 m have distorted flow anomalies, which are likely caused by the gas absorbed to water from the fractures (Appendices KFM24.3.10 and KFM24.3.11). At the length of 82.8–83.8 m there is a flow anomaly in the measurement with 1 m section length, but with a 5 m section the flow fades out. Therefore no flowing fracture is interpreted at that length (Appendix KFM24.3.4.

The sum of the detected fracture flows $8.28 \cdot 10^{-6}$ m^3/s (~0.5 L/min) was substantially smaller than the average pumping rate $2.22 \cdot 10^{-7}$ m^3/s (~0.8 L/min). Gas bubbles and small outflow caused distortion to pumping and uncertainty to the outflow measurement. Also the known leakage of the casing tube could not be measured with pumping. These factors make it difficult to compare the outflow of the pumping and the sum of the detected fracture flows.

6.4.4 Theoretical and practical measurement limits of flow and transmissivity

The theoretical minimum for measurable flow rate in overlapping measurements is some 30 mL/h. The upper limit of flow measurement is 300 000 mL/h. As these upper and lower limits are determined by flow calibration, it is assumed that flows can be reliably detected between the upper and lower theoretical limits in favourable borehole conditions.

In practice, the minimum measurable flow rate may be much higher. Borehole conditions may have an influence on the flow base level (i.e. noise level). Noise levels can be evaluated in intervals along the borehole where no flowing fractures or other complicating structures are lacking, and may vary along a borehole.

There are several known reasons for increased noise in the flow.

1) Roughness of the borehole wall.
2) Solid particles such as clay or drilling debris in the water.
3) Gas bubbles entrained in the water.
4) High flow rate along the borehole.
5) Mixing of waters with different salinity within the test section.

Roughness in the borehole wall always results in high levels of noise, not only in the flow results, but also in the SPR results. The flow curve and SPR curves are typically spiky when the borehole wall is rough.

Drilling debris usually increase noise levels. This kind of noise is typical for both (undisturbed conditions and under pumping.

Pumping results in lower water pressure in the borehole and in fractures located near the borehole. This may lead to the release of dissolved gas and increase the quantity of gas bubbles entrained in the water. Some fractures may produce more gas than others. Sometimes, when the borehole is being measured upwards, increased noise levels are observed just above certain fractures. The reason for this is assumed to be gas bubbles.

The effect of a high flow rate along the borehole can often be seen above fractures with a high flow. Any minor leakage in the seal provided by the lower rubber sealing discs will appear in the measurement as increased levels of noise.

Another reason for increased noise level could be that when the PFL DIFF probe passes a fracture, there still might be less saline water within the test section from other parts of the drillhole. When waters with different salinity mix, it might cause high noise level to the flow rate results.

A high level of noise in a flow will mask the "real" flow if this is smaller than the noise. Real flows are registered correctly if they are about ten times larger than the noise but are undetectable if they are some ten times smaller than the noise. Experience indicates that real flows between one-tenth of the noise level and 10 times the noise level are summed with the noise. Noise levels could therefore be subtracted from measured flows to get real flows. This correction has not yet been carried out because the cases to which it is applicable are unclear.

The practical minimum for measurable flow rate is presented in Appendices KFM24.3.1–KFM24.3.27 using a grey dashed line (Lower limit of flow rate). The practical minimum level of the measurable flow is always evaluated in pumped conditions since this measurement is the most important for transmissivity calculations. The limit is an approximation. It is evaluated to obtain a limit below which there may be fractures or structures that remain undetected.

The noise level ranged from 30 mL/h to 400 mL/h in KFM24. It is possible to detect the existence of flow anomalies below the theoretical limit of the thermal dilution method (30 mL/h). The noise line (grey dashed line) was never drawn below 30 mL/h, because the values of flow rate measured below 30 mL/h are uncertain.

In some boreholes the upper limit of flow measurement (300 000 mL/h) may be exceeded. Such fractures or structures hardly remain undetected (as the fractures below the lower limit). High flow fractures can be measured separately at a smaller drawdown. There was no need for any such additional measurements during this campaign.

The practical minimum for measurable flow rate is also presented in Appendix KFM24.5 (Q-lower limit P) and is obtained from the plots in Appendix KFM24.3 (Lower limit of flow rate). The practical minimum of measurable transmissivity can be evaluated using Q-lower limit and the actual head difference at each measurement location (Appendix KFM24.5 (T_D-measl$_{LP}$). The theoretical minimum for measurable transmissivity (T_D-measl$_{LT}$) is evaluated using a Q value of 30 mL/h (the minimum theoretical flow rate using the thermal dilution method). The upper measurement limit for transmissivity can be evaluated using the maximum flow rate (300 000 mL/h) and the actual head difference as above (Appendix KFM24.5 (T_D-measl$_U$).

All three flow limits are plotted with the measured flow rates (Appendix KFM24.7).

The three transmissivity limits are also presented graphically (Appendix KFM24.8).

Similar flow and transmissivity limits are not provided for the fracture-specific results as the limits for these are harder to define. The situation is similar for the upper flow limit. If several high-flowing fractures are positioned closer to one another than a distance of 1 m, the upper flow limit will depend on the sum of these flows, and this must be below 300 000 mL/h.

6.5 Transmissivity of the entire borehole

The flow period of the pumping during difference flow logging is utilized to evaluate the transmissivity of the entire borehole. This is done with two steady-state methods described in Chapter 3.

In Dupuit's formula (Equation 3-9), R/r_0 is assumed to be 500, Q was 0.8 L/min and the drawdown s = 10 m by the end of the flow period (Appendix KFM24.10.2). The transmissivity calculated with Dupuit's formula is $1.32 \cdot 10^{-6}$ m^2/s. In Moye's formula (Equation 3-10) the length of the test section L is 514.47 m (35.7–550.17 m) and the borehole diameter $2r_0$ is 0.076 m. The transmissivity calculated with Moye's formula is $2.08 \cdot 10^{-6}$ m^2/s.

6.6 Groundwater level and pumping rate

The level of the groundwater table in the borehole during the measurement sequences is presented in Appendix KFM24.10.2. The borehole was pumped between August 4 and August 10 with a drawdown of approximately 10 m. The pumping rates were recorded (Appendix KFM24.10.2). Grey curve is 20 point moving average of pumping rate.

The groundwater recovery was measured after the pumping period, between August 10 and August 11 (Appendix KFM24.10.3). The recovery was measured with two sensors, the water level sensor (pressure sensor for monitoring water level) and the absolute pressure sensor. The absolute pressure sensor was located at the length of 19.1 m.

After the recovery measurement with the PFL DIFF probe and the water level pressure sensor, the recovery measurement was continued using SKB's water level sensor, green line in Appendices KFM24.10.2 and KFM24.10.3.

7 Summary

In this study, the Posiva Flow Log, Difference Flow Method has been used to determine the location and flow rate of flowing fractures or structures in borehole KFM24 at Forsmark, Sweden. Measurements were carried out both when the borehole was at rest and during pumping. A 5 m section length with 0.5 m length increments was used initially. The borehole was also measured with a 1 m section and a 0.1 m measurement interval.

The distribution of saline water along the borehole was logged by electrical conductivity and temperature measurements of the borehole water. In addition, the electrical conductivity of fracture-specific water was measured in selected flowing fractures.

A casing tube leakage was measured with flow along the borehole method just below the casing tube in undisturbed conditions.

The water level in the borehole during pumping and its recovery after the pump was turned off were also measured.

All flow results were length calibrated by synchronizing the SPR logs with the data of the length corrected geophysics resistivity.

The total amount of detected flowing fractures was 34. Transmissivity and hydraulic head were calculated for the measured borehole sections and fractures. The highest estimated fracture transmissivity ($3.1 \cdot 10-7$ m^2/s) was at 185.0 m. The highest section transmissivity ($3.5 \cdot 10^{-7}$ m^2/s) was detected at length interval 184.77 m – 189.77 m. Another high-transmissive section was found at length interval 194.77 m – 199.77 m. No flowing fractures were identified below 414.5 m.

References

SKB's (Svensk Kärnbränslehantering AB) publications can be found at www.skb.com/publications.

de Marsily G, 1986. Quantitative hydrogeology: groundwater hydrology for engineers. Orlando, FL: Academic Press.

Heikkonen J, Heikkinen E, Mäntynen M, 2002. Pohjaveden sähkönjohtavuuden lämpötilakorjauksen matemaattinen mallinnus synteettisten vesinäytteiden mittauksista. (Mathematical modelling of temperature adjustment algorithm for groundwater electrical conductivity on basis of synthetic water sample analysis.) Posiva Työraportti 2002-10, Posiva Oy, Finland. (In Finnish.)

Ludvigson J-E, Hansson K, Rouhiainen P, 2002. Methodology study of Posiva difference flow meter in borehole KLX02 at Laxemar. SKB R-01-52, Svensk Kärnbränslehantering AB.

Moye D G, 1967. Diamond drilling for foundation exploration. Civil Engineering Transactions, Institute of Engineers (Australia), April, 95–100.

Öhberg A, Rouhiainen P, 2000. Posiva groundwater flow measuring techniques. Posiva 2000-12, Posiva Oy, Finland.

Appendices

Appendices	KFM24.1.1–KFM24.1.12	Length corrected resistance measurement and PFL SPR results after the length correction.
Appendix	KFM24.1.13	Length correction.
Appendices	KFM24.2.1–KFM24.2.2	Electrical conductivity of borehole water.
Appendix	KFM24.2.3	Temperature of borehole water.
Appendices	KFM24.3.1–KFM24.3.27	Flow rate and single point resistance.
Appendix	KFM24.3.28	Vertical flow along the borehole.
Appendix	KFM24.4	Explanations for the tables in Appendices 5 and 7.
Appendices	KFM24.5.1–KFM24.5.4	Results of section flows.
Appendix	KFM24.6.1	Plotted flow rates of 5 m sections.
Appendix	KFM24.6.2	Plotted transmissivity and head of 5 m sections.
Appendix	KFM24.6.3	Conductive fracture frequency.
Appendix	KFM24.7	Inferred fracture flow anomalies from flow logging.
Appendix	KFM24.8	Plotted transmissivity and head of detected fractures.
Appendix	KFM24.9	Comparison between section transmissivity and fracture transmissivity.
Appendix	KFM24.10.1	Head in the borehole during flow logging.
Appendix	KFM24.10.2	Air pressure, water level in the borehole and pumping rate during flow logging.
Appendix	KFM24.10.3	Groundwater recovery after pumping.
Appendices	KFM24.11.1–KFM24.11.5	Fracture-specific EC results by date.

Forsmark, borehole KFM24
Length corrected resistance measurement and
PFL SPR results after the length correction

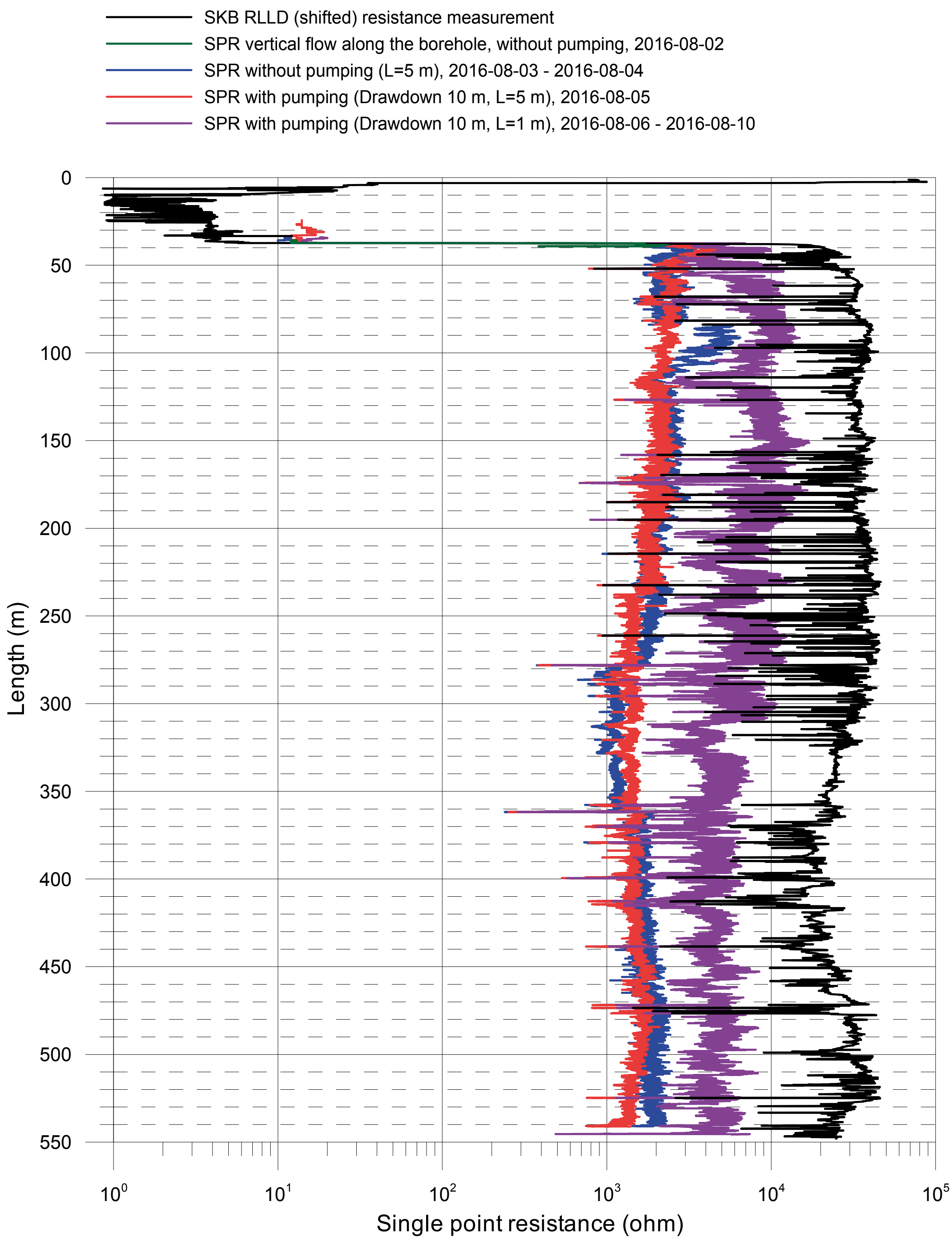

Forsmark, borehole KFM24
Length corrected resistance measurement and
PFL SPR results after the length correction

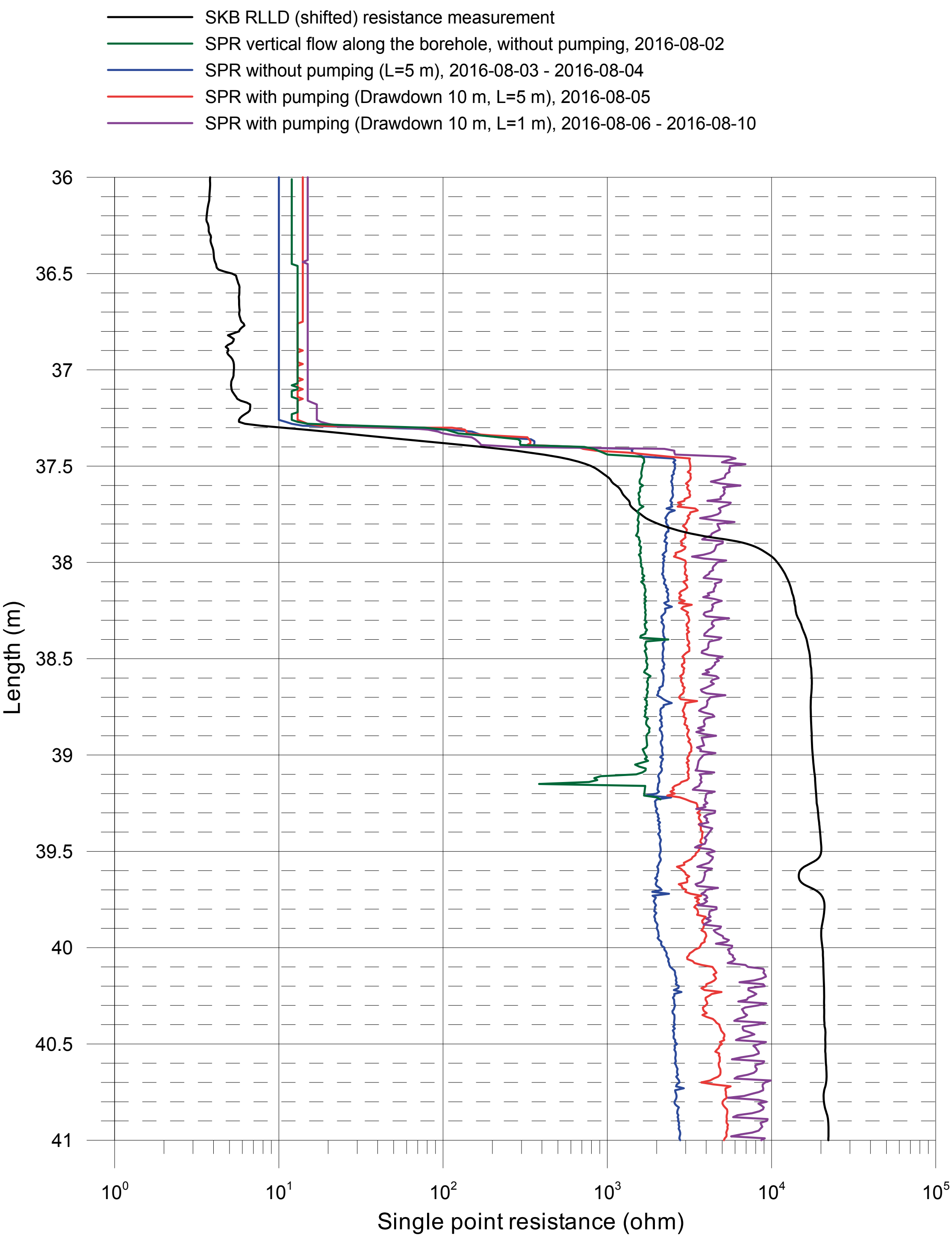

Forsmark, borehole KFM24
Length corrected resistance measurement and
PFL SPR results after the length correction

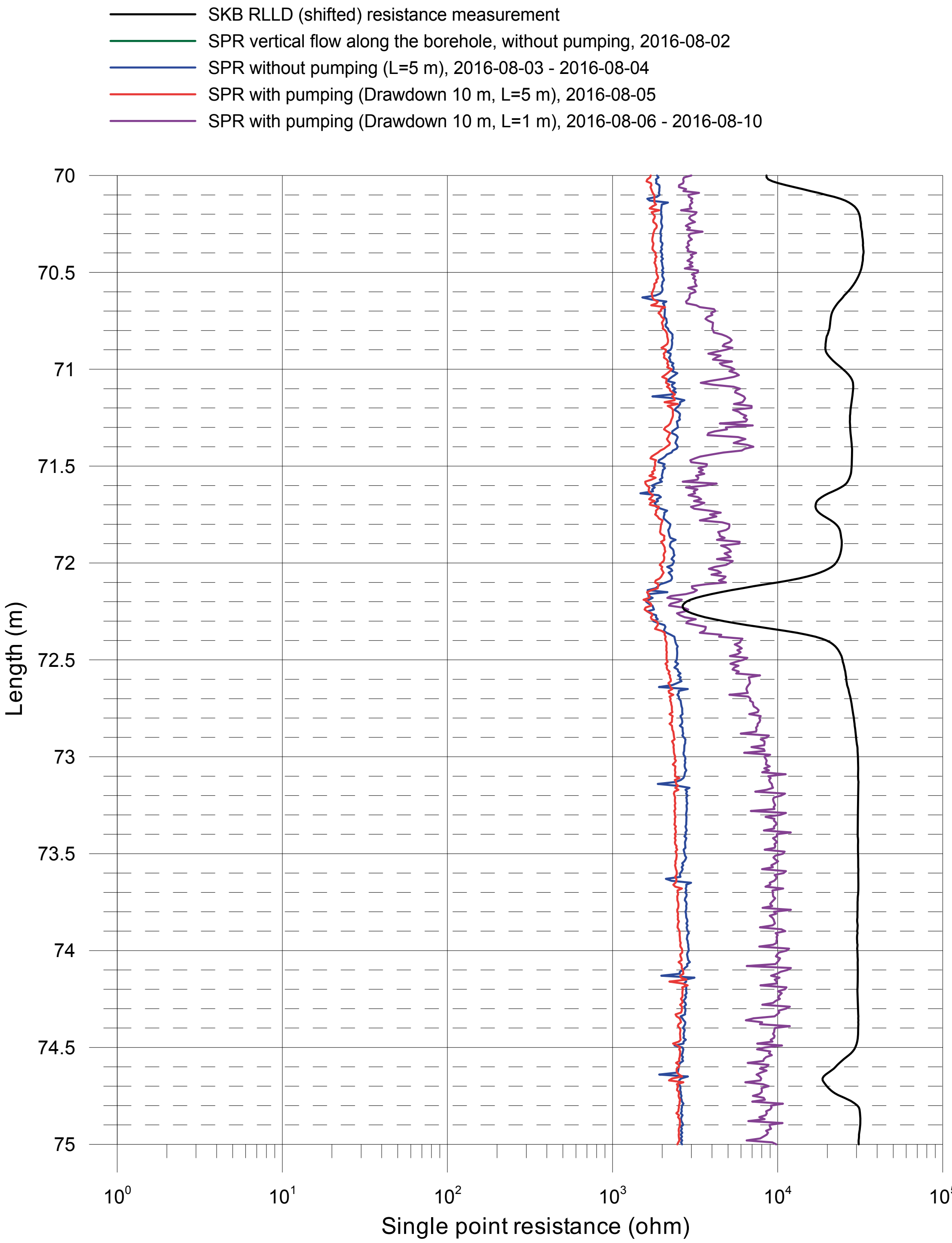

Forsmark, borehole KFM24
Length corrected resistance measurement and
PFL SPR results after the length correction

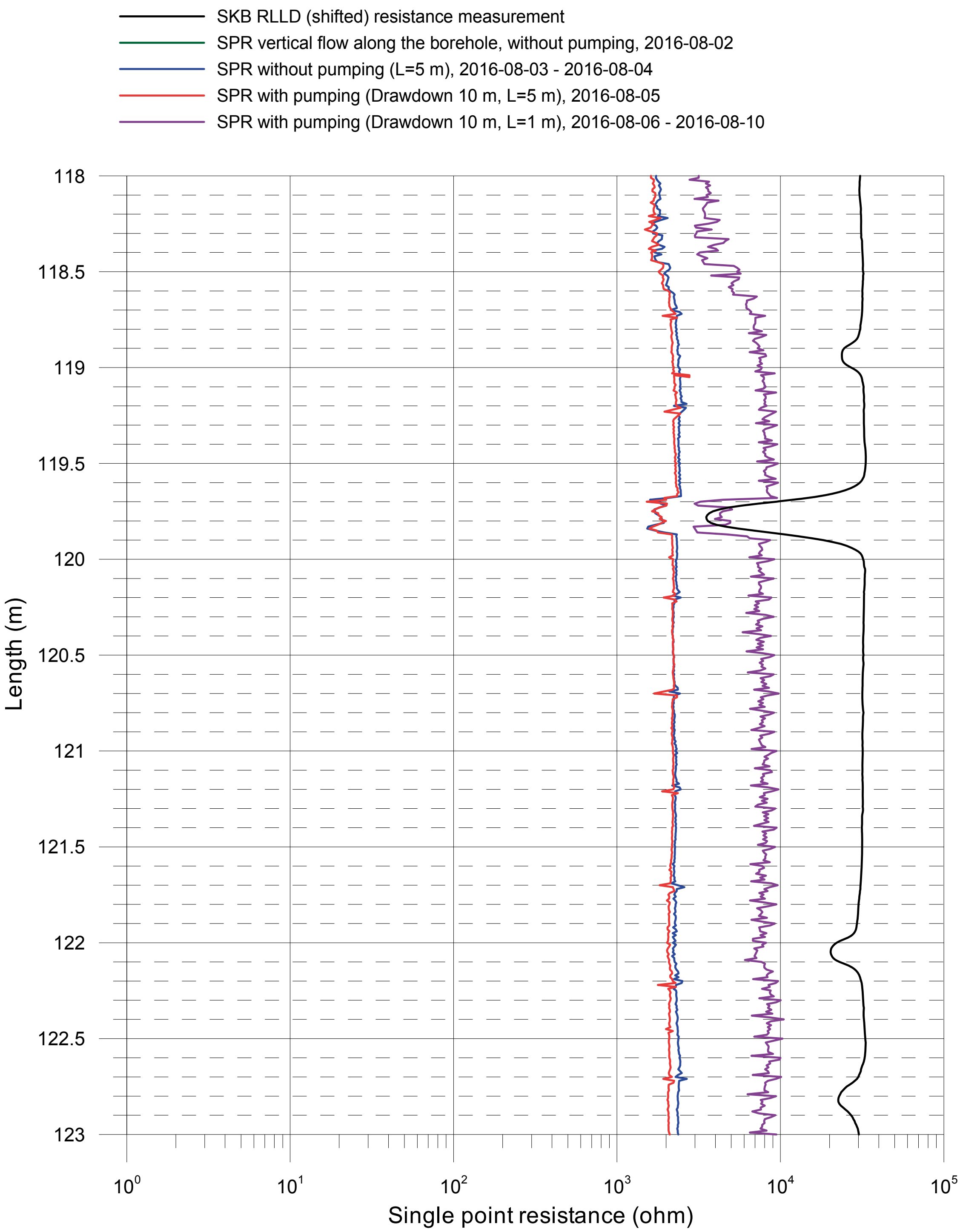

Forsmark, borehole KFM24
Length corrected resistance measurement and
PFL SPR results after the length correction

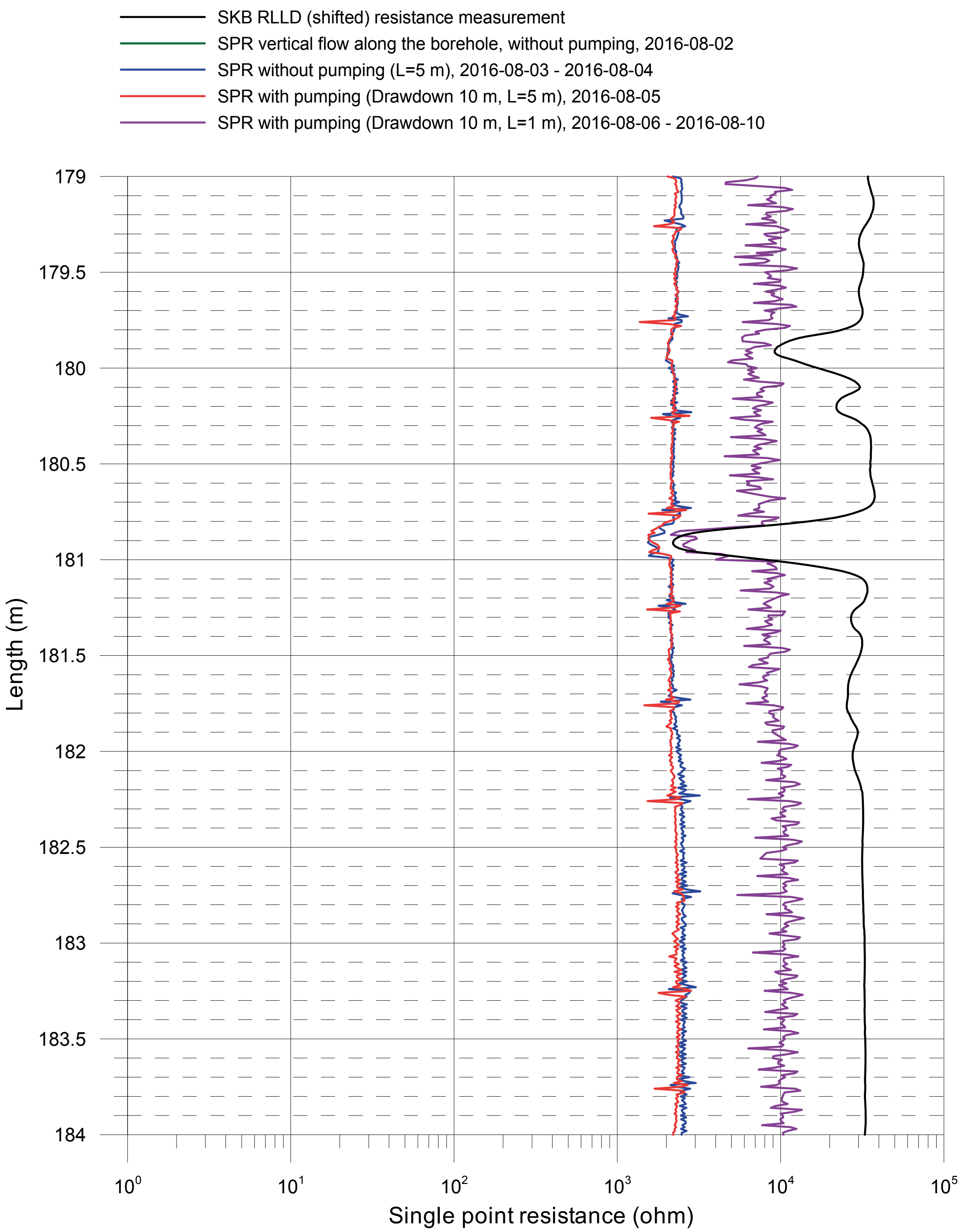

Forsmark, borehole KFM24
Length corrected resistance measurement and
PFL SPR results after the length correction

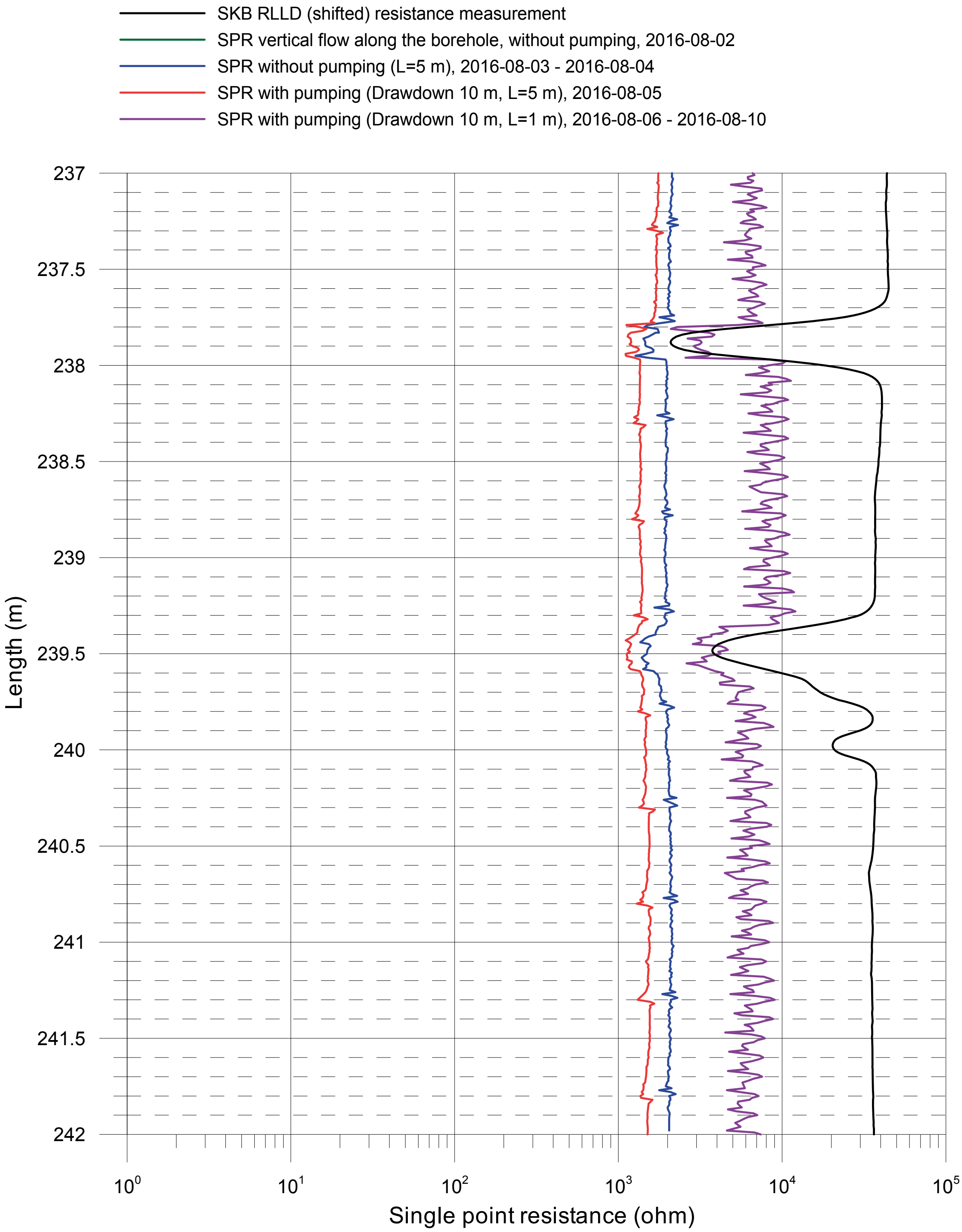

Forsmark, borehole KFM24
Length corrected resistance measurement and
PFL SPR results after the length correction

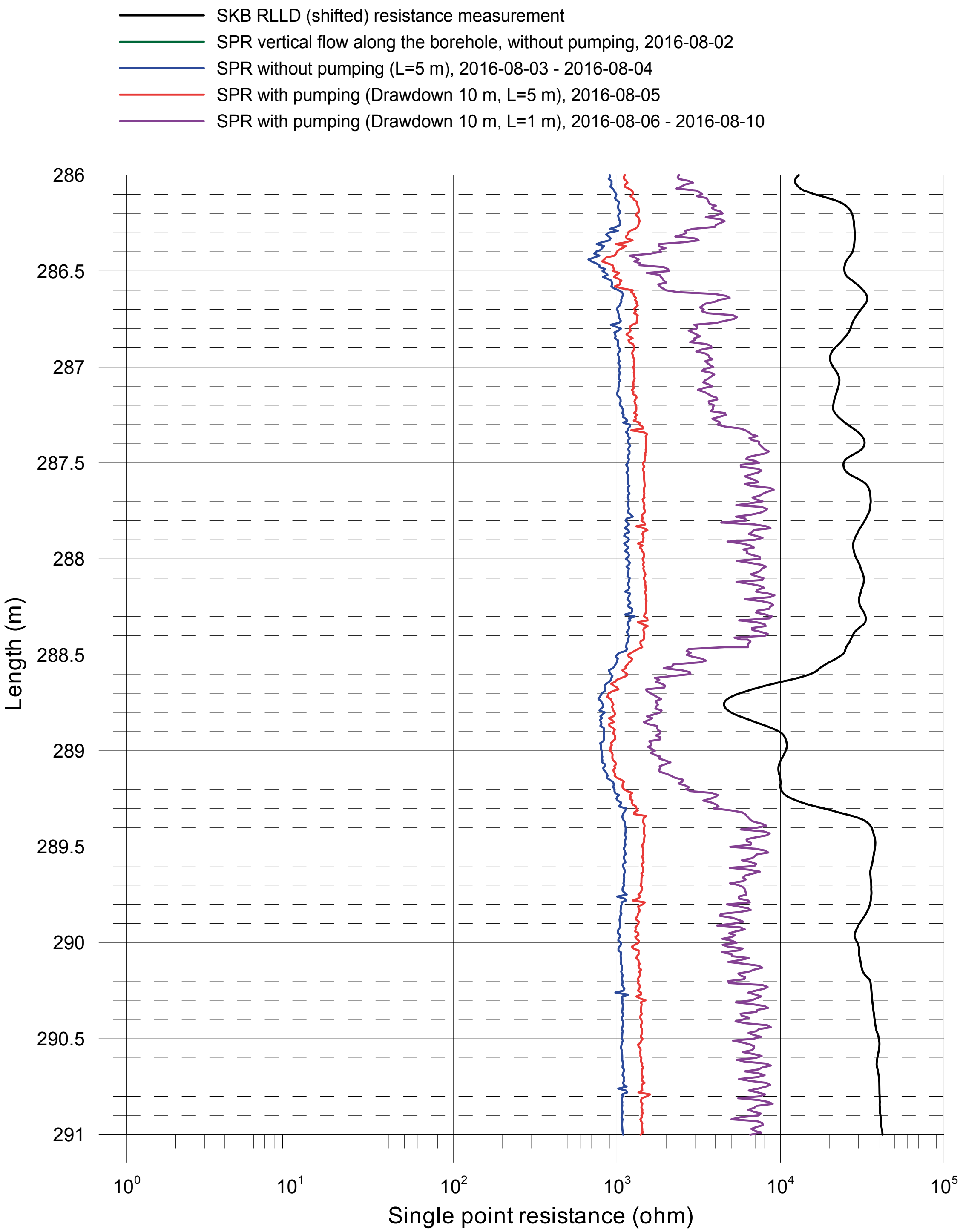

Forsmark, borehole KFM24
Length corrected resistance measurement and
PFL SPR results after the length correction

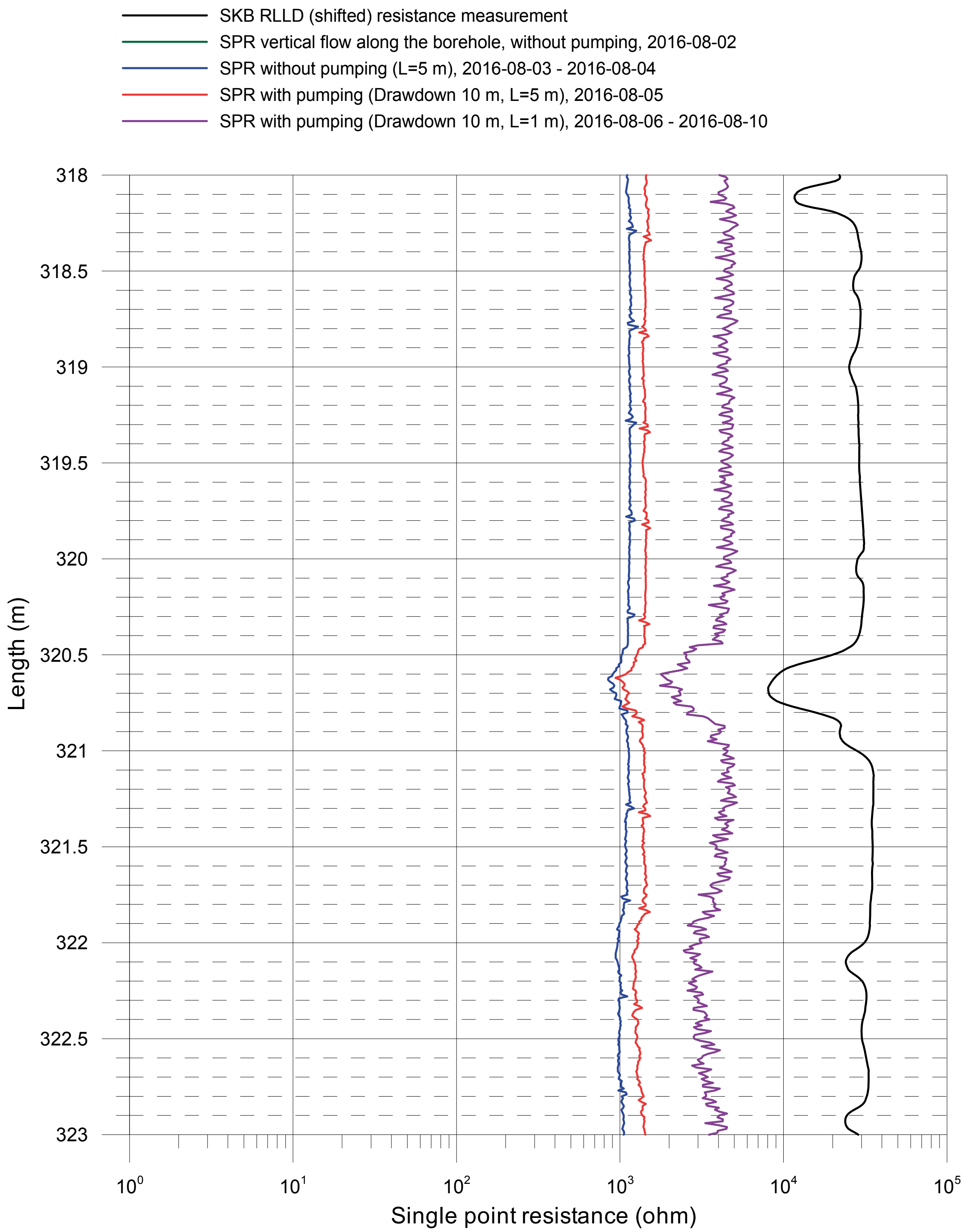

Forsmark, borehole KFM24
Length corrected resistance measurement and
PFL SPR results after the length correction

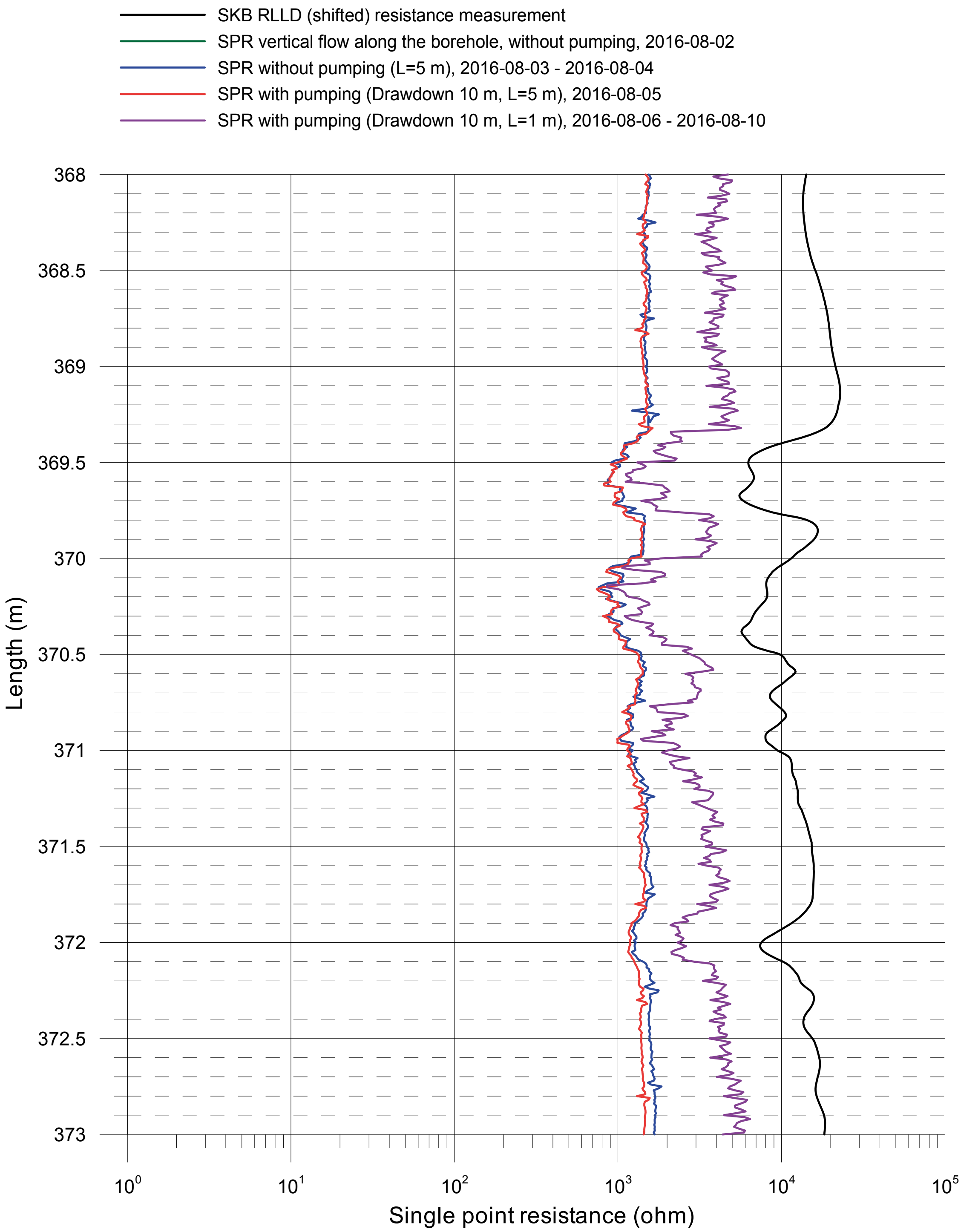

Forsmark, borehole KFM24
Length corrected resistance measurement and
PFL SPR results after the length correction

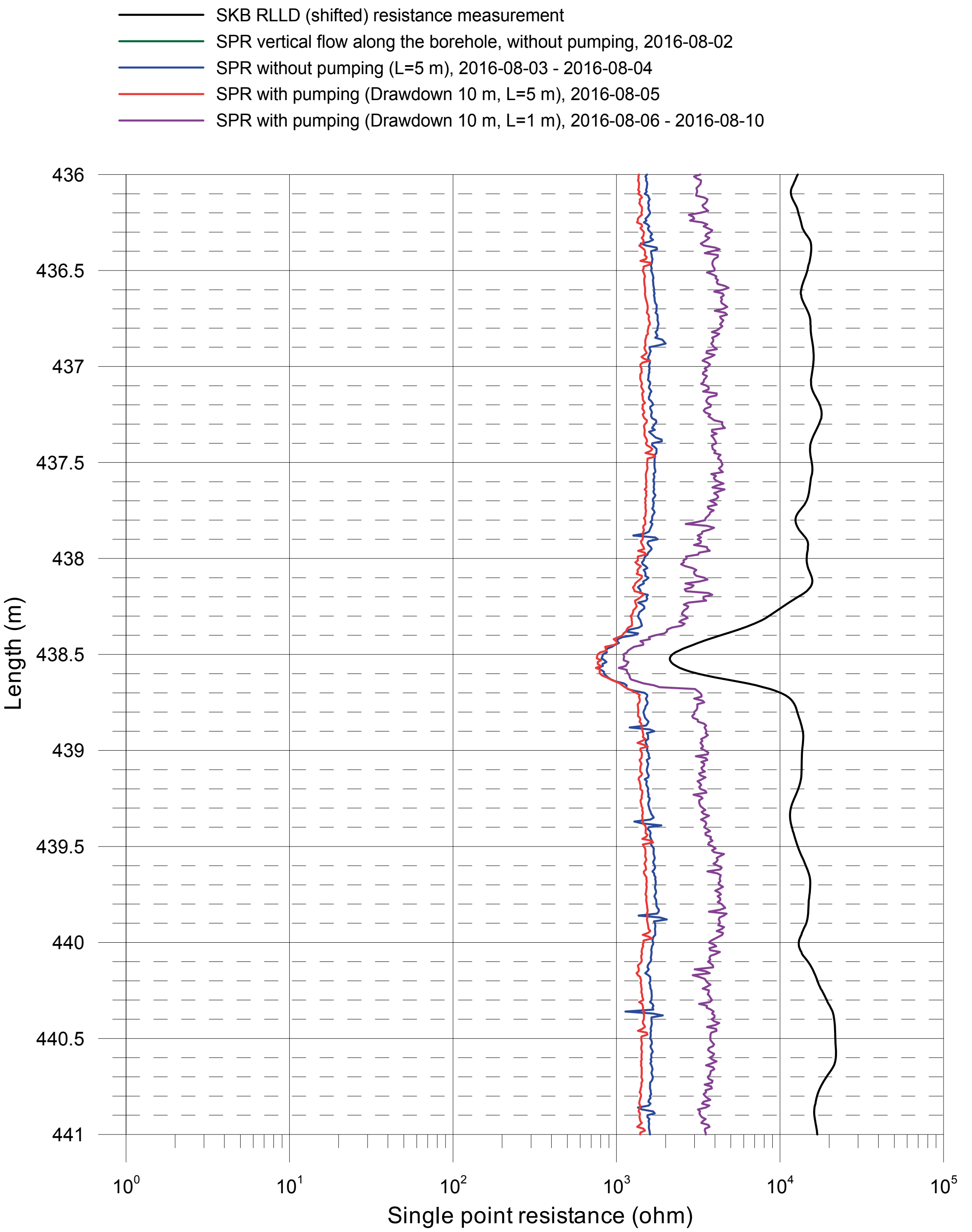

Forsmark, borehole KFM24
Length corrected resistance measurement and
PFL SPR results after the length correction

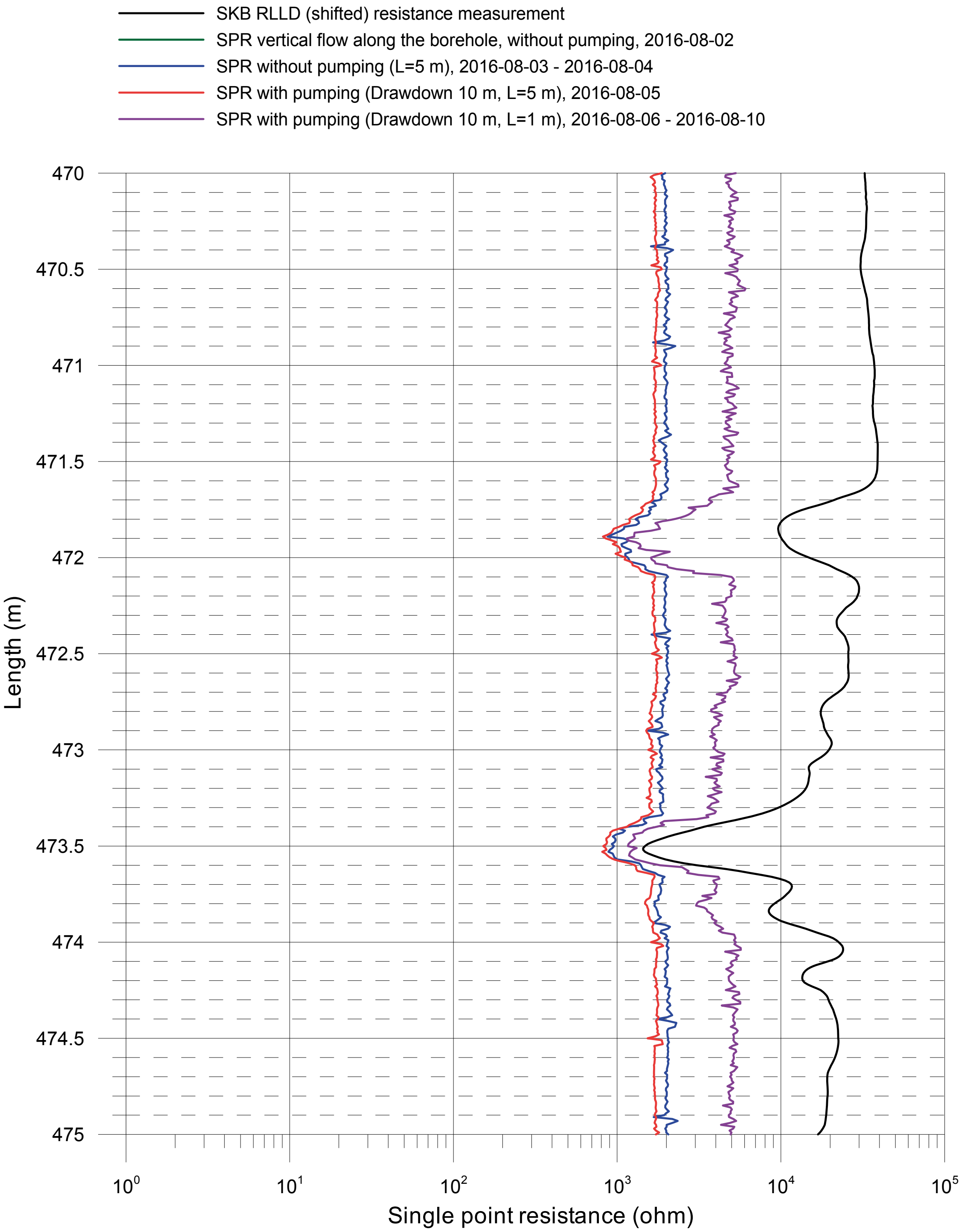

Forsmark, borehole KFM24
Length corrected resistance measurement and
PFL SPR results after the length correction

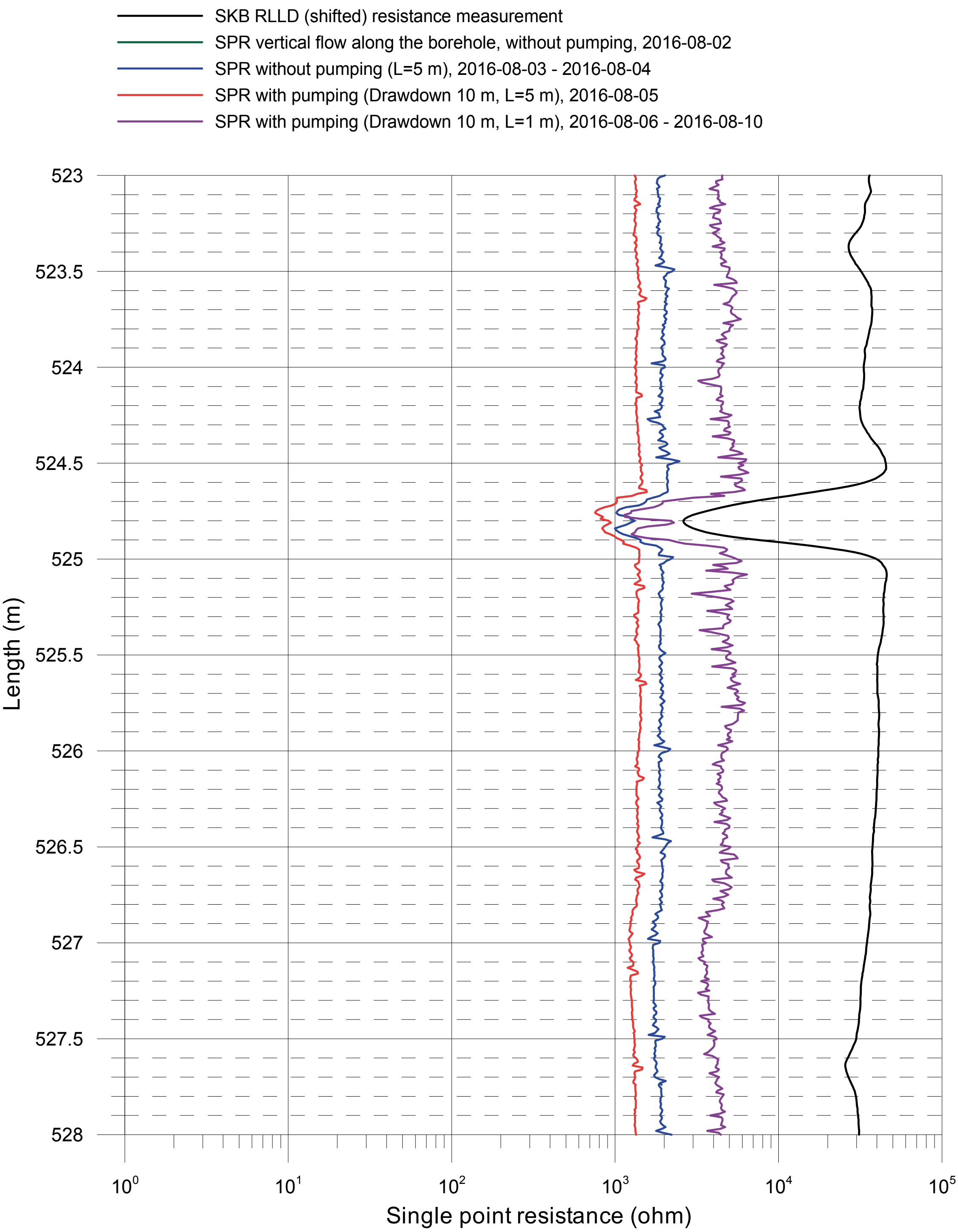

Forsmark, borehole KFM24
Length correction

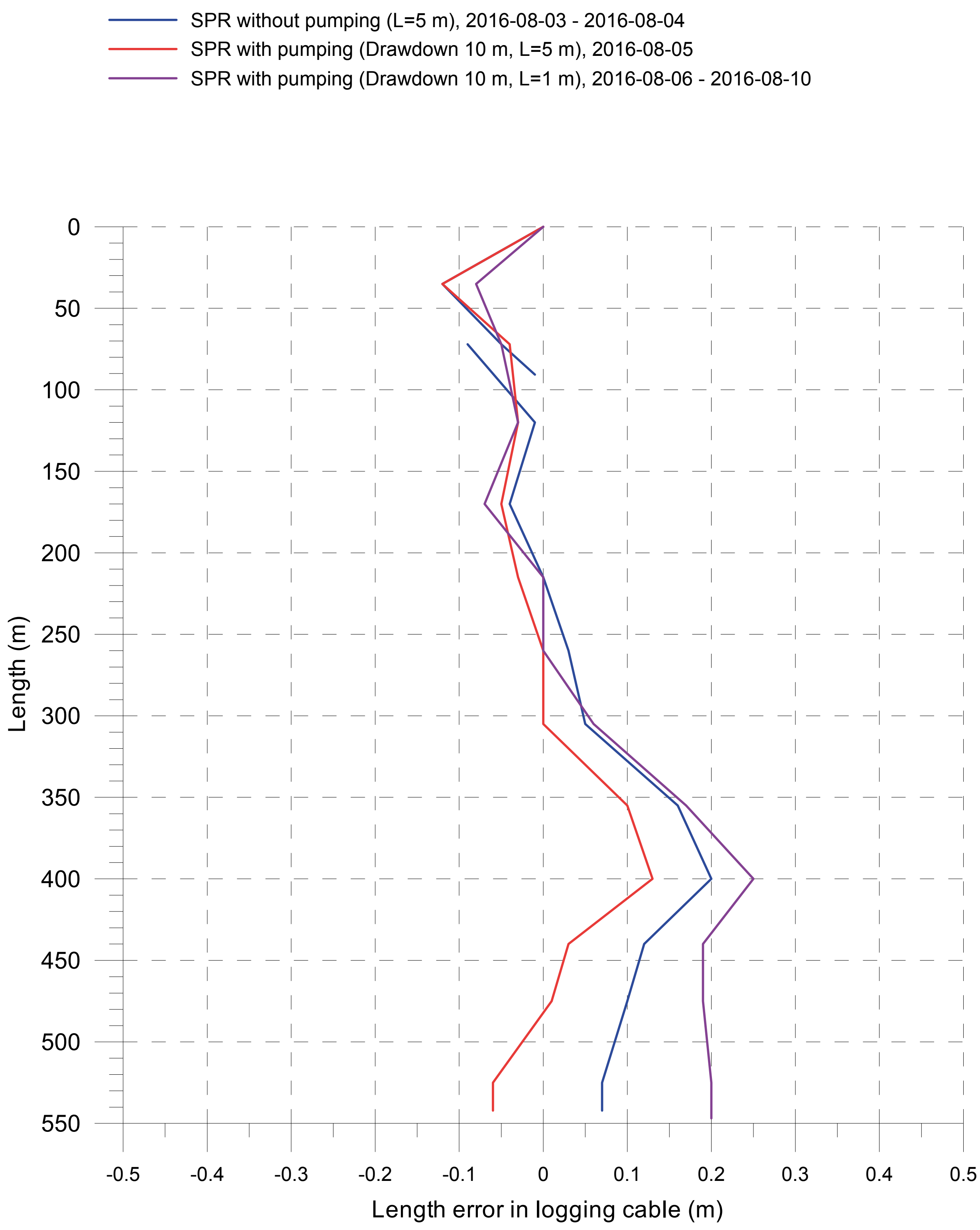

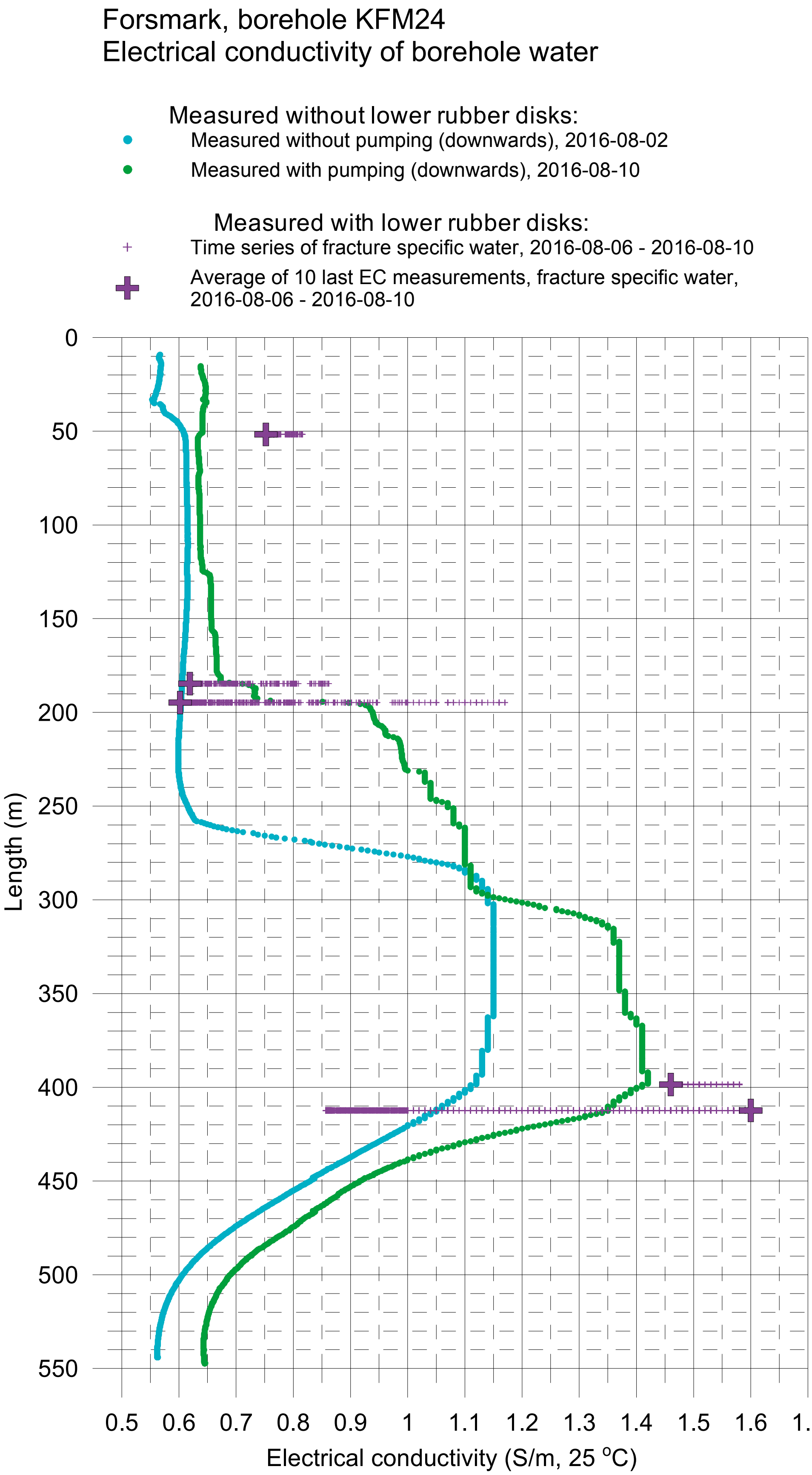
Forsmark, borehole KFM24
Electrical conductivity of borehole water
Measured without lower rubber disks:
Measured without pumping (downwards), 2016-08-02
Measured with pumping (downwards), 2016-08-10
Measured with lower rubber disks:
Time series of fracture specific water, 2016-08-06 - 2016-08-10
Average of 10 last EC measurements, fracture specific water, 2016-08-06 - 2016-08-10
Length (m)
0
50
100
150
200
250
300
350
400
450
500
550
0.5
0.6
0.7
0.8
0.9
1
1.1
1.2
1.3
1.4
1.5
1.6
1.7
Electrical conductivity (S/m, 25 °C)

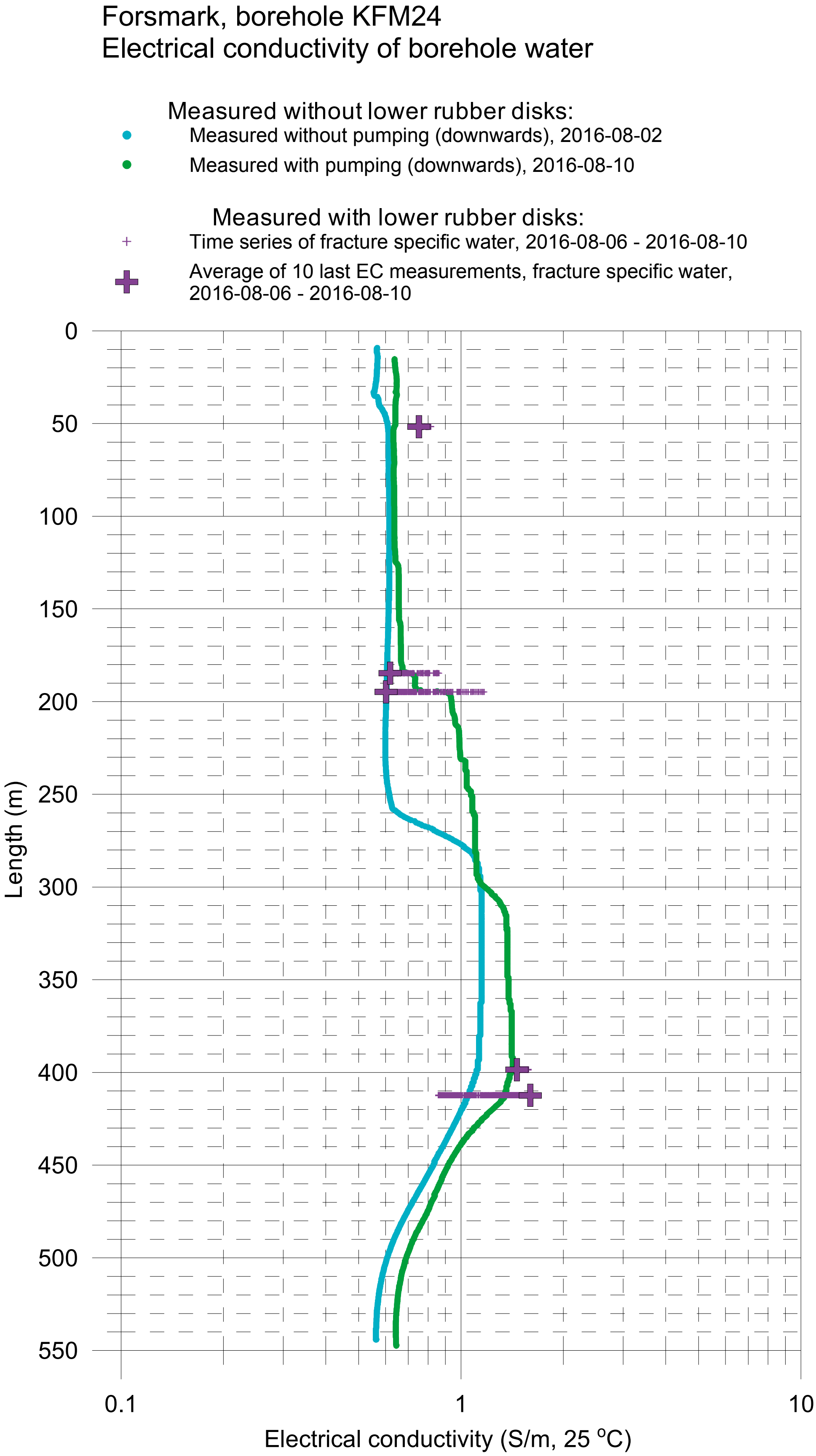
Forsmark, borehole KFM24
Electrical conductivity of borehole water
Measured without lower rubber disks:
Measured without pumping (downwards), 2016-08-02
Measured with pumping (downwards), 2016-08-10
Measured with lower rubber disks:
Time series of fracture specific water, 2016-08-06 - 2016-08-10
Average of 10 last EC measurements, fracture specific water, 2016-08-06 - 2016-08-10
Length (m)
0
50
100
150
200
250
300
350
400
450
500
550
0.1
1
10
Electrical conductivity (S/m, 25 °C)

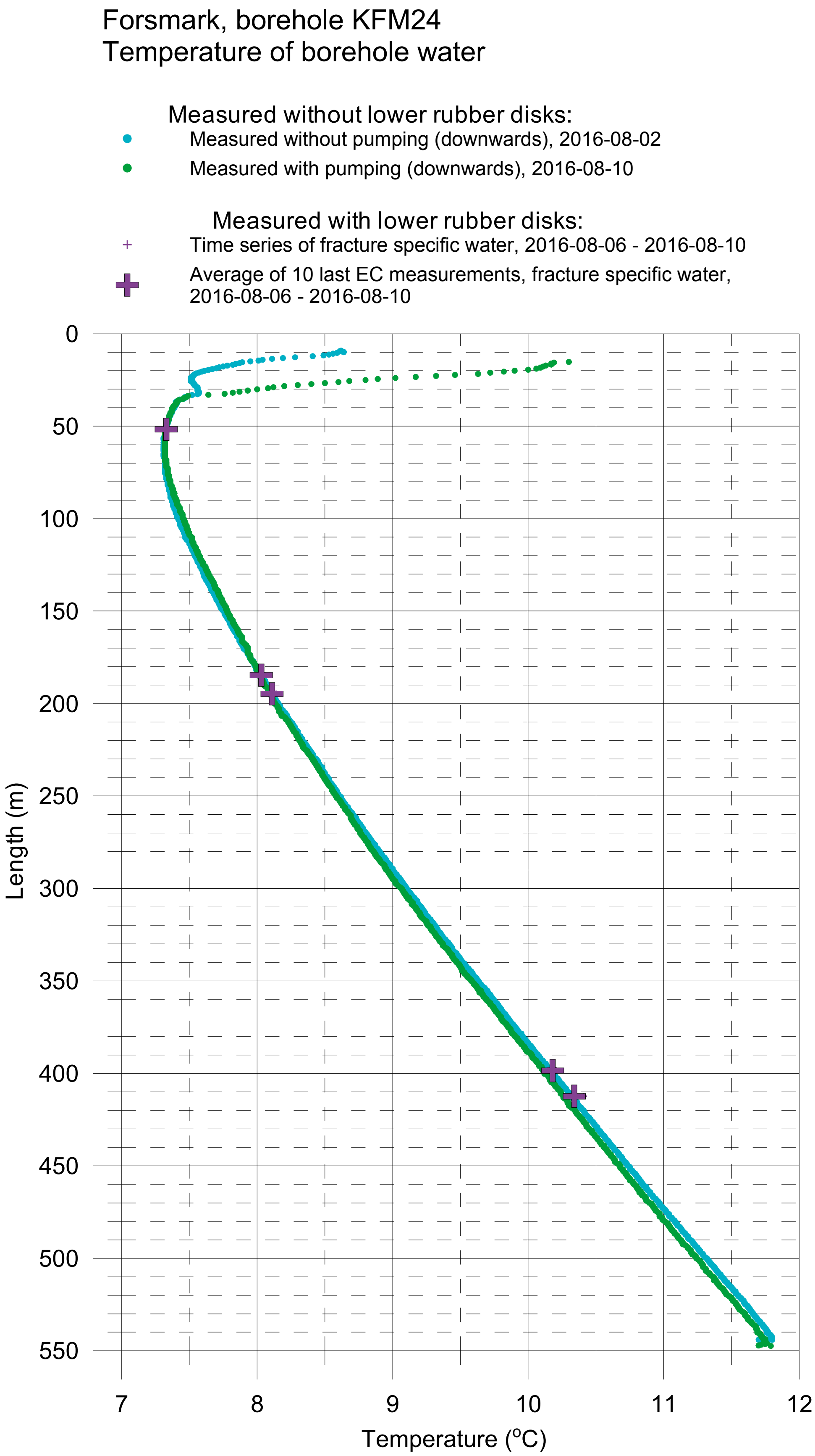
Forsmark, borehole KFM24
Temperature of borehole water
Measured without lower rubber disks:
Measured without pumping (downwards), 2016-08-02
Measured with pumping (downwards), 2016-08-10
Measured with lower rubber disks:
Time series of fracture specific water, 2016-08-06 - 2016-08-10
Average of 10 last EC measurements, fracture specific water, 2016-08-06 - 2016-08-10
Length (m)
0
50
100
150
200
250
300
350
400
450
500
550
7
8
9
10
11
12
Temperature (°C)

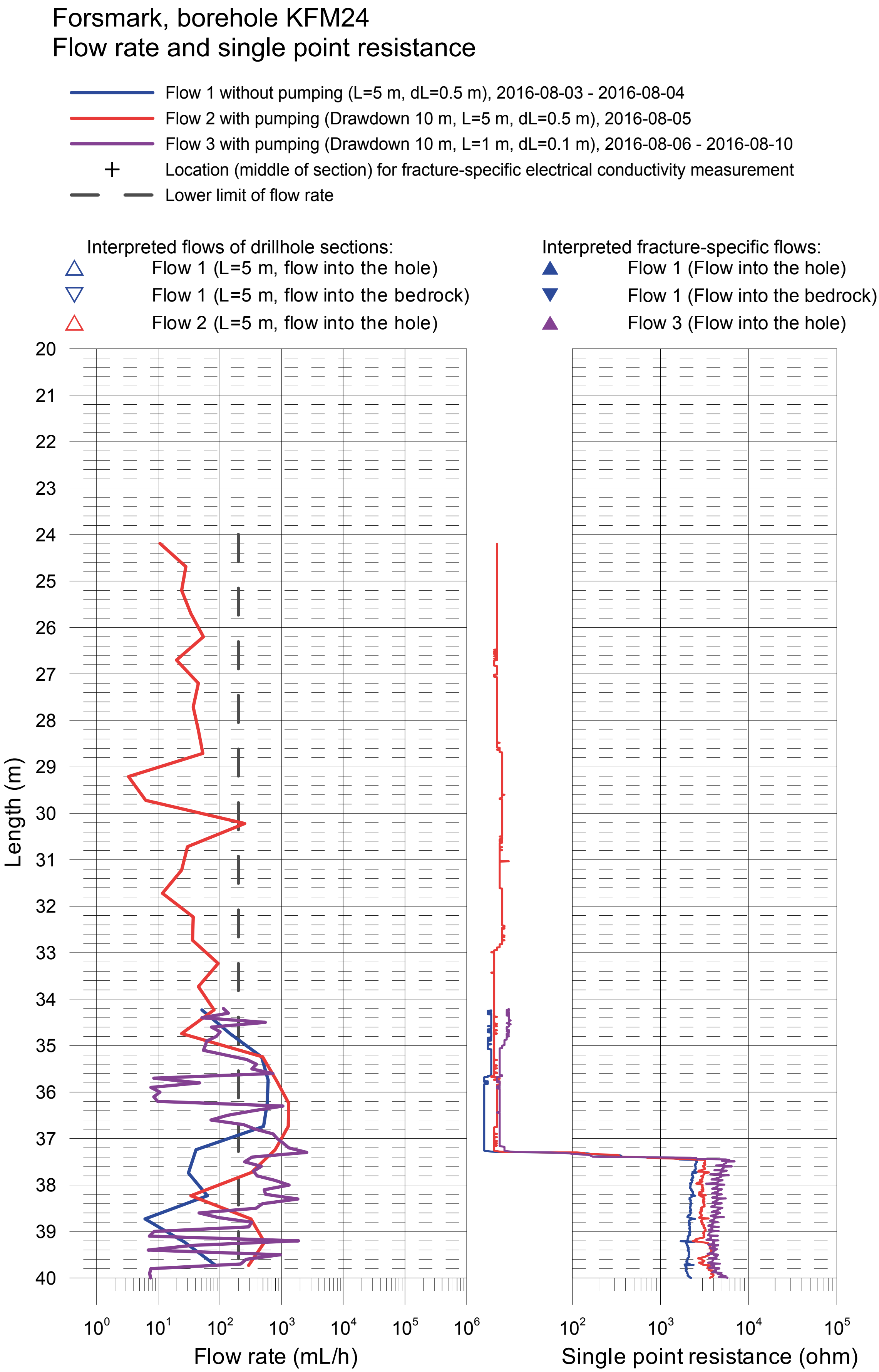

Forsmark, borehole KFM24
Flow rate and single point resistance
Flow 1 without pumping (L=5 m, dL=0.5 m), 2016-08-03 - 2016-08-04
Flow 2 with pumping (Drawdown 10 m, L=5 m, dL=0.5 m), 2016-08-05
Flow 3 with pumping (Drawdown 10 m, L=1 m, dL=0.1 m), 2016-08-06 - 2016-08-10
Location (middle of section) for fracture-specific electrical conductivity measurement
Lower limit of flow rate
Interpreted flows of drillhole sections:
Flow 1 (L=5 m, flow into the hole)
Flow 1 (L=5 m, flow into the bedrock)
Flow 2 (L=5 m, flow into the hole)
Interpreted fracture-specific flows:
Flow 1 (Flow into the hole)
Flow 1 (Flow into the bedrock)
Flow 3 (Flow into the hole)
Length (m)
20
21
22
23
24
25
26
27
28
29
30
31
32
33
34
35
36
37
38
39
40
10^0 10^1 10^2 10^3 10^4 10^5 10^6
Flow rate (mL/h)
10^2 10^3 10^4 10^5
Single point resistance (ohm)

Forsmark, borehole KFM24
Flow rate and single point resistance

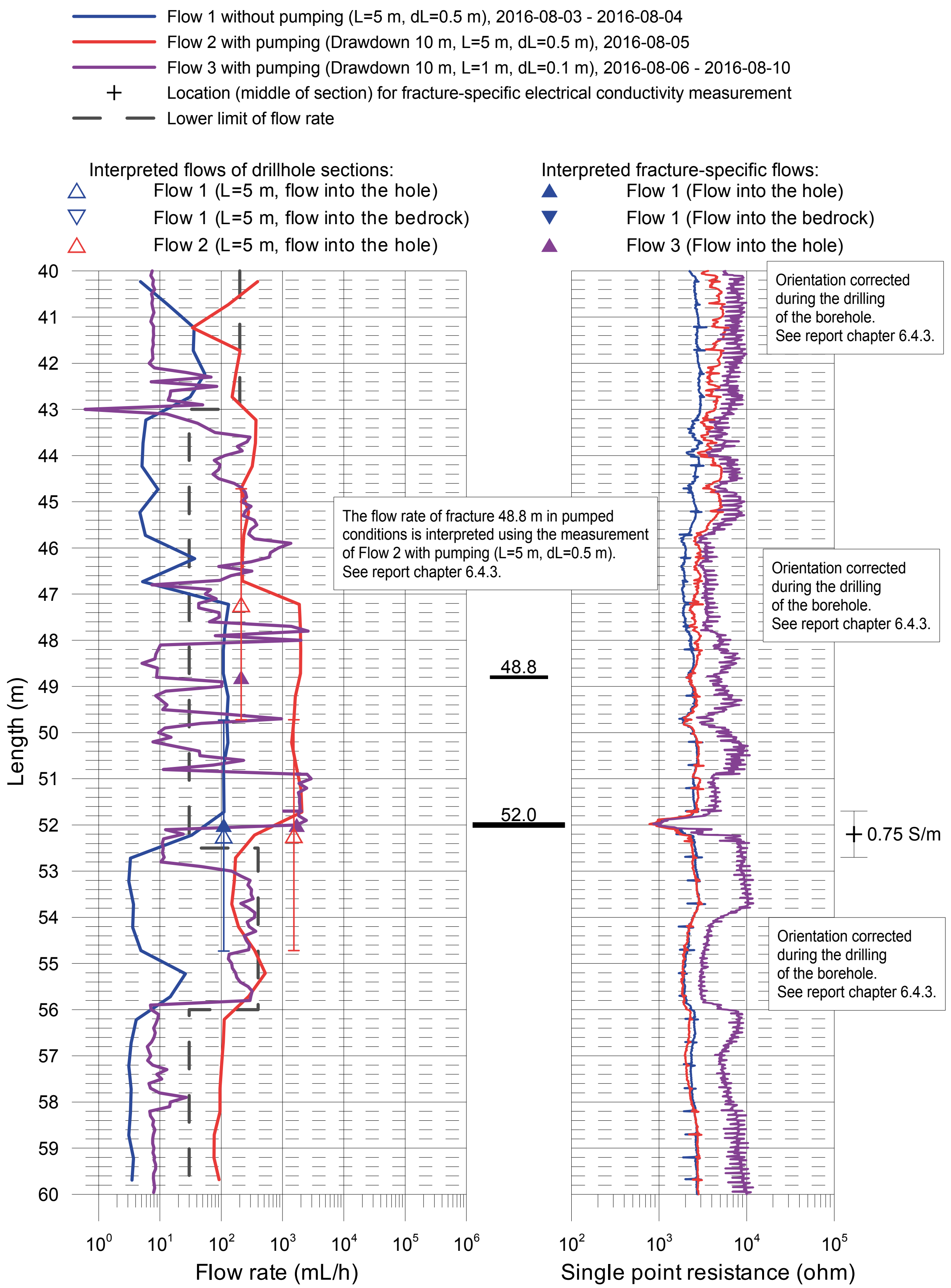

Forsmark, borehole KFM24
Flow rate and single point resistance

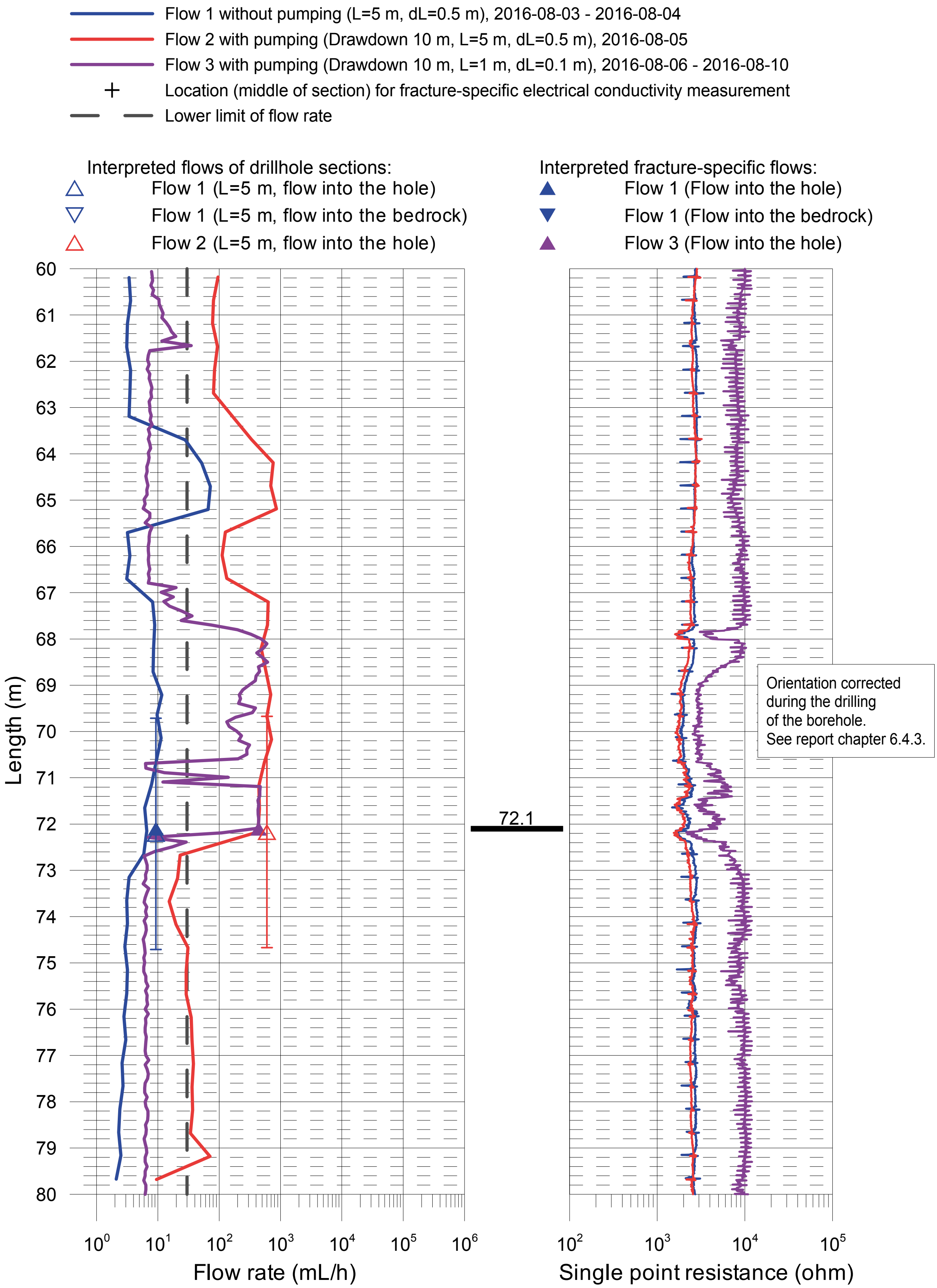

Forsmark, borehole KFM24
Flow rate and single point resistance

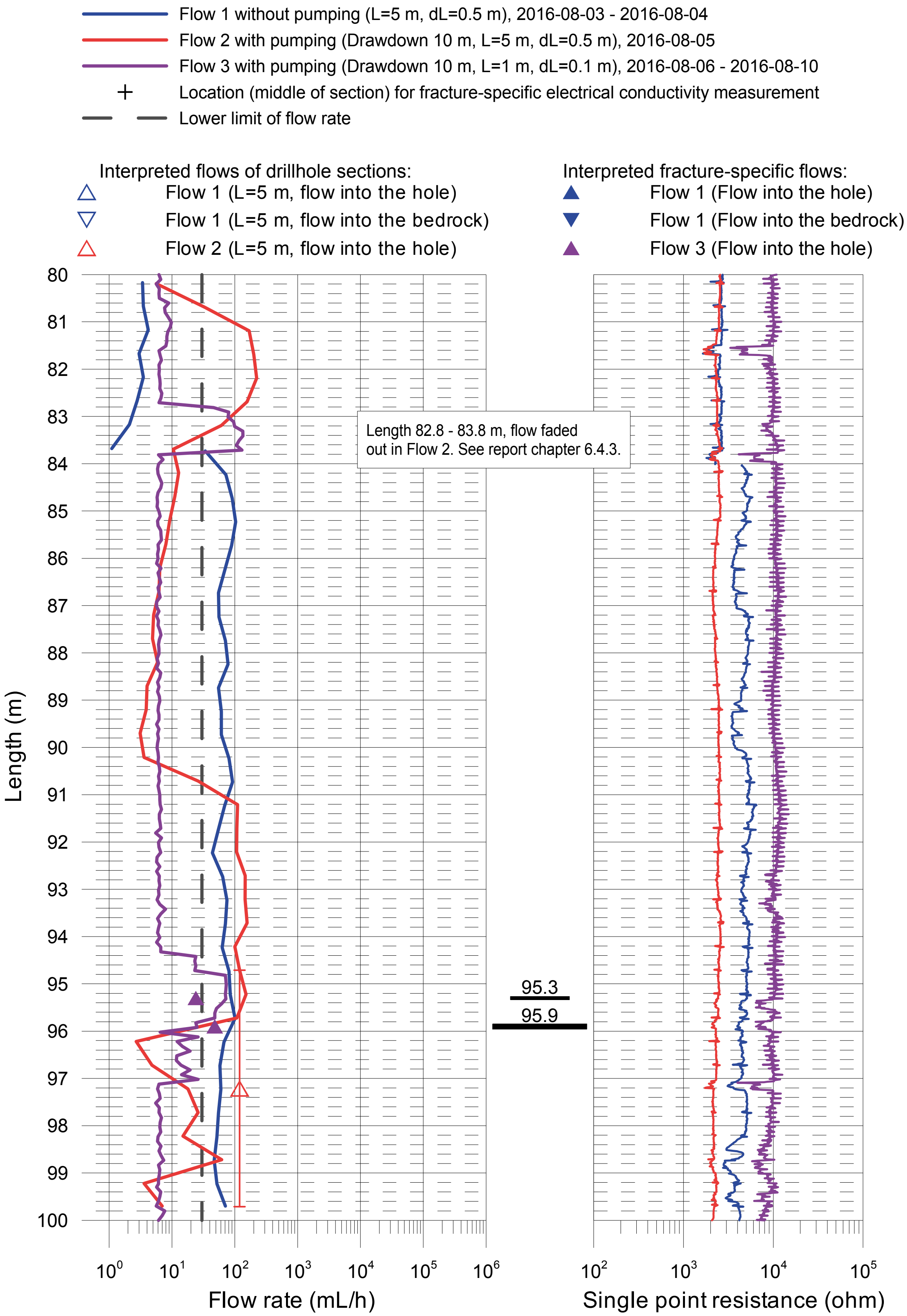

Forsmark, borehole KFM24
Flow rate and single point resistance

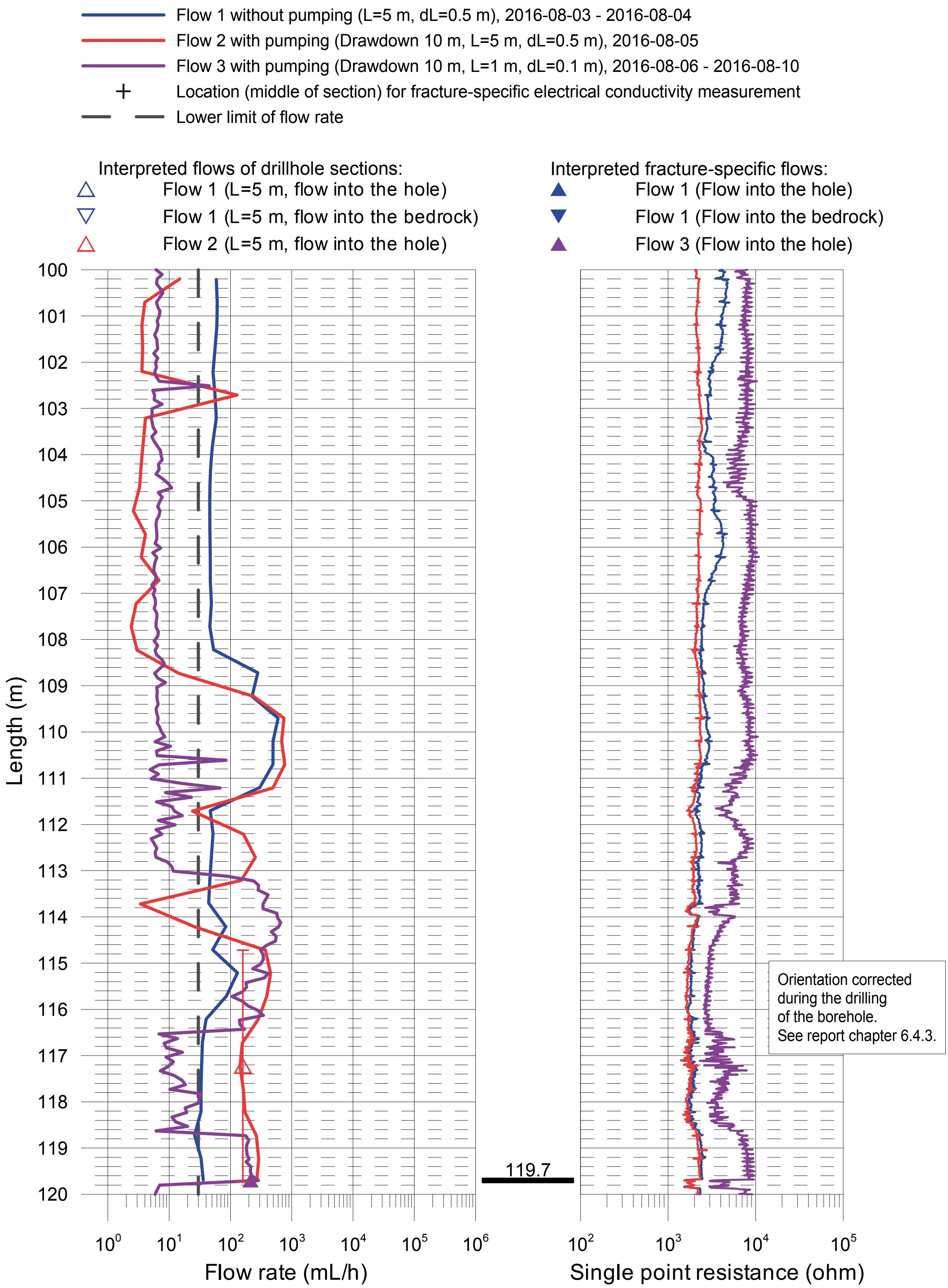

Forsmark, borehole KFM24
Flow rate and single point resistance

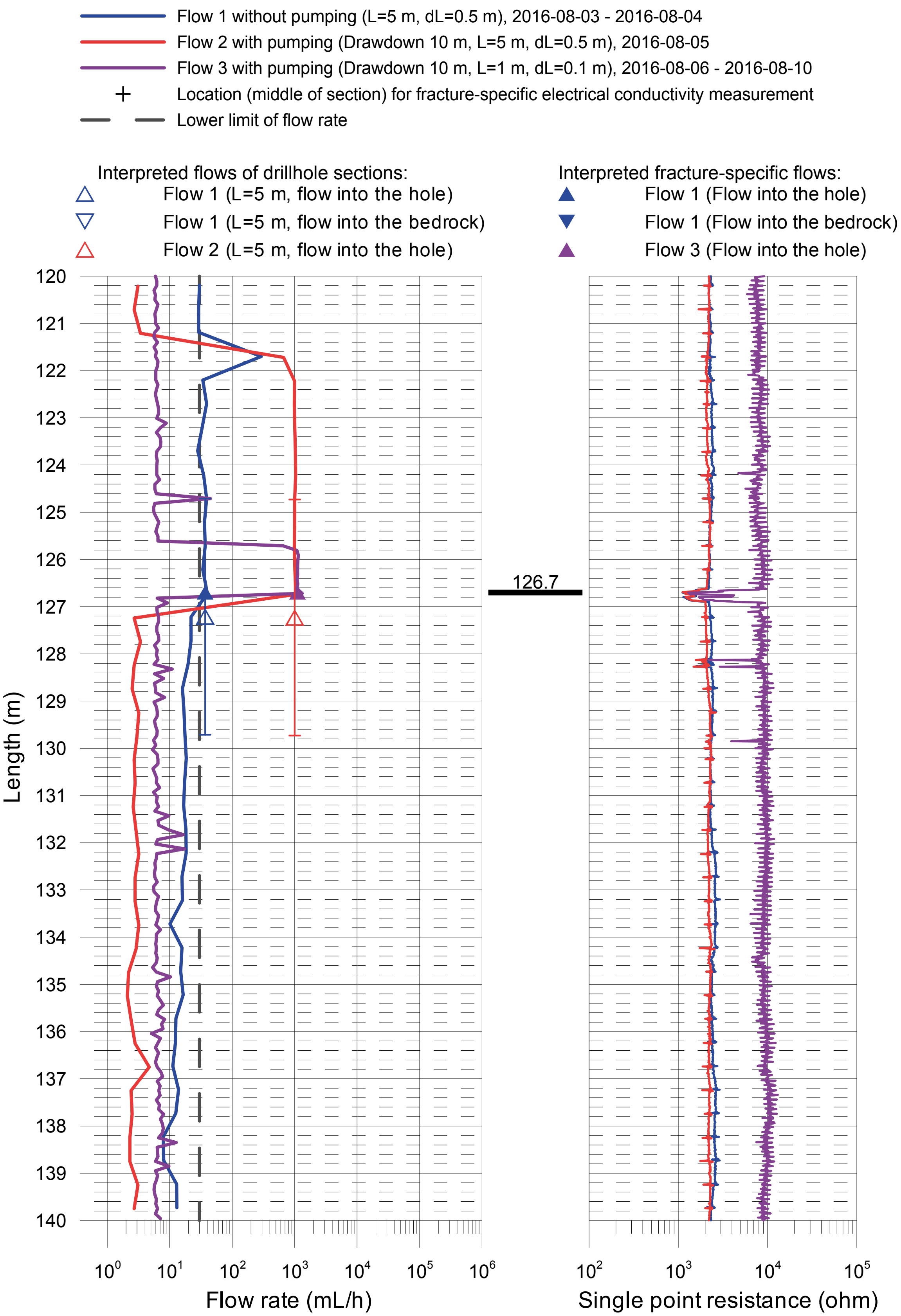

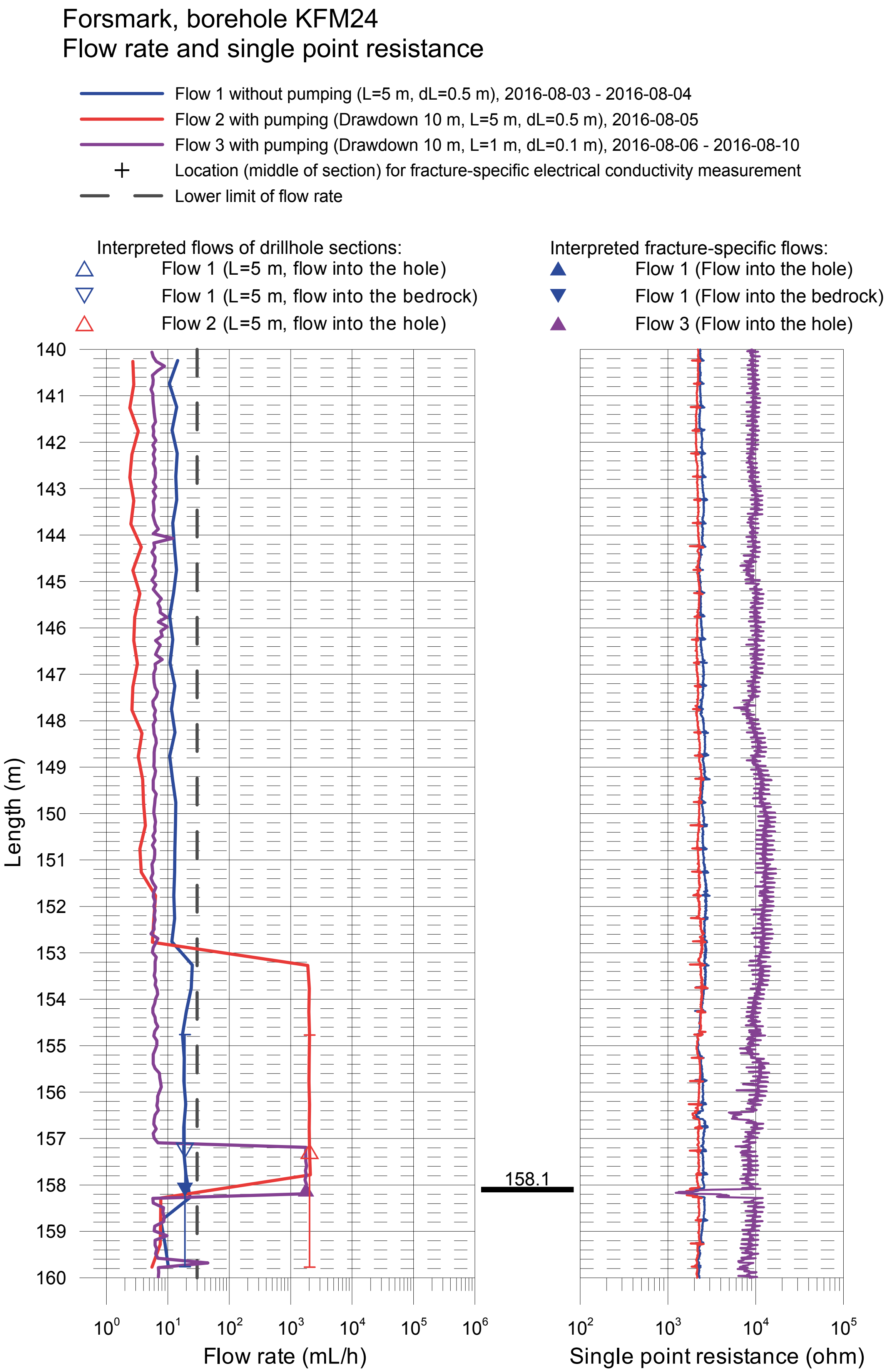
Forsmark, borehole KFM24
Flow rate and single point resistance
Flow 1 without pumping (L=5 m, dL=0.5 m), 2016-08-03 - 2016-08-04
Flow 2 with pumping (Drawdown 10 m, L=5 m, dL=0.5 m), 2016-08-05
Flow 3 with pumping (Drawdown 10 m, L=1 m, dL=0.1 m), 2016-08-06 - 2016-08-10
Location (middle of section) for fracture-specific electrical conductivity measurement
Lower limit of flow rate
Interpreted flows of drillhole sections:
Flow 1 (L=5 m, flow into the hole)
Flow 1 (L=5 m, flow into the bedrock)
Flow 2 (L=5 m, flow into the hole)
Interpreted fracture-specific flows:
Flow 1 (Flow into the hole)
Flow 1 (Flow into the bedrock)
Flow 3 (Flow into the hole)
Length (m)
140
141
142
143
144
145
146
147
148
149
150
151
152
153
154
155
156
157
158
159
160
158.1
10^0 10^1 10^2 10^3 10^4 10^5 10^6
Flow rate (mL/h)
10^2 10^3 10^4 10^5
Single point resistance (ohm)

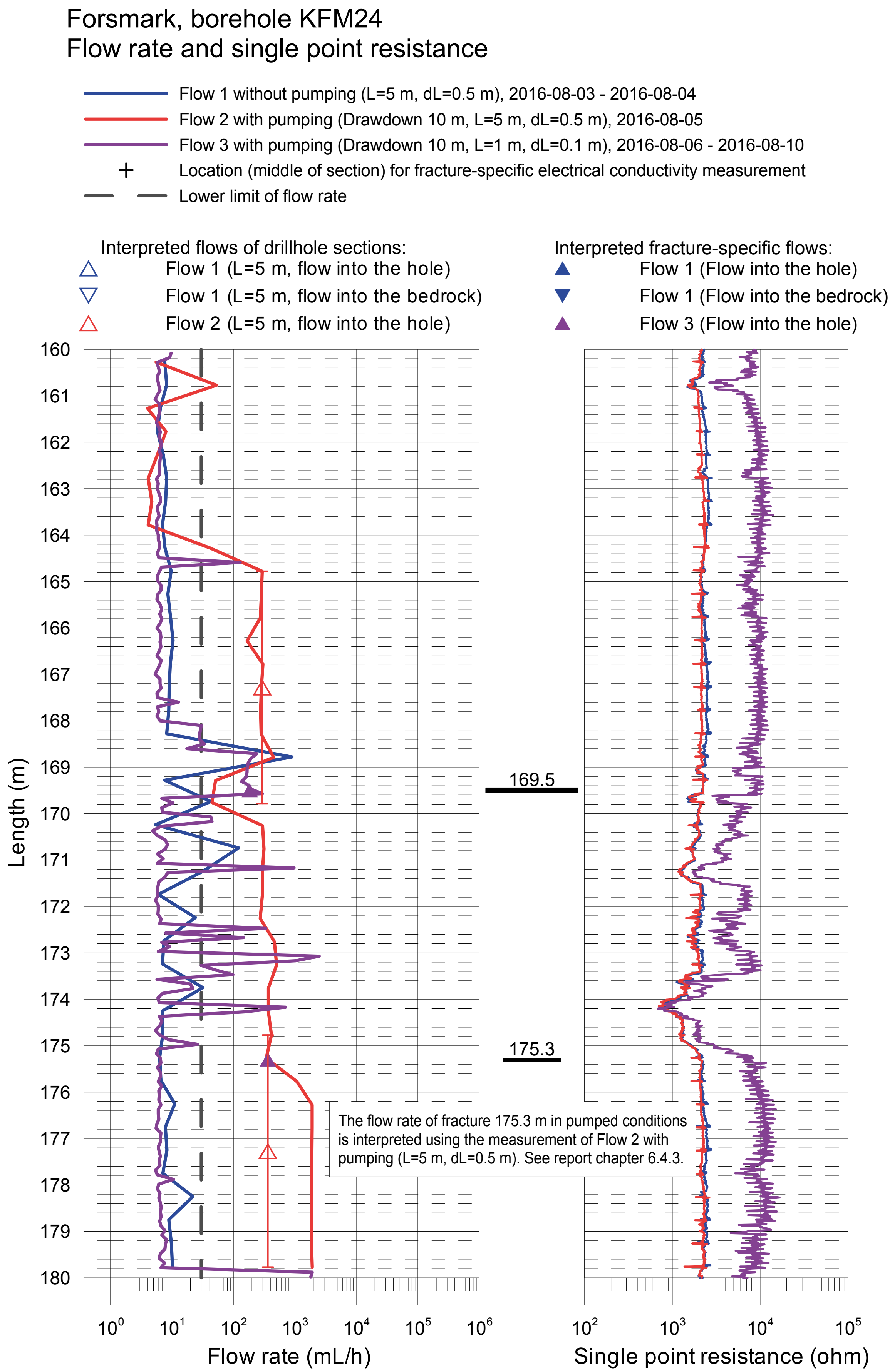
Forsmark, borehole KFM24
Flow rate and single point resistance
Flow 1 without pumping (L=5 m, dL=0.5 m), 2016-08-03 - 2016-08-04
Flow 2 with pumping (Drawdown 10 m, L=5 m, dL=0.5 m), 2016-08-05
Flow 3 with pumping (Drawdown 10 m, L=1 m, dL=0.1 m), 2016-08-06 - 2016-08-10
Location (middle of section) for fracture-specific electrical conductivity measurement
Lower limit of flow rate
Interpreted flows of drillhole sections:
Flow 1 (L=5 m, flow into the hole)
Flow 1 (L=5 m, flow into the bedrock)
Flow 2 (L=5 m, flow into the hole)
Interpreted fracture-specific flows:
Flow 1 (Flow into the hole)
Flow 1 (Flow into the bedrock)
Flow 3 (Flow into the hole)
Length (m)
169.5
175.3
The flow rate of fracture 175.3 m in pumped conditions is interpreted using the measurement of Flow 2 with pumping (L=5 m, dL=0.5 m). See report chapter 6.4.3.
Flow rate (mL/h)
Single point resistance (ohm)

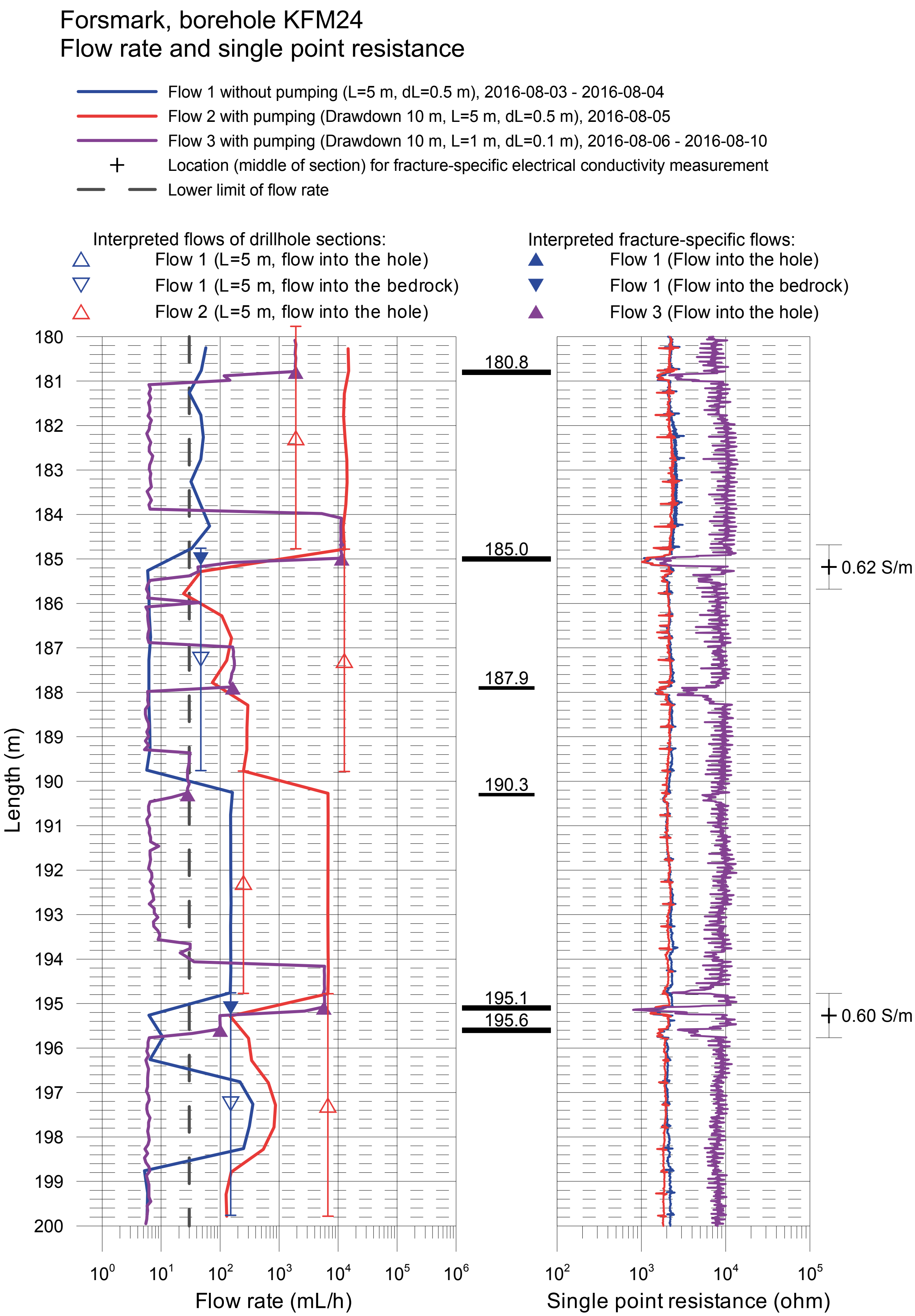

Forsmark, borehole KFM24
Flow rate and single point resistance
Flow 1 without pumping (L=5 m, dL=0.5 m), 2016-08-03 - 2016-08-04
Flow 2 with pumping (Drawdown 10 m, L=5 m, dL=0.5 m), 2016-08-05
Flow 3 with pumping (Drawdown 10 m, L=1 m, dL=0.1 m), 2016-08-06 - 2016-08-10
Location (middle of section) for fracture-specific electrical conductivity measurement
Lower limit of flow rate
Interpreted flows of drillhole sections:
Flow 1 (L=5 m, flow into the hole)
Flow 1 (L=5 m, flow into the bedrock)
Flow 2 (L=5 m, flow into the hole)
Interpreted fracture-specific flows:
Flow 1 (Flow into the hole)
Flow 1 (Flow into the bedrock)
Flow 3 (Flow into the hole)
180.8
185.0
187.9
190.3
195.1
195.6
0.62 S/m
0.60 S/m
Length (m)
Flow rate (mL/h)
Single point resistance (ohm)

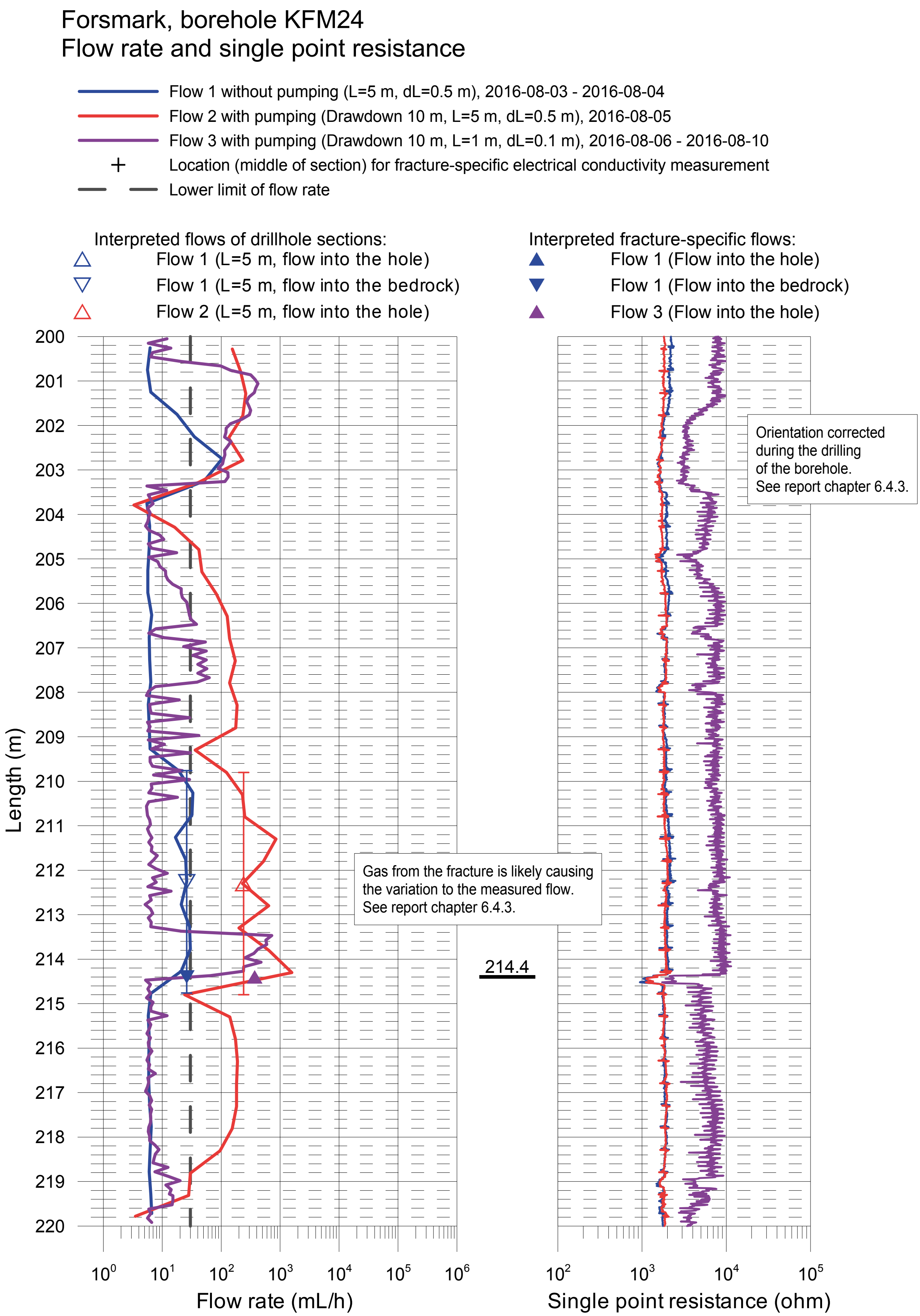
Forsmark, borehole KFM24
Flow rate and single point resistance
Flow 1 without pumping (L=5 m, dL=0.5 m), 2016-08-03 - 2016-08-04
Flow 2 with pumping (Drawdown 10 m, L=5 m, dL=0.5 m), 2016-08-05
Flow 3 with pumping (Drawdown 10 m, L=1 m, dL=0.1 m), 2016-08-06 - 2016-08-10
Location (middle of section) for fracture-specific electrical conductivity measurement
Lower limit of flow rate
Interpreted flows of drillhole sections:
Flow 1 (L=5 m, flow into the hole)
Flow 1 (L=5 m, flow into the bedrock)
Flow 2 (L=5 m, flow into the hole)
Interpreted fracture-specific flows:
Flow 1 (Flow into the hole)
Flow 1 (Flow into the bedrock)
Flow 3 (Flow into the hole)
Orientation corrected during the drilling of the borehole. See report chapter 6.4.3.
Gas from the fracture is likely causing the variation to the measured flow. See report chapter 6.4.3.
214.4
Length (m)
Flow rate (mL/h)
Single point resistance (ohm)

Forsmark, borehole KFM24
Flow rate and single point resistance

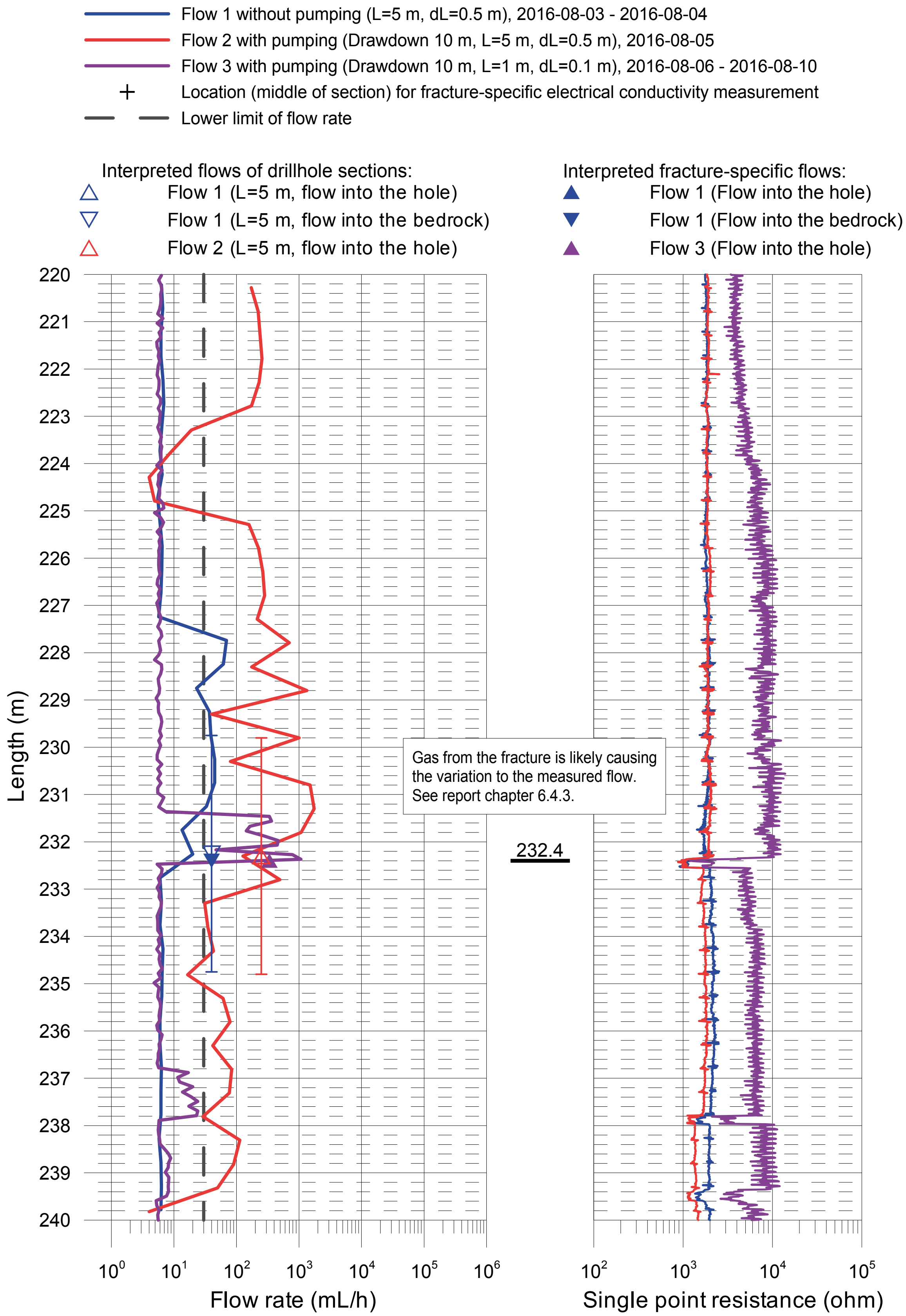

Forsmark, borehole KFM24
Flow rate and single point resistance

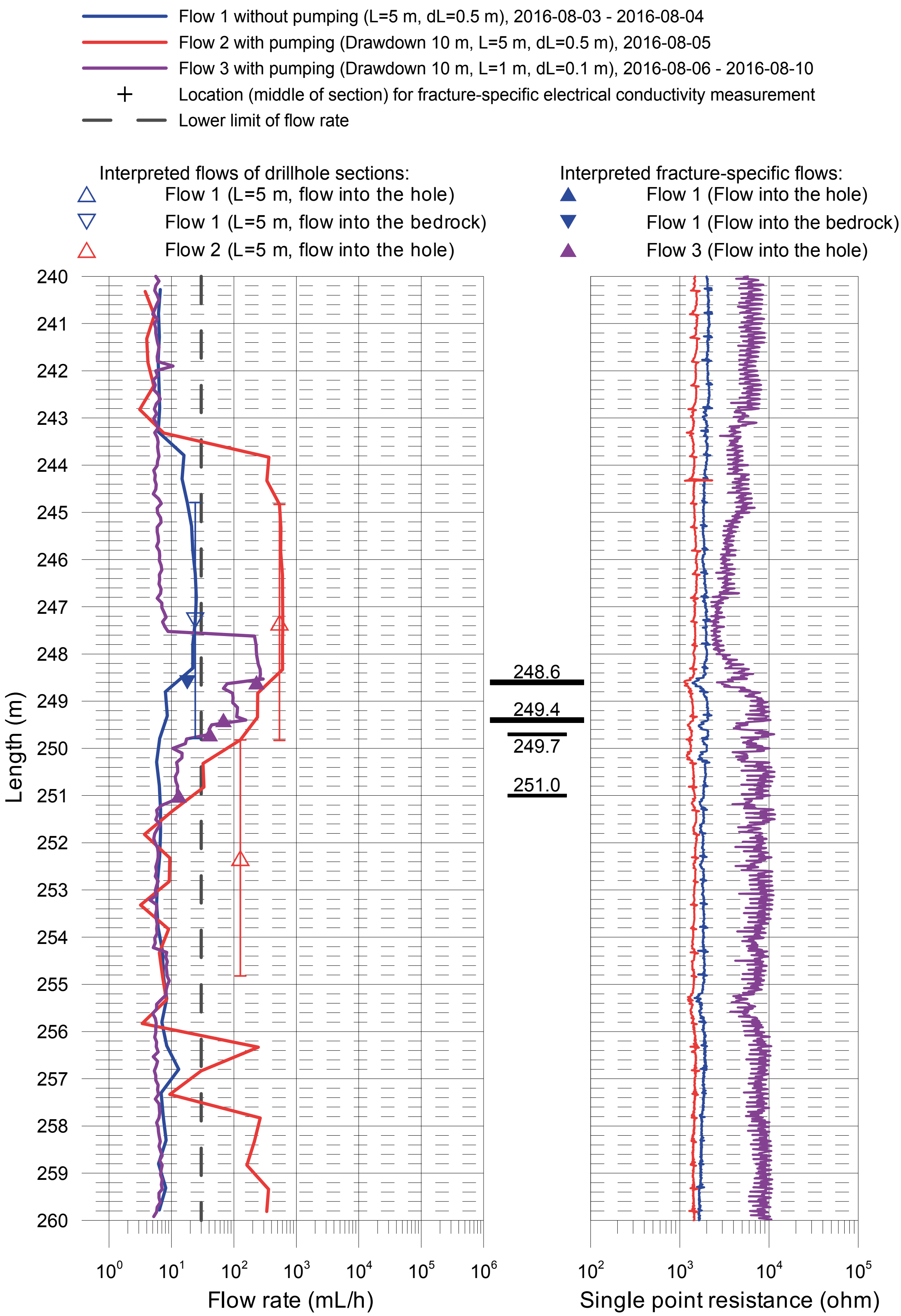

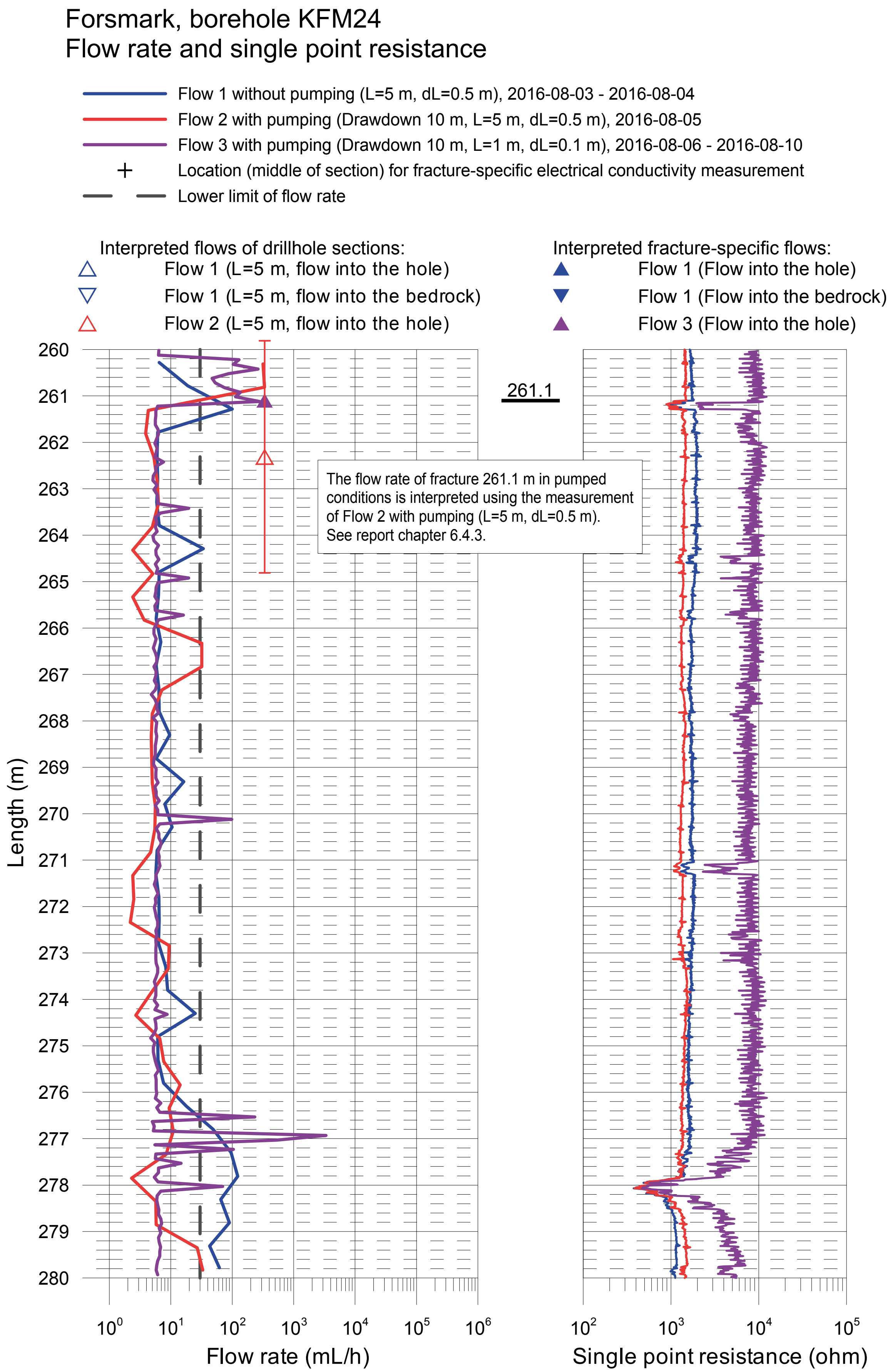
Forsmark, borehole KFM24
Flow rate and single point resistance
Flow 1 without pumping (L=5 m, dL=0.5 m), 2016-08-03 - 2016-08-04
Flow 2 with pumping (Drawdown 10 m, L=5 m, dL=0.5 m), 2016-08-05
Flow 3 with pumping (Drawdown 10 m, L=1 m, dL=0.1 m), 2016-08-06 - 2016-08-10
Location (middle of section) for fracture-specific electrical conductivity measurement
Lower limit of flow rate
Interpreted flows of drillhole sections:
Flow 1 (L=5 m, flow into the hole)
Flow 1 (L=5 m, flow into the bedrock)
Flow 2 (L=5 m, flow into the hole)
Interpreted fracture-specific flows:
Flow 1 (Flow into the hole)
Flow 1 (Flow into the bedrock)
Flow 3 (Flow into the hole)
261.1
The flow rate of fracture 261.1 m in pumped conditions is interpreted using the measurement of Flow 2 with pumping (L=5 m, dL=0.5 m). See report chapter 6.4.3.
Length (m)
Flow rate (mL/h)
Single point resistance (ohm)

Forsmark, borehole KFM24
Flow rate and single point resistance

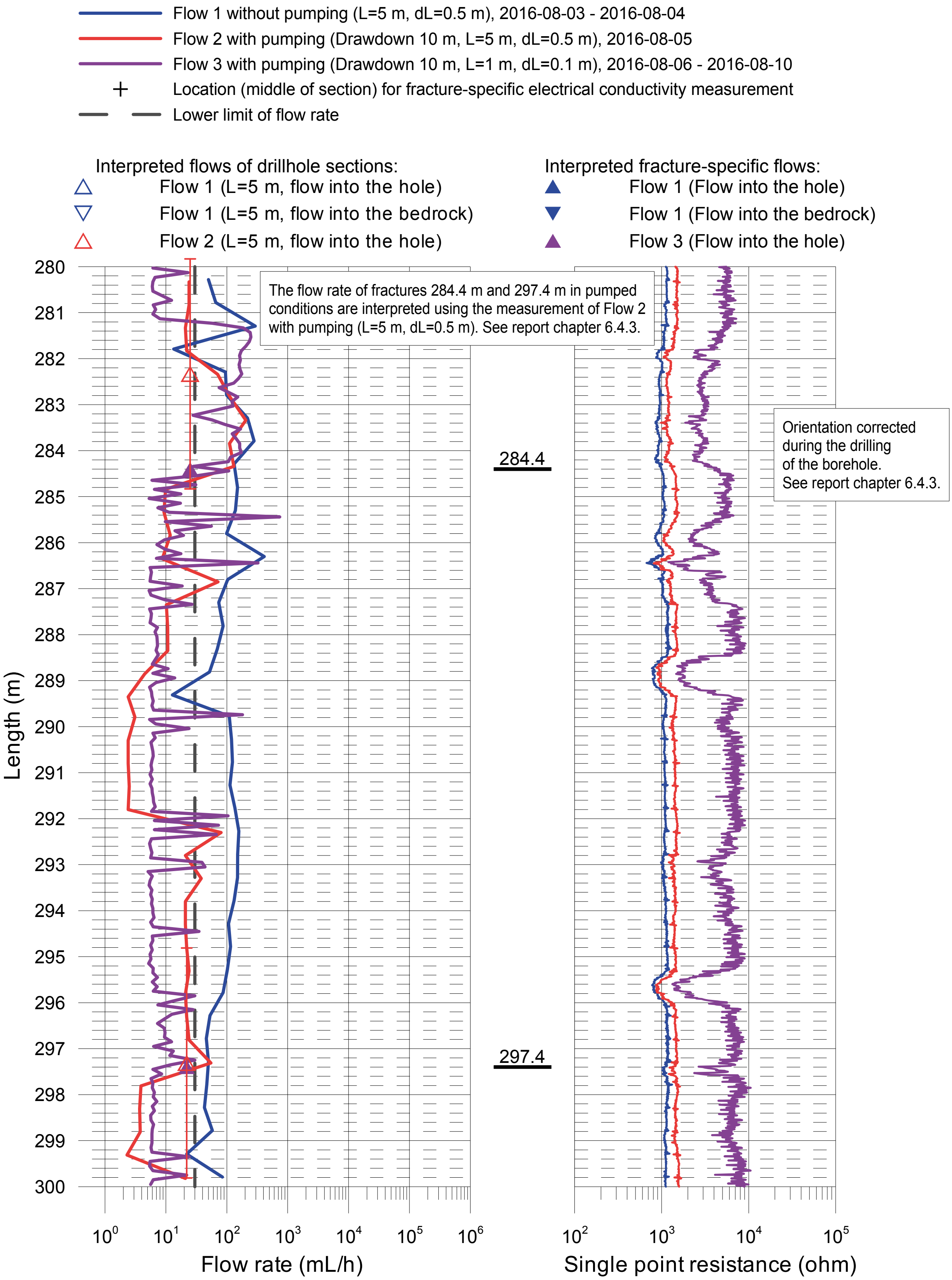

Forsmark, borehole KFM24
Flow rate and single point resistance

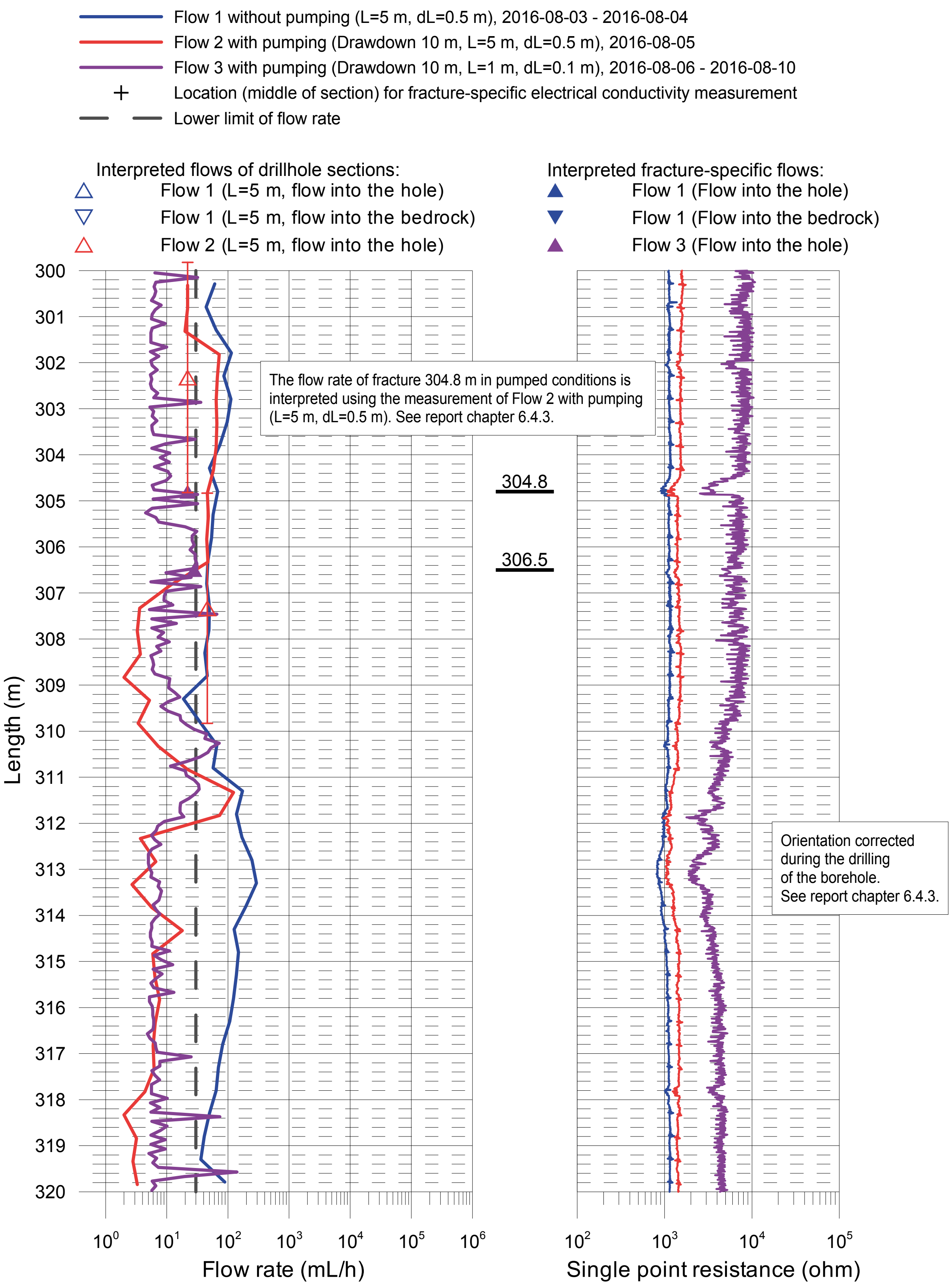

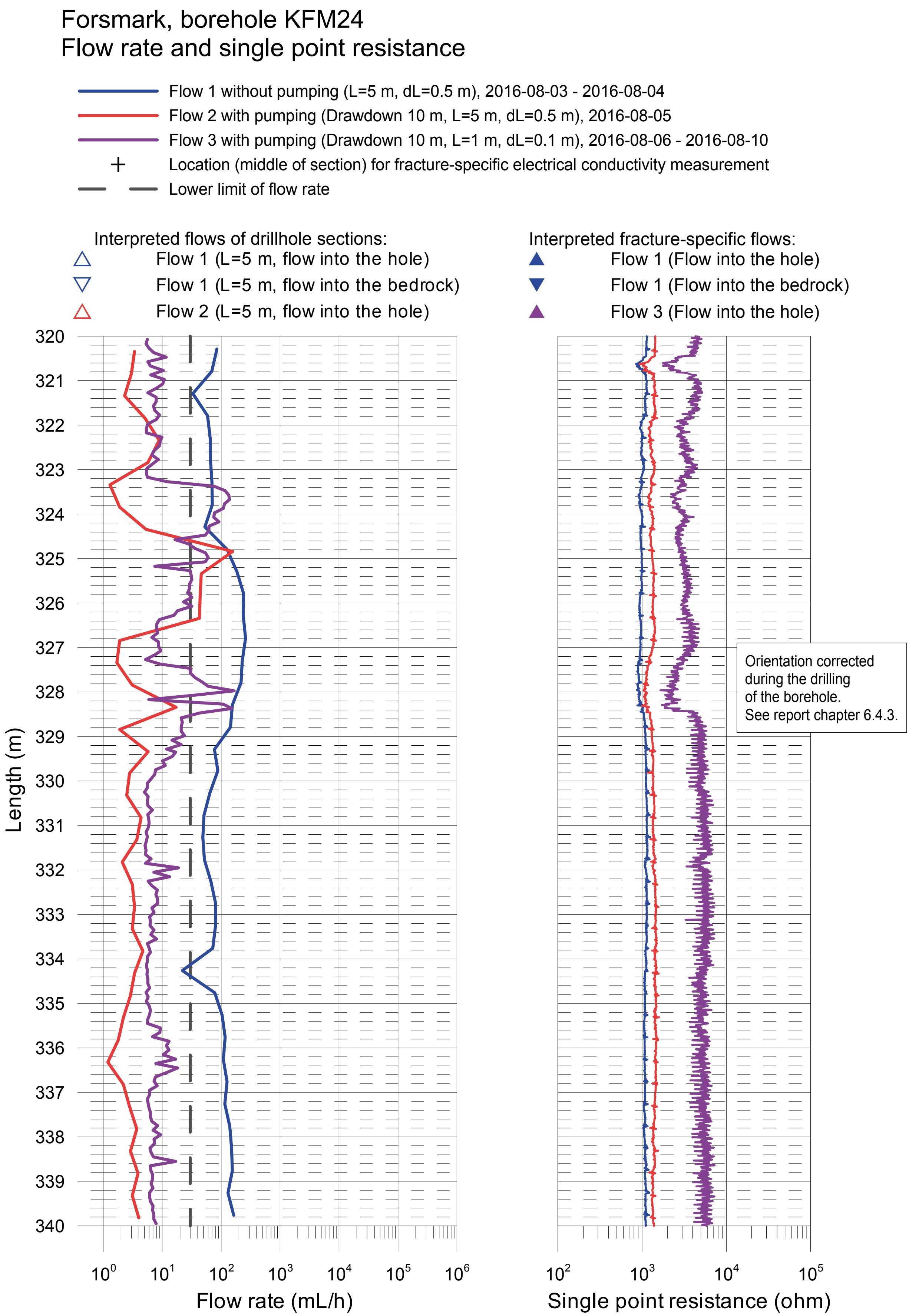
Forsmark, borehole KFM24
Flow rate and single point resistance
Flow 1 without pumping (L=5 m, dL=0.5 m), 2016-08-03 - 2016-08-04
Flow 2 with pumping (Drawdown 10 m, L=5 m, dL=0.5 m), 2016-08-05
Flow 3 with pumping (Drawdown 10 m, L=1 m, dL=0.1 m), 2016-08-06 - 2016-08-10
Location (middle of section) for fracture-specific electrical conductivity measurement
Lower limit of flow rate
Interpreted flows of drillhole sections:
Flow 1 (L=5 m, flow into the hole)
Flow 1 (L=5 m, flow into the bedrock)
Flow 2 (L=5 m, flow into the hole)
Interpreted fracture-specific flows:
Flow 1 (Flow into the hole)
Flow 1 (Flow into the bedrock)
Flow 3 (Flow into the hole)
Length (m)
320
321
322
323
324
325
326
327
328
329
330
331
332
333
334
335
336
337
338
339
340
10^0 10^1 10^2 10^3 10^4 10^5 10^6
Flow rate (mL/h)
10^2 10^3 10^4 10^5
Single point resistance (ohm)
Orientation corrected during the drilling of the borehole. See report chapter 6.4.3.

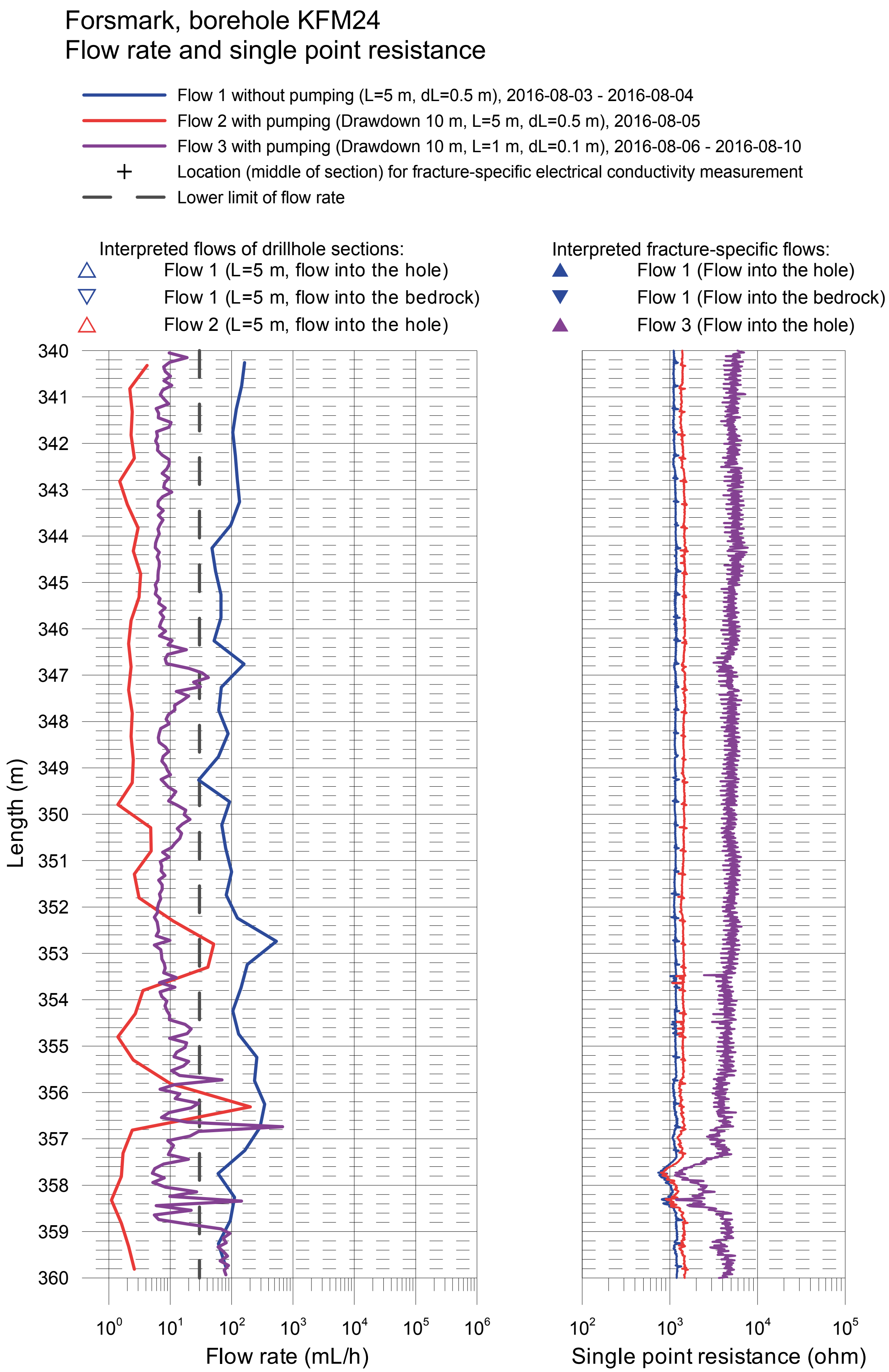

Forsmark, borehole KFM24
Flow rate and single point resistance
Flow 1 without pumping (L=5 m, dL=0.5 m), 2016-08-03 - 2016-08-04
Flow 2 with pumping (Drawdown 10 m, L=5 m, dL=0.5 m), 2016-08-05
Flow 3 with pumping (Drawdown 10 m, L=1 m, dL=0.1 m), 2016-08-06 - 2016-08-10
Location (middle of section) for fracture-specific electrical conductivity measurement
Lower limit of flow rate
Interpreted flows of drillhole sections:
Flow 1 (L=5 m, flow into the hole)
Flow 1 (L=5 m, flow into the bedrock)
Flow 2 (L=5 m, flow into the hole)
Interpreted fracture-specific flows:
Flow 1 (Flow into the hole)
Flow 1 (Flow into the bedrock)
Flow 3 (Flow into the hole)
Length (m)
340
341
342
343
344
345
346
347
348
349
350
351
352
353
354
355
356
357
358
359
360
10^0
10^1
10^2
10^3
10^4
10^5
10^6
Flow rate (mL/h)
10^2
10^3
10^4
10^5
Single point resistance (ohm)

Forsmark, borehole KFM24
Flow rate and single point resistance

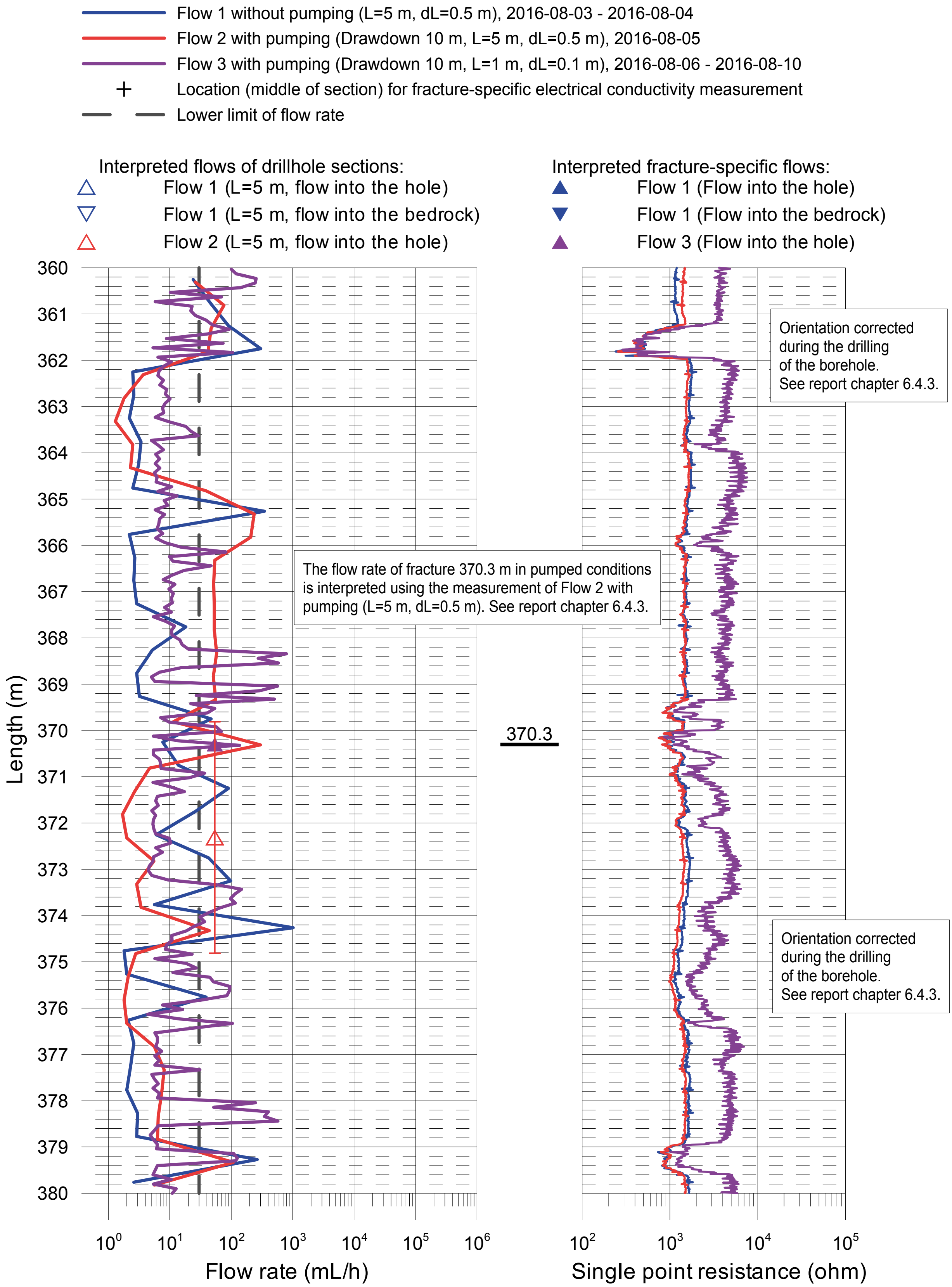

Forsmark, borehole KFM24
Flow rate and single point resistance

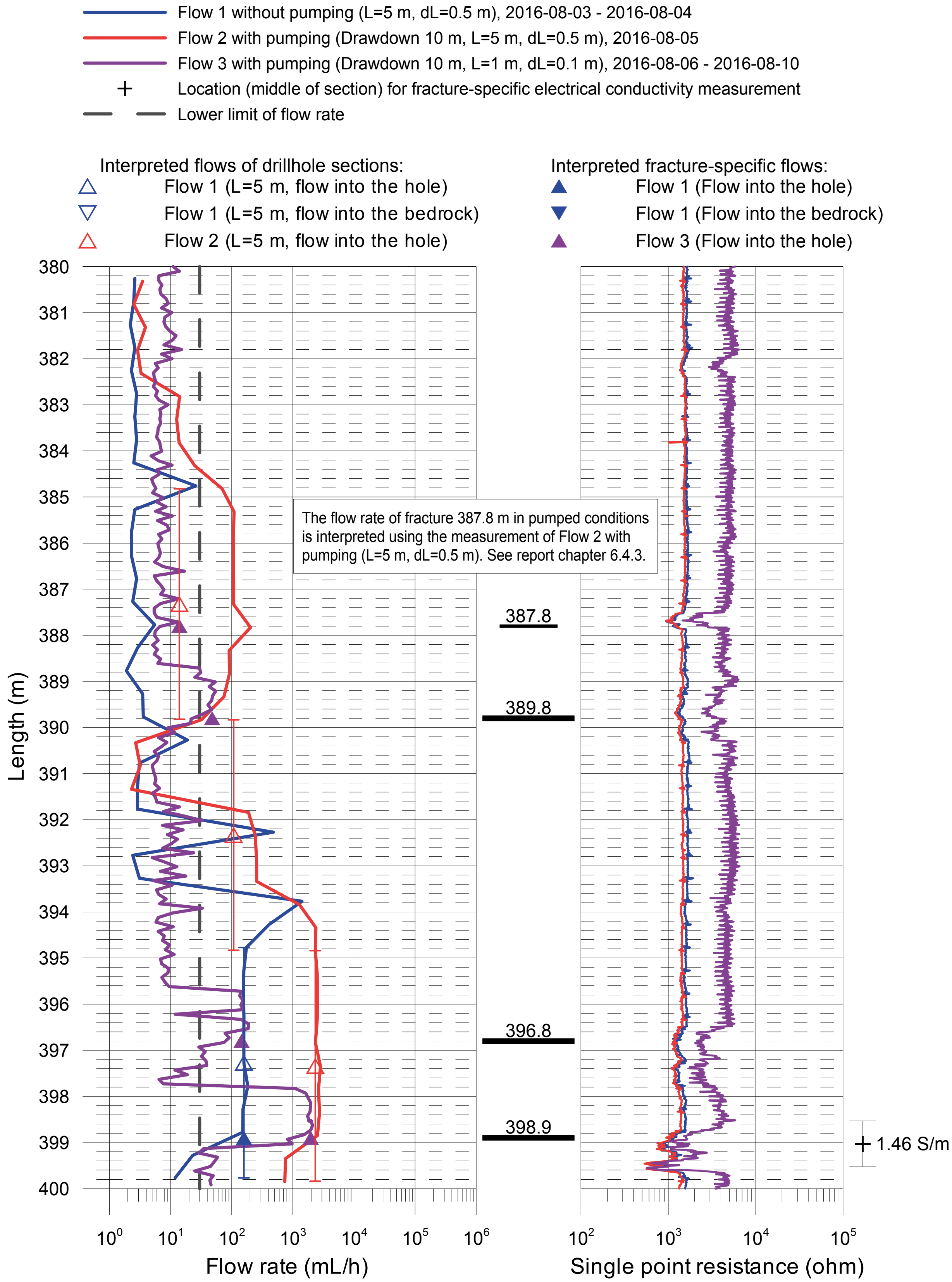

Forsmark, borehole KFM24
Flow rate and single point resistance

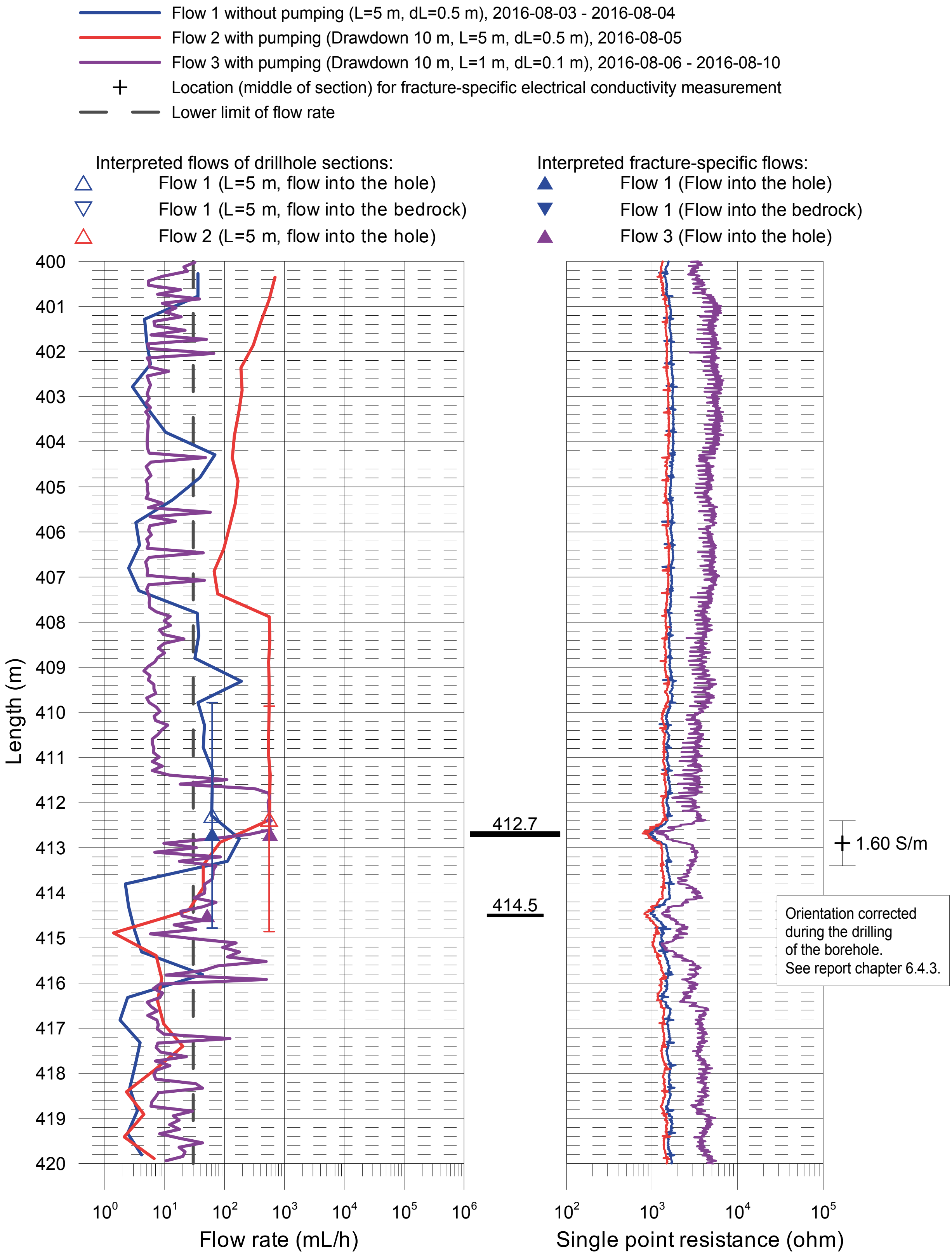

Forsmark, borehole KFM24
Flow rate and single point resistance

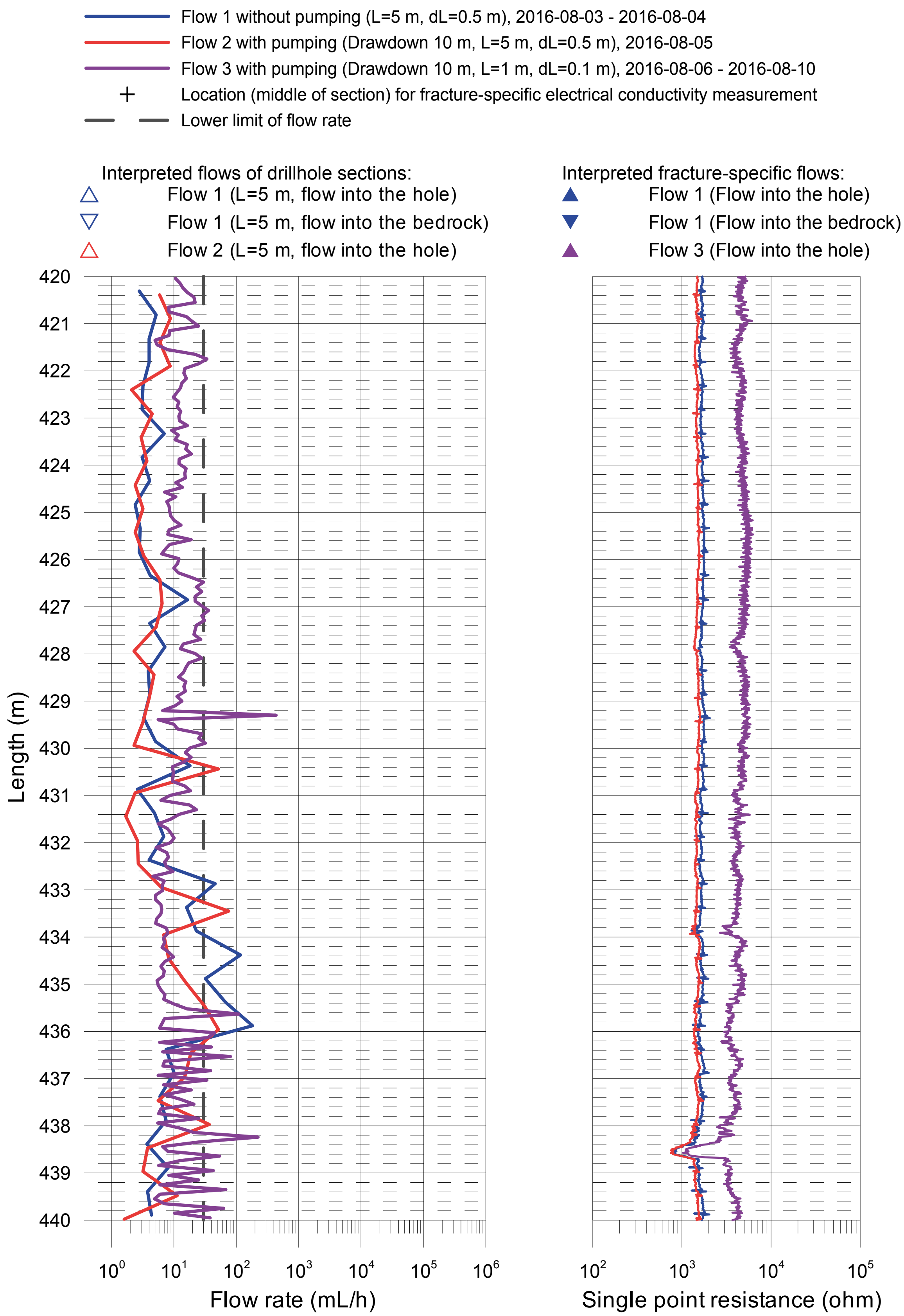

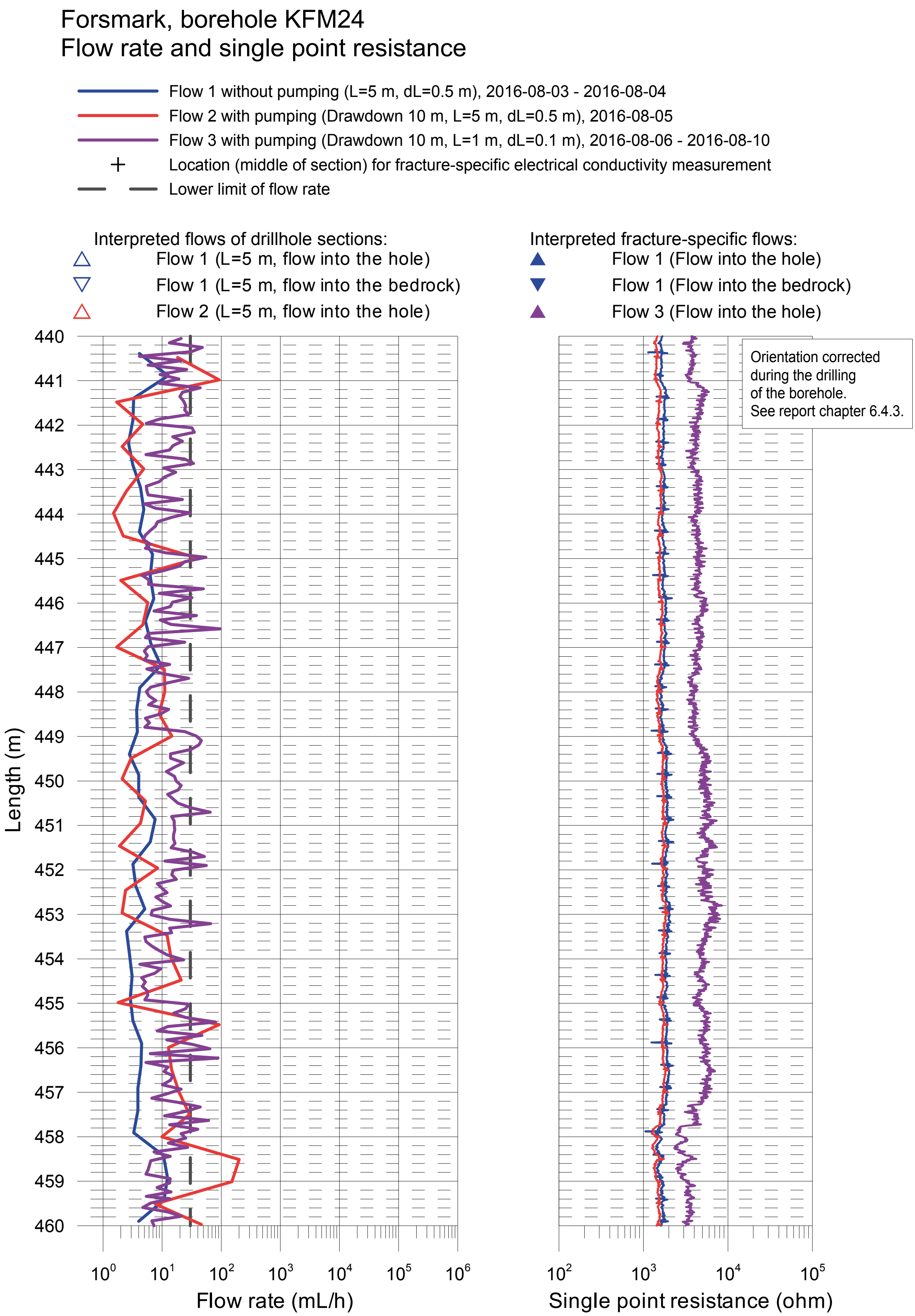
Forsmark, borehole KFM24
Flow rate and single point resistance
Flow 1 without pumping (L=5 m, dL=0.5 m), 2016-08-03 - 2016-08-04
Flow 2 with pumping (Drawdown 10 m, L=5 m, dL=0.5 m), 2016-08-05
Flow 3 with pumping (Drawdown 10 m, L=1 m, dL=0.1 m), 2016-08-06 - 2016-08-10
Location (middle of section) for fracture-specific electrical conductivity measurement
Lower limit of flow rate
Interpreted flows of drillhole sections:
Flow 1 (L=5 m, flow into the hole)
Flow 1 (L=5 m, flow into the bedrock)
Flow 2 (L=5 m, flow into the hole)
Interpreted fracture-specific flows:
Flow 1 (Flow into the hole)
Flow 1 (Flow into the bedrock)
Flow 3 (Flow into the hole)
Orientation corrected
during the drilling
of the borehole.
See report chapter 6.4.3.
Length (m)
440
441
442
443
444
445
446
447
448
449
450
451
452
453
454
455
456
457
458
459
460
10^0 10^1 10^2 10^3 10^4 10^5 10^6
Flow rate (mL/h)
10^2 10^3 10^4 10^5
Single point resistance (ohm)

Forsmark, borehole KFM24
Flow rate and single point resistance

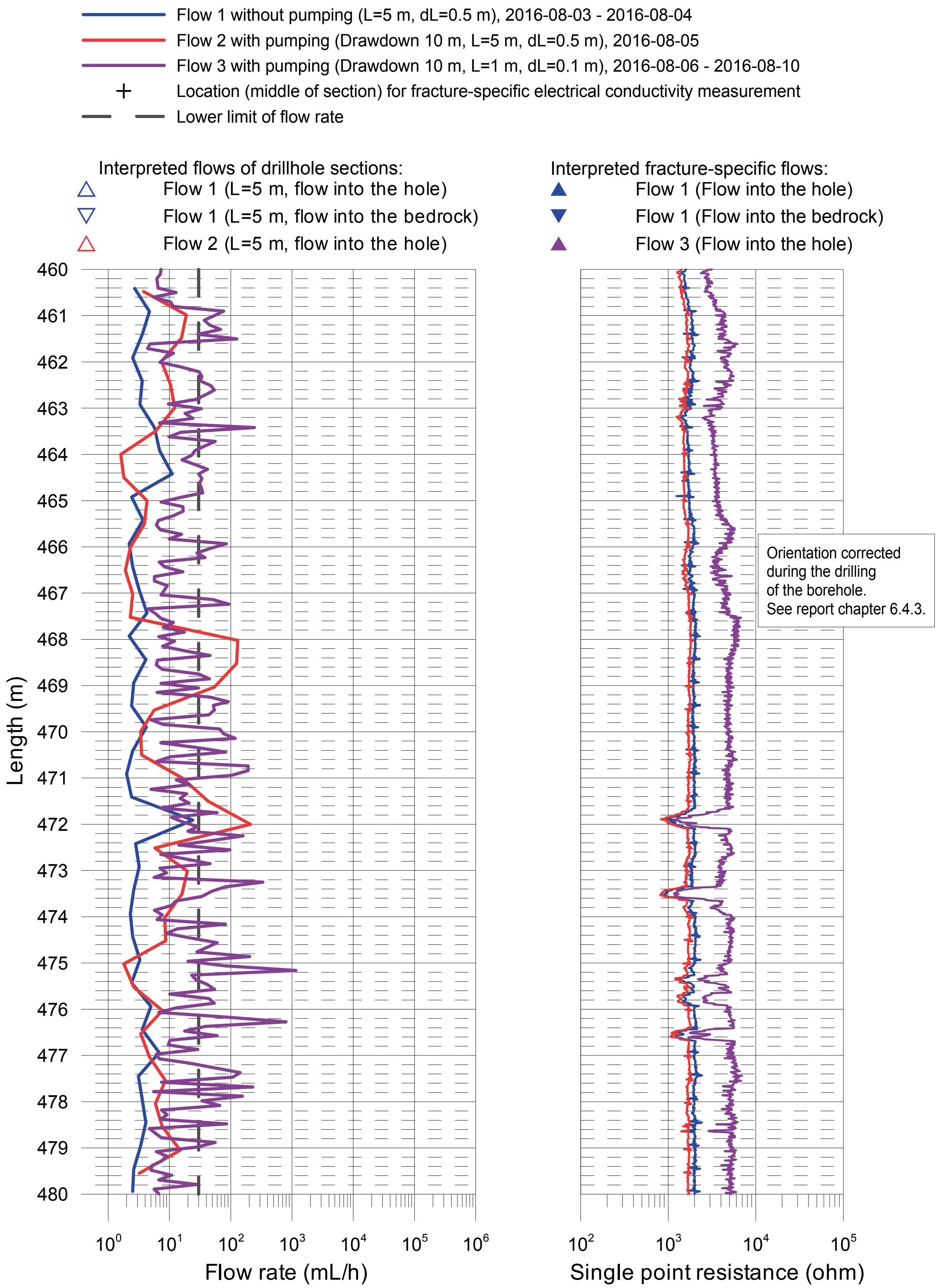

Forsmark, borehole KFM24
Flow rate and single point resistance

Flow 1 without pumping (L=5 m, dL=0.5 m), 2016-08-03 - 2016-08-04
Flow 2 with pumping (Drawdown 10 m, L=5 m, dL=0.5 m), 2016-08-05
Flow 3 with pumping (Drawdown 10 m, L=1 m, dL=0.1 m), 2016-08-06 - 2016-08-10
+ Location (middle of section) for fracture-specific electrical conductivity measurement
Lower limit of flow rate

Interpreted flows of drillhole sections:
△ Flow 1 (L=5 m, flow into the hole)
▽ Flow 1 (L=5 m, flow into the bedrock)
△ Flow 2 (L=5 m, flow into the hole)

Interpreted fracture-specific flows:
▲ Flow 1 (Flow into the hole)
▼ Flow 1 (Flow into the bedrock)
▲ Flow 3 (Flow into the hole)

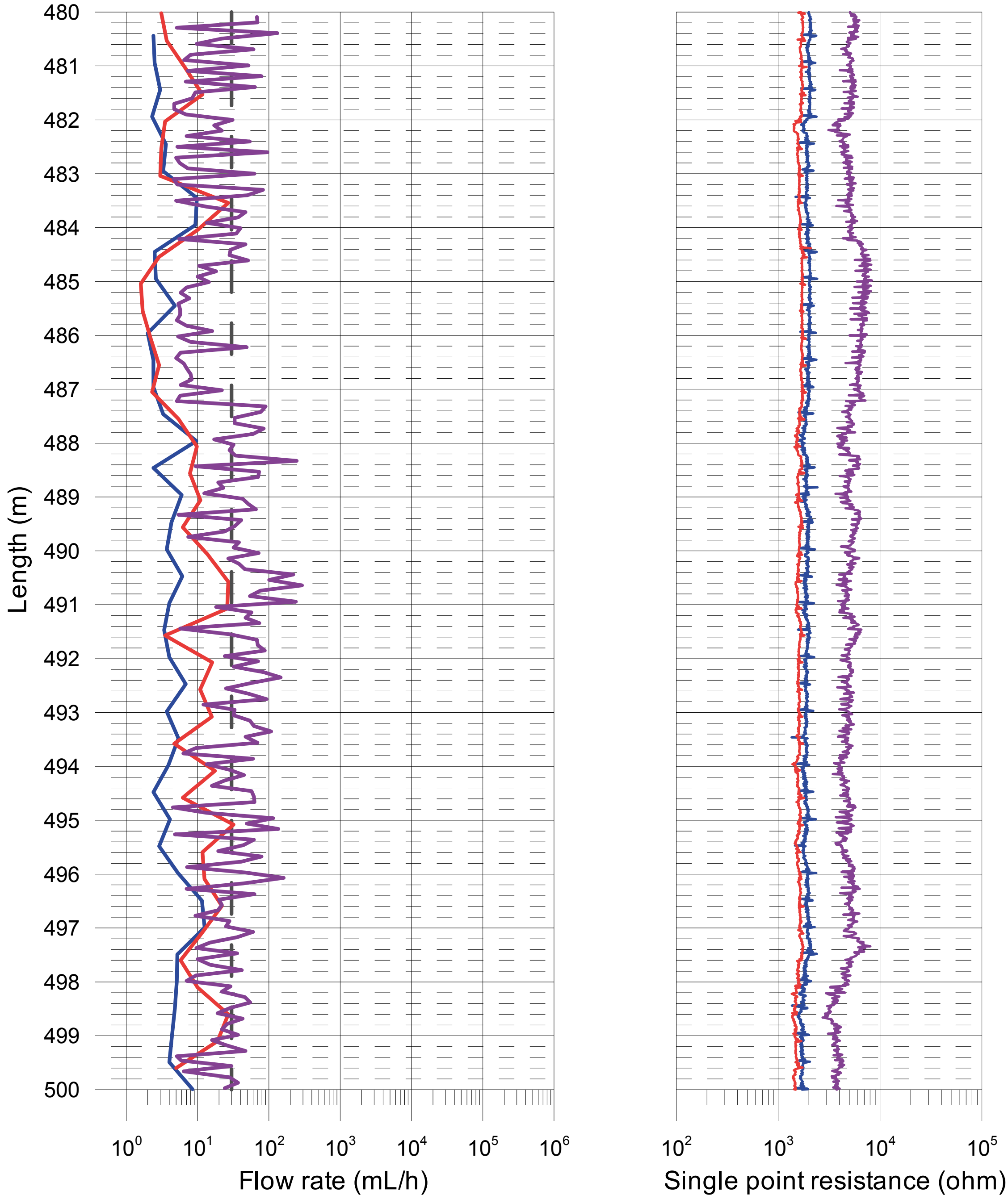

Forsmark, borehole KFM24
Flow rate and single point resistance

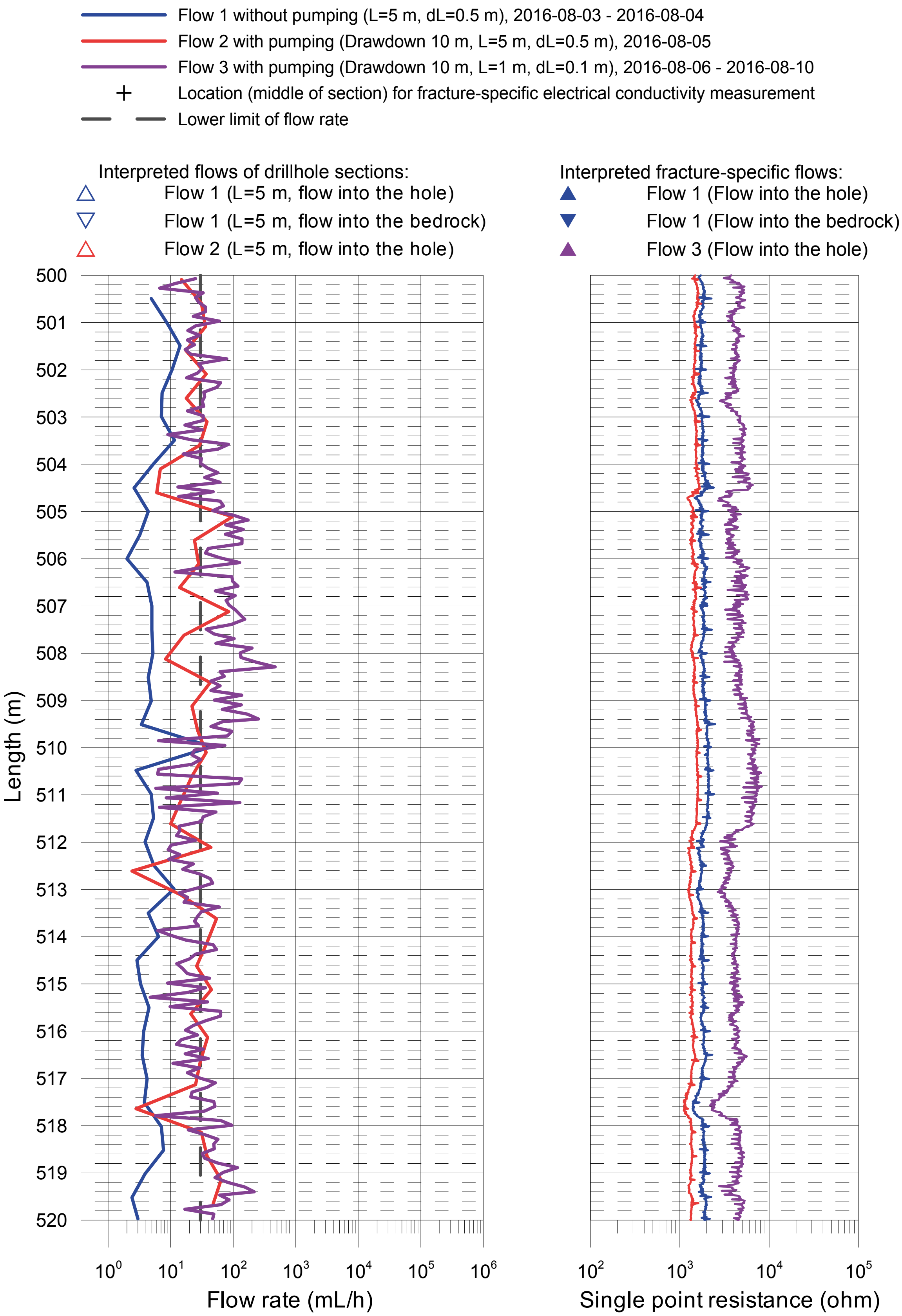

Forsmark, borehole KFM24
Flow rate and single point resistance

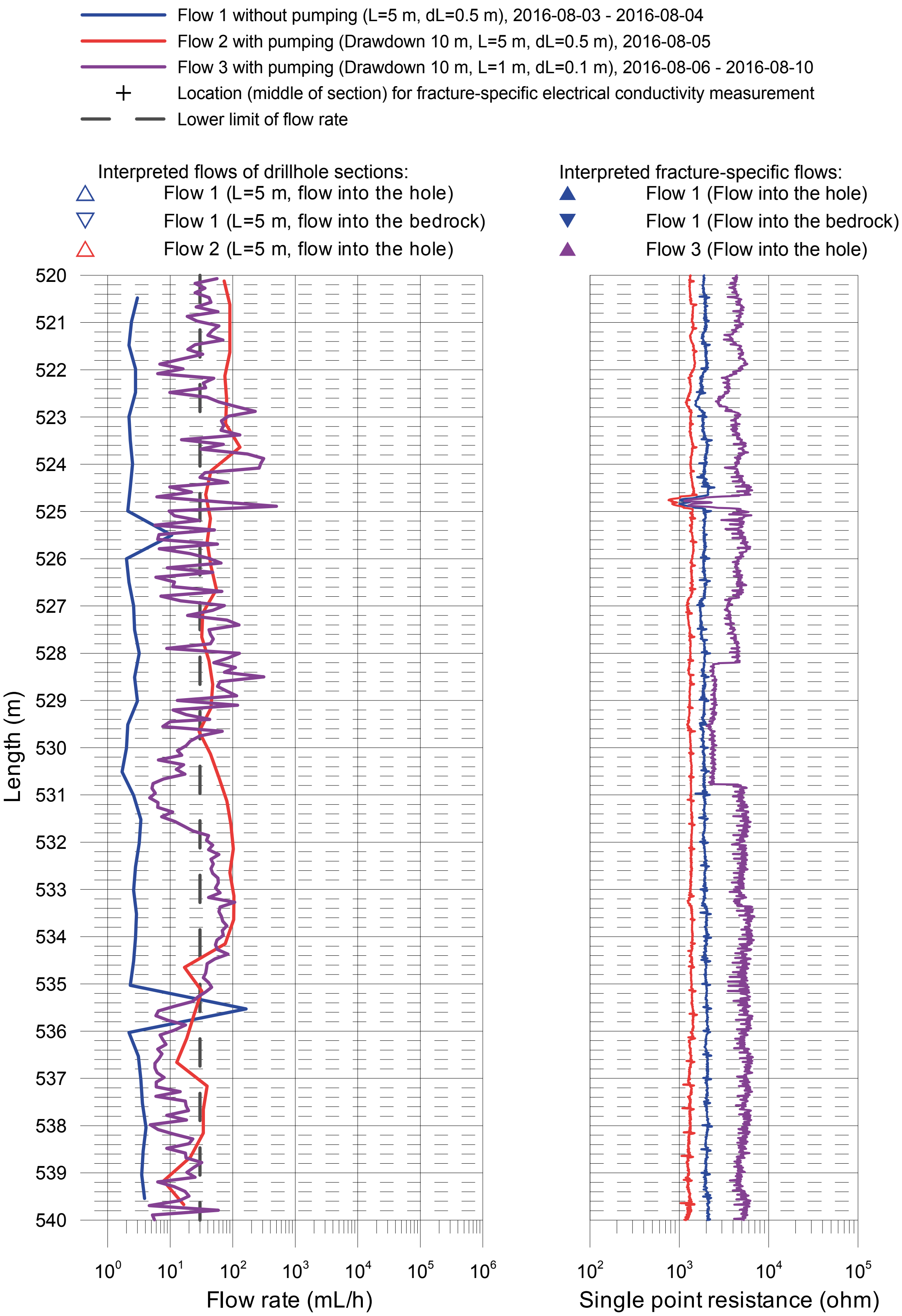

Forsmark, borehole KFM24
Flow rate and single point resistance

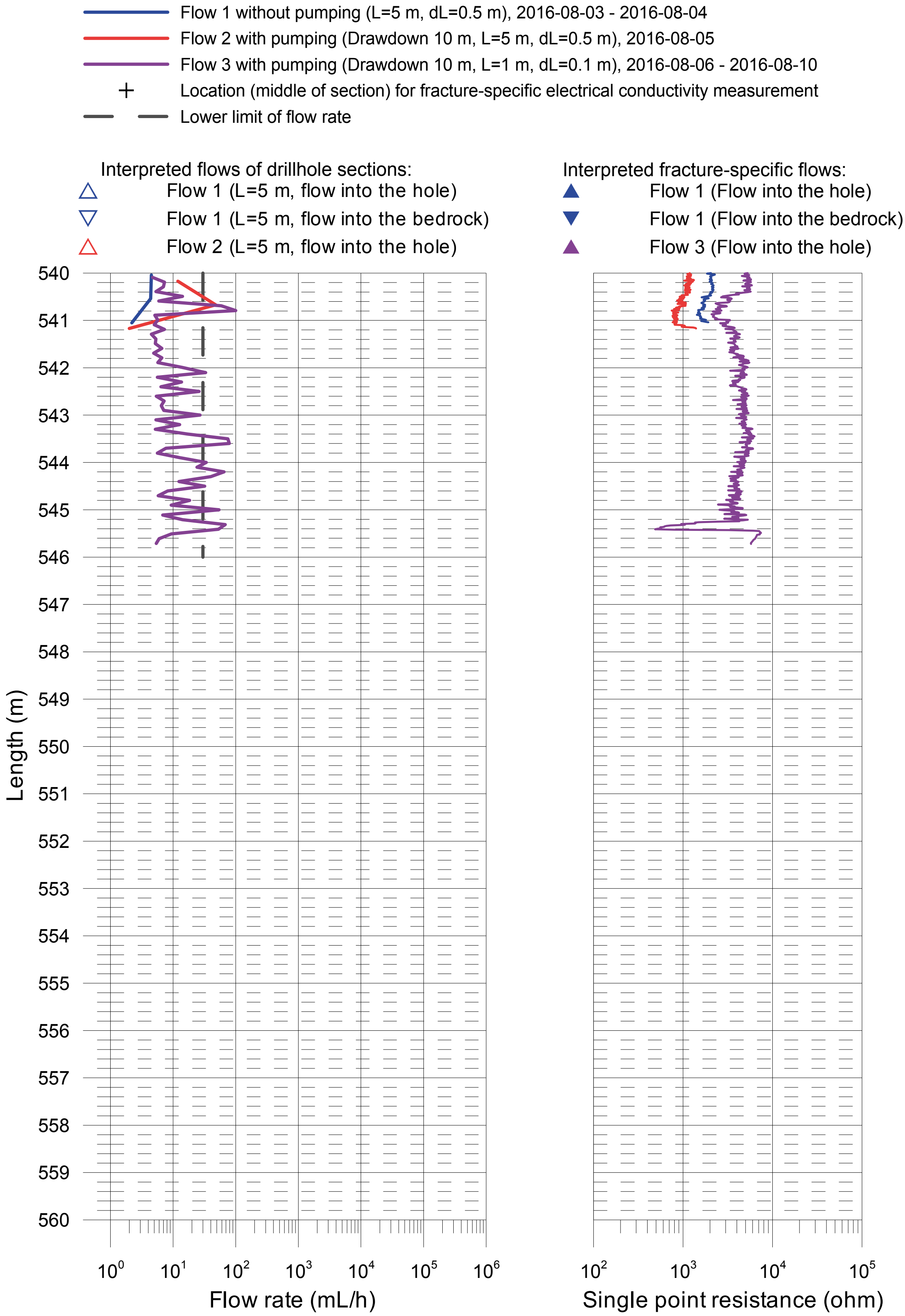

Forsmark, borehole KFM24
Vertical flow along the borehole at the length of 37.54 m

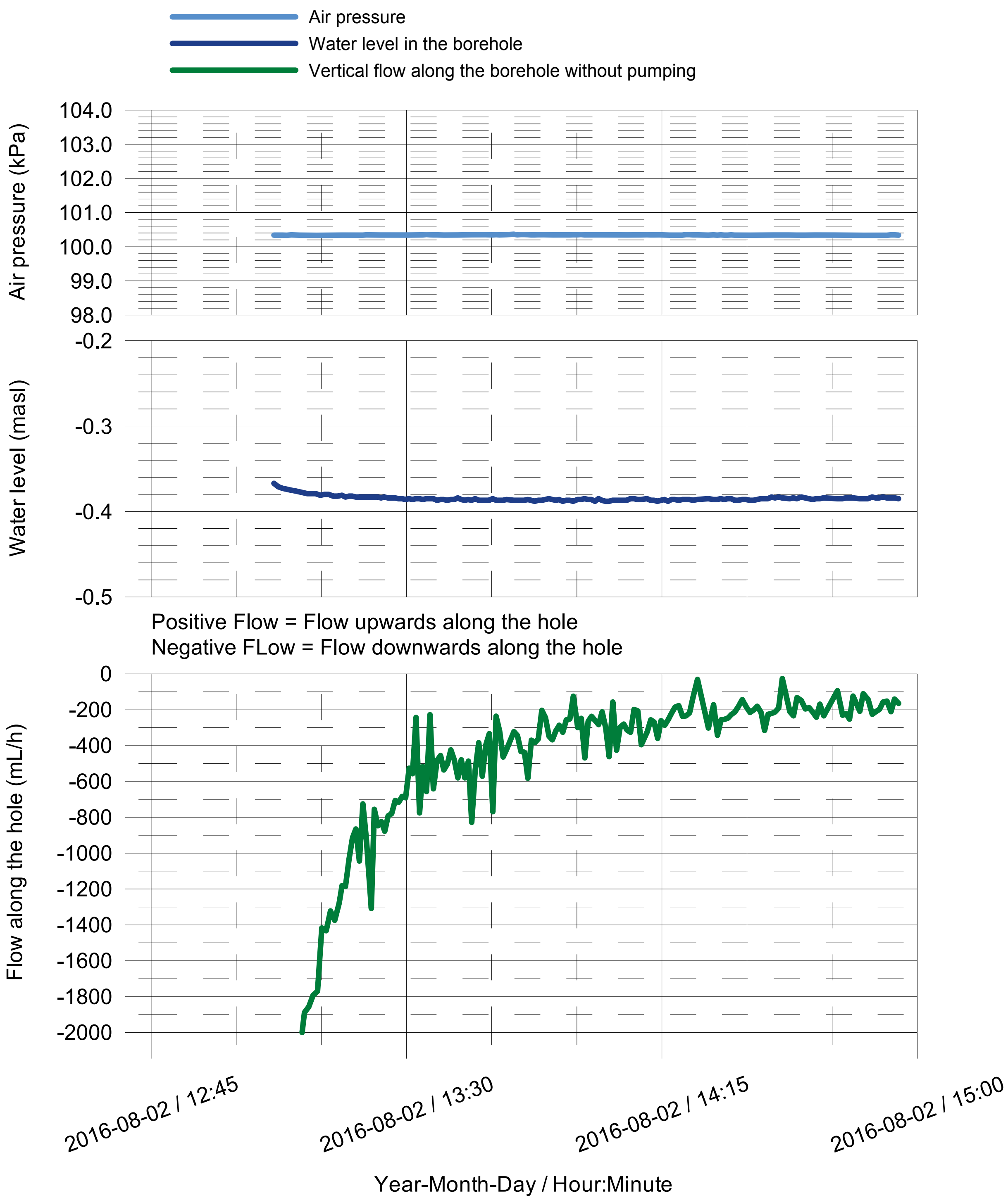

Header	Unit	Explanations
Borehole		ID for borehole.
Secup	m	Length along the borehole for the upper limit of the test section (based on corrected length L).
Seclow	m	Length along the borehole for the lower limit of the test section (based on corrected length L).
L	m	Corrected length along borehole based on SKB procedures for length correction.
Length to flow anom.	m	Length along the borehole to inferred flow anomaly during overlapping flow logging.
Test type (1–6)	(–)	1A: Pumping test – wire-line eq., 1B:Pumping test-submersible pump, 1C: Pumping test-airlift pumping, 2: Interference test, 3: Injection test, 4: Slug test, 5A: Difference flow logging – PFL-DIFF-Sequential, 5B: Difference flow logging – PFL-DIFF-Overlapping, 6: Flow logging-Impeller.
Date of test, start	YY-MM-DD	Date for start of pumping.
Time of test, start	hh:mm	Time for start of pumping.
Date of flowl., start .	YY-MM-DD	Date for start of the flow logging.
Time of flowl., start	hh:mm	Time for start of the flow logging.
Date of test, stop	YY-MM-DD	Date for stop of the test.
Time of test, stop	hh:mm	Time for stop of the test.
L_w	m	Section length used in the difference flow logging.
dL	m	Step length (increment) used in the difference flow logging.
Q_{p1}	m^3/s	Flow rate at surface by the end of the first pumping period of the flow logging.
Q_{p2}	m^3/s	Flow rate at surface by the end of the second pumping period of the flow logging.
t_{p1}	s	Duration of the first pumping period.
t_{p2}	s	Duration of the second pumping period.
t_{F1}	s	Duration of the first recovery period.
t_{F2}	s	Duration of the second recovery period.
h_0	m.a.s.l.	Initial hydraulic head before pumping. Elevation of water level in open borehole in the local co-ordinates system with z=0 m.
h_1	m.a.s.l.	Stabilized hydraulic head during the first pumping period. Elevation of water level in open borehole in the local co-ordinates system with z=0 m.
h_2	m.a.s.l.	Stabilized hydraulic head during the second pumping period. Elevation of water level in open borehole in the local co-ordinates system with z=0 m.
s_1	m	Drawdown of the water level in the borehole during first pumping period. Difference between the actual hydraulic head and the initial head (s1= h1−h0).
s_2	m	Drawdown of the water level in the borehole during second pumping period. Difference between the actual hydraulic head and the initial head (s2=h2−h0).
T	m^2/s	Transmissivity of the entire borehole.
Q_0	m^3/s	Measured flow rate through the test section or flow anomaly under natural conditions (no pumping) with h=h0 in the open borehole.
Q_1	m^3/s	Measured flow rate through the test section or flow anomaly during the first pumping period.
Q_2	m^3/s	Measured flow rate through the test section or flow anomaly during the second pumping period.
h_{0FW}	m.a.s.l.	Corrected initial hydraulic head along the hole due to e.g. varying salinity conditions of the borehole fluid before pumping.
h_{1FW}	m.a.s.l.	Corrected hydraulic head along the hole due to e.g. varying salinity conditions of the borehole fluid during the first pumping period.
h_{2FW}	m.a.s.l.	Corrected hydraulic head along the hole due to e.g. varying salinity conditions of the borehole fluid during the second pumping period.
EC_w	S/m	Measured electric conductivity of the borehole fluid in the test section during difference flow logging.
Te_w	°C	Measured borehole fluid temperature in the test section during difference flow logging.
EC_f	S/m	Measured fracture-specific electric conductivity of the fluid in flow anomaly during difference flow logging.
Te_f	°C	Measured fracture-specific fluid temperature in flow anomaly during difference flow logging.
T_D	m^2/s	Transmissivity of section or flow anomaly based on 2D model for evaluation of formation properties of the test section based on PFL-DIFF.
T-$measl_{LT}$	m^2/s	Estimated theoretical lower measurement limit for evaluated TD. If the estimated TD equals TD-measlim, the actual TD is considered to be equal or less than TD-measlim.
T-$measl_{LP}$	m^2/s	Estimated practical lower measurement limit for evaluated TD. If the estimated TD equals TD-measlim, the actual TD is considered to be equal or less than TD-measlim.
T-$meas_{lU}$	m^2/s	Estimated upper measurement limit for evaluated TD. If the estimated TD equals TD-measlim, the actual TD is considered to be equal or less than TD-measlim.
h_i	m.a.s.l.	Calculated relative, natural freshwater head for test section or flow anomaly (undisturbed conditions).

Results of section flows

Borehole ID	Secup L(m)	Seclow L(m)	L_w (m)	Q_0 (m^3/s)	h_{0FW} (m.a.s.l.)	Q_1 (m^3/s)	h_{1FW} (m.a.s.l.)	T_D (m^2/s)	h_i (m.a.s.l.)	Q-lower limit P (mL/h)	T_D-measl$_{LT}$ (m^2/s)	T_D-measl$_{LP}$ (m^2/s)	T_D-measl$_U$ (m^2/s)	Comments
KFM24	29.72	34.72	5	–	−0.41	–	−10.47	–	–	200	8.2E−10	5.5E−09	8.2E−06	
KFM24	34.74	39.74	5	–	−0.37	–	−10.44	–	–	200	8.2E−10	5.5E−09	8.2E−06	
KFM24	39.73	44.73	5	–	−0.36	–	−10.45	–	–	200	8.2E−10	5.4E−09	8.2E−06	
KFM24	44.73	49.73	5	–	−0.35	5.89E−08	−10.40	5.8E−09	–	30	8.2E−10	8.2E−10	8.2E−06	
KFM24	49.73	54.73	5	3.06E−08	−0.32	4.24E−07	−10.39	3.9E−08	0.5	30	8.2E−10	8.2E−10	8.2E−06	
KFM24	54.72	59.72	5	–	−0.26	–	−10.34	–	–	400	8.2E−10	1.1E−08	8.2E−06	
KFM24	59.70	64.70	5	–	−0.24	–	−10.33	–	–	30	8.2E−10	8.2E−10	8.2E−06	
KFM24	64.71	69.71	5	–	−0.24	–	−10.32	–	–	30	8.2E−10	8.2E−10	8.2E−06	
KFM24	69.69	74.69	5	2.58E−09	−0.24	1.67E−07	−10.29	1.6E−08	−0.1	30	8.2E−10	8.2E−10	8.2E−06	*
KFM24	74.70	79.70	5	–	−0.22	–	−10.31	–	–	30	8.2E−10	8.2E−10	8.2E−06	
KFM24	79.70	84.70	5	–	−0.11	–	−10.24	–	–	30	8.1E−10	8.1E−10	8.1E−06	
KFM24	84.71	89.71	5	–	−0.18	–	−10.26	–	–	30	8.2E−10	8.2E−10	8.2E−06	
KFM24	89.72	94.72	5	–	−0.16	–	−10.26	–	–	30	8.2E−10	8.2E−10	8.2E−06	
KFM24	94.72	99.72	5	–	−0.13	3.31E−08	−10.23	3.2E−09	–	30	8.2E−10	8.2E−10	8.2E−06	
KFM24	99.70	104.70	5	–	−0.11	–	−10.20	–	–	30	8.2E−10	8.2E−10	8.2E−06	
KFM24	104.72	109.72	5	–	−0.11	–	−10.19	–	–	30	8.2E−10	8.2E−10	8.2E−06	
KFM24	109.70	114.70	5	–	−0.09	–	−10.19	–	–	30	8.2E−10	8.2E−10	8.2E−06	
KFM24	114.72	119.72	5	–	−0.06	4.44E−08	−10.14	4.4E−09	–	30	8.2E−10	8.2E−10	8.2E−06	
KFM24	119.70	124.70	5	–	−0.03	–	−10.14	–	–	30	8.2E−10	8.2E−10	8.2E−06	
KFM24	124.72	129.72	5	1.03E−08	−0.04	2.78E−07	−10.16	2.6E−08	0.4	30	8.1E−10	8.1E−10	8.1E−06	
KFM24	129.73	134.73	5	–	−0.02	–	−10.08	–	–	30	8.2E−10	8.2E−10	8.2E−06	
KFM24	134.74	139.74	5	–	−0.02	–	−10.11	–	–	30	8.2E−10	8.2E−10	8.2E−06	
KFM24	139.74	144.74	5	–	0.00	–	−10.07	–	–	30	8.2E−10	8.2E−10	8.2E−06	
KFM24	144.76	149.76	5	–	0.02	–	−10.05	–	–	30	8.2E−10	8.2E−10	8.2E−06	
KFM24	149.76	154.76	5	–	0.04	–	−10.05	–	–	30	8.2E−10	8.2E−10	8.2E−06	
KFM24	154.77	159.77	5	−5.28E−09	0.06	5.63E−07	−10.05	5.6E−08	0.0	30	8.2E−10	8.2E−10	8.2E−06	*
KFM24	159.77	164.77	5	–	0.08	–	−9.95	–	–	30	8.2E−10	8.2E−10	8.2E−06	
KFM24	164.78	169.78	5	–	0.10	8.17E−08	−9.96	8.0E−09	–	30	8.2E−10	8.2E−10	8.2E−06	
KFM24	169.75	174.75	5	–	0.11	–	−9.95	–	–	30	8.2E−10	8.2E−10	8.2E−06	
KFM24	174.76	179.76	5	–	0.13	1.01E−07	−9.97	9.9E−09	–	30	8.2E−10	8.2E−10	8.2E−06	
KFM24	179.76	184.76	5	–	0.16	5.33E−07	−9.96	5.2E−08	–	30	8.1E−10	8.1E−10	8.1E−06	
KFM24	184.77	189.77	5	−1.31E−08	0.19	3.55E−06	−9.89	3.5E−07	0.2	30	8.2E−10	8.2E−10	8.2E−06	
KFM24	189.76	194.76	5	–	0.22	6.89E−08	−9.86	6.8E−09	–	30	8.2E−10	8.2E−10	8.2E−06	
KFM24	194.77	199.77	5	−4.19E−08	0.27	1.87E−06	−9.80	1.9E−07	0.1	30	8.2E−10	8.2E−10	8.2E−06	

Borehole ID	Secup L(m)	Seclow L(m)	L_w (m)	Q_0 (m^3/s)	h_{0FW} (m.a.s.l.)	Q_1 (m^3/s)	h_{1FW} (m.a.s.l.)	T_D (m^2/s)	h_i (m.a.s.l.)	Q-lower limit P (mL/h)	T_D-measl$_{LT}$ (m^2/s)	T_D-measl$_{LP}$ (m^2/s)	T_D-measl$_U$ (m^2/s)	Comments
KFM24	199.76	204.76	5	–	0.33	–	−9.78	–	–	30	8.2E−10	8.2E−10	8.2E−06	
KFM24	204.78	209.78	5	–	0.35	–	−9.75	–	–	30	8.2E−10	8.2E−10	8.2E−06	
KFM24	209.78	214.78	5	−7.22E−09	0.34	6.67E−08	−9.74	7.3E−09	−0.7	30	8.2E−10	8.2E−10	8.2E−06	*
KFM24	214.79	219.79	5	–	0.34	–	−9.74	–	–	30	8.2E−10	8.2E−10	8.2E−06	
KFM24	219.75	224.75	5	–	0.34	–	−9.68	–	–	30	8.2E−10	8.2E−10	8.2E−06	
KFM24	224.76	229.76	5	–	0.38	–	−9.66	–	–	30	8.2E−10	8.2E−10	8.2E−06	
KFM24	229.78	234.78	5	−1.11E−08	0.44	6.94E−08	−9.59	7.9E−09	−0.9	30	8.2E−10	8.2E−10	8.2E−06	
KFM24	234.79	239.79	5	–	0.47	–	−9.57	–	–	30	8.2E−10	8.2E−10	8.2E−06	
KFM24	239.80	244.80	5	–	0.44	–	−9.64	–	–	30	8.2E−10	8.2E−10	8.2E−06	
KFM24	244.81	249.81	5	−6.67E−09	0.46	1.49E−07	−9.58	1.5E−08	0.0	30	8.2E−10	8.2E−10	8.2E−06	*
KFM24	249.81	254.81	5	–	0.52	3.53E−08	−9.55	3.5E−09	–	30	8.2E−10	8.2E−10	8.2E−06	
KFM24	254.82	259.82	5	–	0.54	–	−9.53	–	–	30	8.2E−10	8.2E−10	8.2E−06	
KFM24	259.79	264.79	5	–	0.52	9.36E−08	−9.52	9.2E−09	–	30	8.2E−10	8.2E−10	8.2E−06	
KFM24	264.81	269.81	5	–	0.59	–	−9.48	–	–	30	8.2E−10	8.2E−10	8.2E−06	
KFM24	269.81	274.81	5	–	0.63	–	−9.52	–	–	30	8.1E−10	8.1E−10	8.1E−06	
KFM24	274.82	279.82	5	–	0.62	–	−9.44	–	–	30	8.2E−10	8.2E−10	8.2E−06	
KFM24	279.81	284.81	5	–	0.71	6.94E−09	−9.39	6.8E−10	–	30	8.2E−10	8.2E−10	8.2E−06	*
KFM24	284.82	289.82	5	–	0.71	–	−9.31	–	–	30	8.2E−10	8.2E−10	8.2E−06	
KFM24	289.78	294.78	5	–	0.74	–	−9.32	–	–	30	8.2E−10	8.2E−10	8.2E−06	
KFM24	294.79	299.79	5	–	0.77	6.11E−09	−9.30	6.0E−10	–	30	8.2E−10	8.2E−10	8.2E−06	*
KFM24	299.81	304.81	5	–	0.81	6.11E−09	−9.23	6.0E−10	–	30	8.2E−10	8.2E−10	8.2E−06	*
KFM24	304.82	309.82	5	–	0.85	1.28E−08	−9.20	1.3E−09	–	30	8.2E−10	8.2E−10	8.2E−06	
KFM24	309.82	314.82	5	–	0.94	–	−9.14	–	–	30	8.2E−10	8.2E−10	8.2E−06	
KFM24	314.82	319.82	5	–	0.93	–	−9.08	–	–	30	8.2E−10	8.2E−10	8.2E−06	
KFM24	319.82	324.82	5	–	1.04	–	−9.10	–	–	30	8.1E−10	8.1E−10	8.1E−06	
KFM24	324.82	329.82	5	–	1.04	–	−9.00	–	–	30	8.2E−10	8.2E−10	8.2E−06	
KFM24	329.80	334.80	5	–	1.11	–	−9.02	–	–	30	8.1E−10	8.1E−10	8.1E−06	
KFM24	334.79	339.79	5	–	1.16	–	−8.89	–	–	30	8.2E−10	8.2E−10	8.2E−06	
KFM24	339.79	344.79	5	–	1.17	–	−8.91	–	–	30	8.2E−10	8.2E−10	8.2E−06	
KFM24	344.79	349.79	5	–	1.27	–	−8.79	–	–	30	8.2E−10	8.2E−10	8.2E−06	
KFM24	349.76	354.76	5	–	1.30	–	−8.79	–	–	30	8.2E−10	8.2E−10	8.2E−06	
KFM24	354.77	359.77	5	–	1.30	–	−8.79	–	–	30	8.2E−10	8.2E−10	8.2E−06	
KFM24	359.78	364.78	5	–	1.38	–	−8.68	–	–	30	8.2E−10	8.2E−10	8.2E−06	
KFM24	364.79	369.79	5	–	1.45	–	−8.63	–	–	30	8.2E−10	8.2E−10	8.2E−06	
KFM24	369.78	374.78	5	–	1.45	1.50E−08	−8.63	1.5E−09	–	30	8.2E−10	8.2E−10	8.2E−06	

Borehole ID	Secup L(m)	Seclow L(m)	L_w (m)	Q_0 (m^3/s)	h_{0FW} (m.a.s.l.)	Q_1 (m^3/s)	h_{1FW} (m.a.s.l.)	T_D (m^2/s)	h_i (m.a.s.l.)	Q-lower limit P (mL/h)	T_D-measl$_{LT}$ (m^2/s)	T_D-measl$_{LP}$ (m^2/s)	T_D-measl$_U$ (m^2/s)	Comments
KFM24	374.79	379.79	5	–	1.48	–	−8.60	–	–	30	8.2E−10	8.2E−10	8.2E−06	
KFM24	379.79	384.79	5	–	1.52	–	−8.54	–	–	30	8.2E−10	8.2E−10	8.2E−06	
KFM24	384.79	389.79	5	–	1.59	3.89E−09	−8.47	3.8E−10	–	30	8.2E−10	8.2E−10	8.2E−06	*
KFM24	389.80	394.80	5	–	1.67	3.00E−08	−8.43	2.9E−09	–	30	8.2E−10	8.2E−10	8.2E−06	
KFM24	394.81	399.81	5	4.42E−08	1.70	6.46E−07	−8.38	5.9E−08	2.4	30	8.2E−10	8.2E−10	8.2E−06	
KFM24	399.81	404.81	5	–	1.72	–	−8.31	–	–	30	8.2E−10	8.2E−10	8.2E−06	
KFM24	404.83	409.83	5	–	1.75	–	−8.32	–	–	30	8.2E−10	8.2E−10	8.2E−06	
KFM24	409.82	414.82	5	1.72E−08	1.77	1.55E−07	−8.30	1.4E−08	3.0	30	8.2E−10	8.2E−10	8.2E−06	
KFM24	414.85	419.85	5	–	1.79	–	−8.27	–	–	30	8.2E−10	8.2E−10	8.2E−06	
KFM24	419.85	424.85	5	–	1.81	–	−8.28	–	–	30	8.2E−10	8.2E−10	8.2E−06	
KFM24	424.88	429.88	5	–	1.82	–	−8.25	–	–	30	8.2E−10	8.2E−10	8.2E−06	
KFM24	429.90	434.90	5	–	1.85	–	−8.21	–	–	30	8.2E−10	8.2E−10	8.2E−06	
KFM24	434.92	439.92	5	–	1.89	–	−8.19	–	–	30	8.2E−10	8.2E−10	8.2E−06	
KFM24	439.94	444.94	5	–	1.93	–	−8.12	–	–	30	8.2E−10	8.2E−10	8.2E−06	
KFM24	444.95	449.95	5	–	2.00	–	−8.06	–	–	30	8.2E−10	8.2E−10	8.2E−06	
KFM24	449.91	454.91	5	–	2.03	–	−8.00	–	–	30	8.2E−10	8.2E−10	8.2E−06	
KFM24	454.94	459.94	5	–	2.04	–	−8.05	–	–	30	8.2E−10	8.2E−10	8.2E−06	
KFM24	459.94	464.94	5	–	2.07	–	−8.02	–	–	30	8.2E−10	8.2E−10	8.2E−06	
KFM24	464.96	469.96	5	–	2.13	–	−7.96	–	–	30	8.2E−10	8.2E−10	8.2E−06	
KFM24	469.95	474.95	5	–	2.15	–	−7.93	–	–	30	8.2E−10	8.2E−10	8.2E−06	
KFM24	474.97	479.97	5	–	2.19	–	−7.88	–	–	30	8.2E−10	8.2E−10	8.2E−06	
KFM24	479.98	484.98	5	–	2.21	–	−7.88	–	–	30	8.2E−10	8.2E−10	8.2E−06	
KFM24	485.00	490.00	5	–	2.22	–	−7.83	–	–	30	8.2E−10	8.2E−10	8.2E−06	
KFM24	490.02	495.02	5	–	2.25	–	−7.79	–	–	30	8.2E−10	8.2E−10	8.2E−06	
KFM24	495.03	500.03	5	–	2.30	–	−7.80	–	–	30	8.2E−10	8.2E−10	8.2E−06	
KFM24	500.04	505.04	5	–	2.34	–	−7.79	–	–	30	8.1E−10	8.1E−10	8.1E−06	
KFM24	505.06	510.06	5	–	2.41	–	−7.73	–	–	30	8.1E−10	8.1E−10	8.1E−06	
KFM24	510.04	515.04	5	–	2.43	–	−7.66	–	–	30	8.2E−10	8.2E−10	8.2E−06	
KFM24	515.06	520.06	5	–	2.47	–	−7.68	–	–	30	8.1E−10	8.1E−10	8.1E−06	
KFM24	520.05	525.05	5	–	2.45	–	−7.60	–	–	30	8.2E−10	8.2E−10	8.2E−06	
KFM24	525.07	530.07	5	–	2.47	–	−7.65	–	–	30	8.1E−10	8.1E−10	8.1E−06	
KFM24	530.07	535.07	5	–	2.53	–	−7.56	–	–	30	8.2E−10	8.2E−10	8.2E−06	
KFM24	535.09	540.09	5	–	2.60	–	−7.58	–	–	30	8.1E−10	8.1E−10	8.1E−06	
KFM24	540.11	545.11	5	–	2.63	–	−7.52	–	–	30	8.1E−10	8.1E−10	8.1E−06	

* Flow rate Flow 1 (Q_0) and/or Flow 2 (Q_1) below 30 mL/h or the flow anomalies are overlapping or they are unclear because of noise.

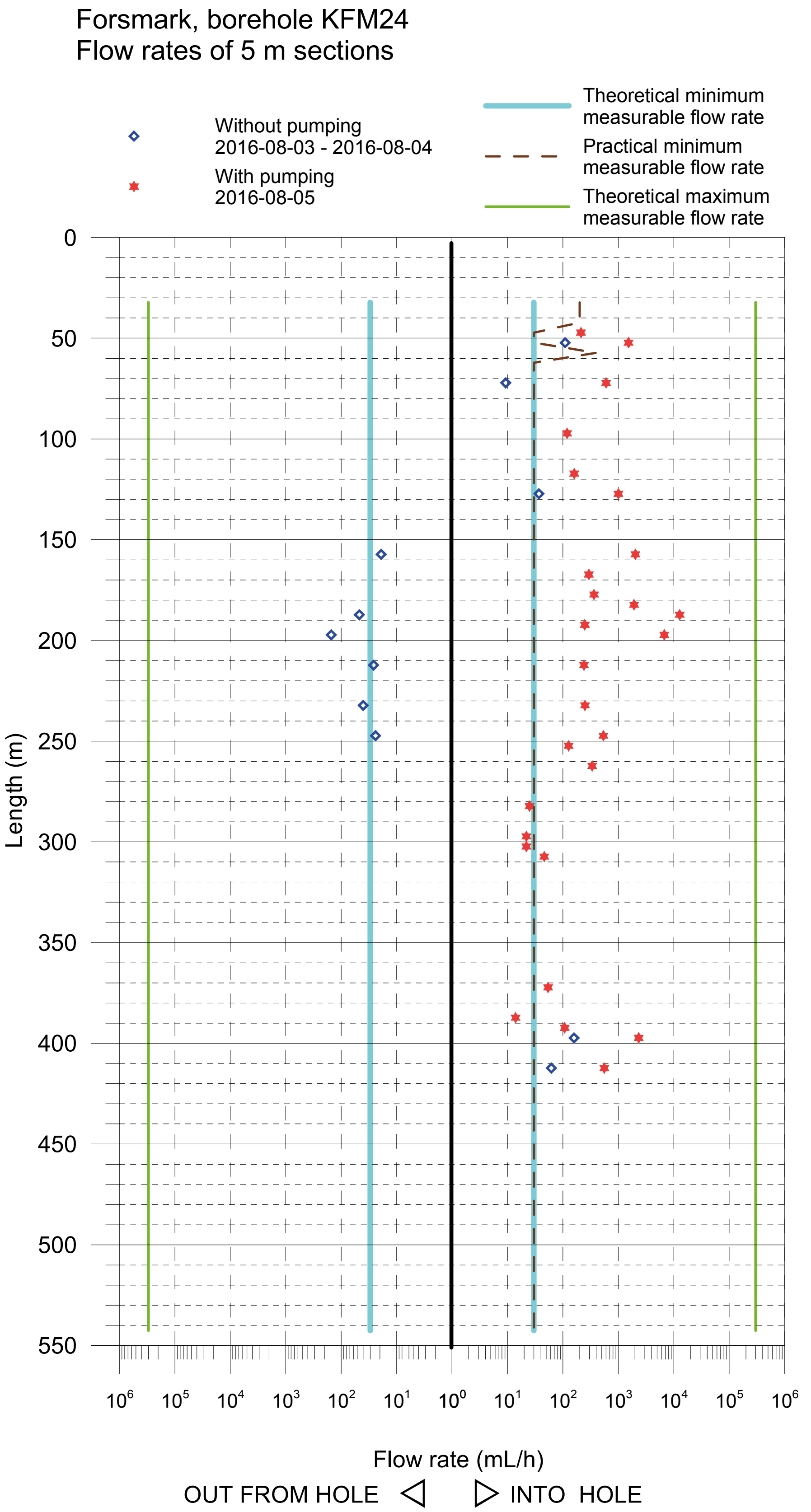
Forsmark, borehole KFM24
Flow rates of 5 m sections
Without pumping
2016-08-03 - 2016-08-04
With pumping
2016-08-05
Theoretical minimum measurable flow rate
Practical minimum measurable flow rate
Theoretical maximum measurable flow rate
Length (m)
0
50
100
150
200
250
300
350
400
450
500
550
10^6 10^5 10^4 10^3 10^2 10^1 10^0 10^1 10^2 10^3 10^4 10^5 10^6
Flow rate (mL/h)
OUT FROM HOLE
INTO HOLE

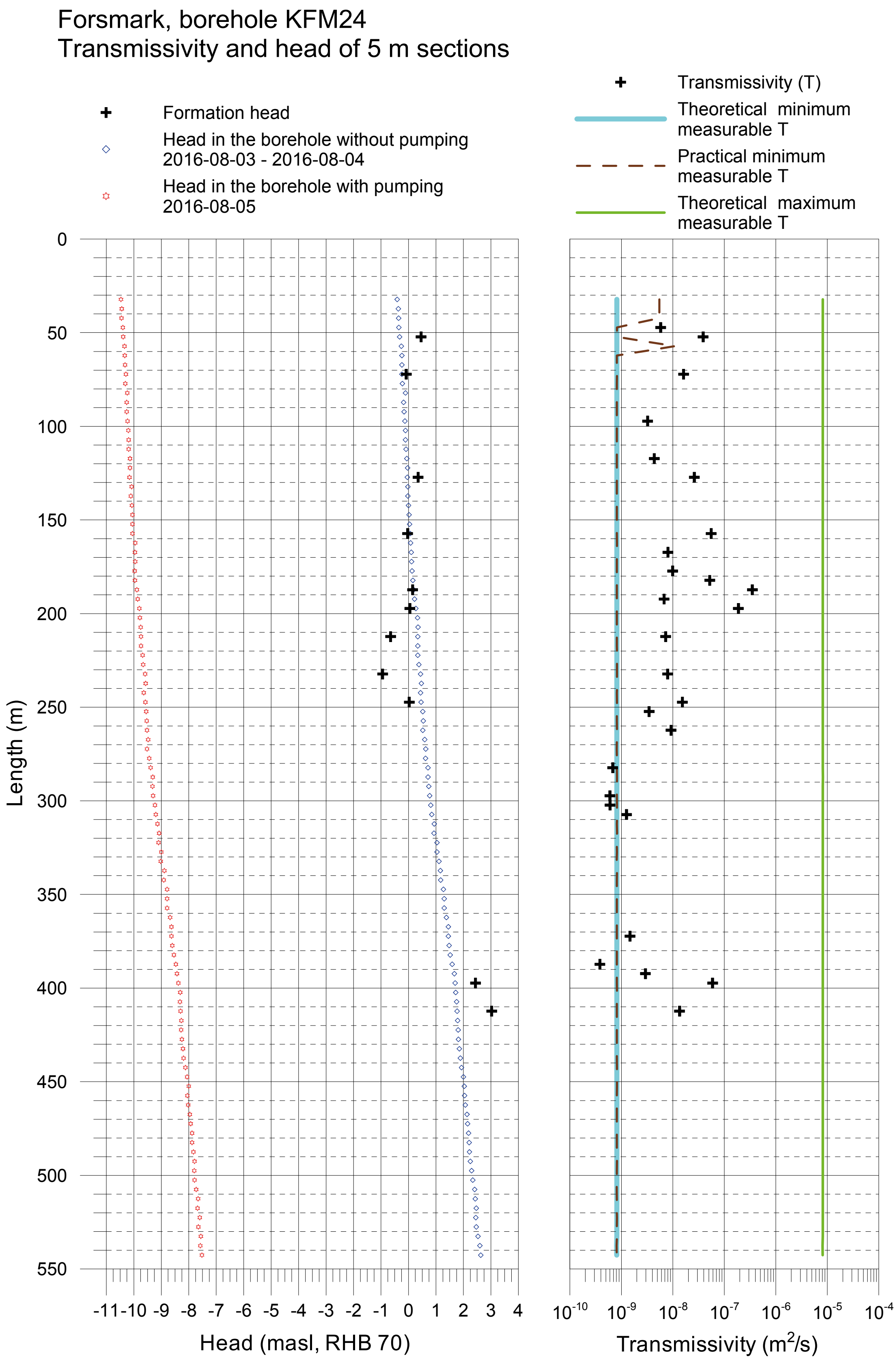

Forsmark, borehole KFM24
Transmissivity and head of 5 m sections
Formation head
Head in the borehole without pumping
2016-08-03 - 2016-08-04
Head in the borehole with pumping
2016-08-05
Transmissivity (T)
Theoretical minimum measurable T
Practical minimum measurable T
Theoretical maximum measurable T
Length (m)
Head (masl, RHB 70)
Transmissivity (m²/s)

Forsmark, borehole KFM24
Calculation of conductive fracture frequency

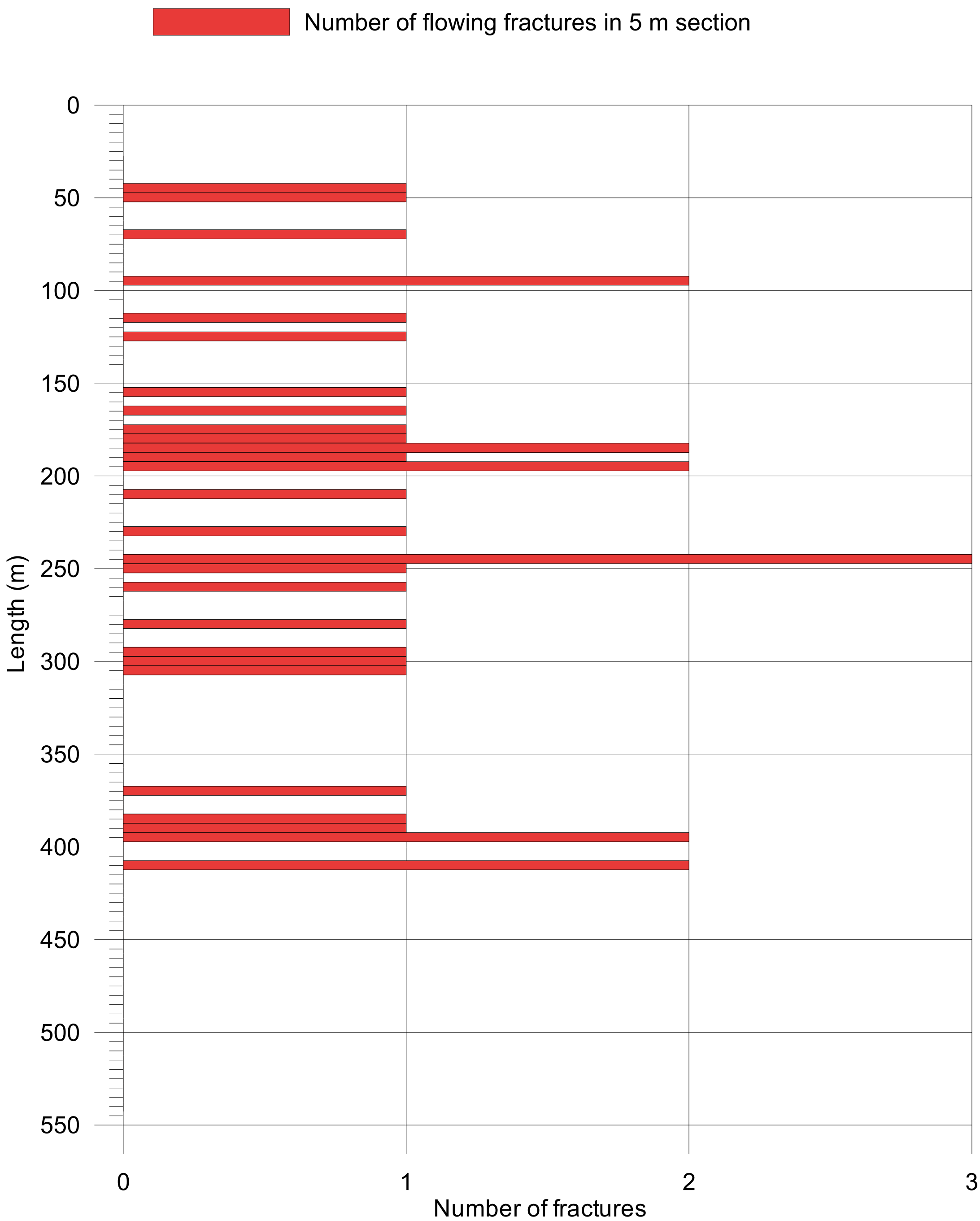

Inferred fracture flow anomalies from flow logging

Borehole ID	Length to flow anom. L (m)	L_w (m)	dL (m)	Q_0 (m^3/s)	h_{0FW} (m.a.s.l.)	Q_1 (m^3/s)	h_{1FW} (m.a.s.l.)	T_D (m^2/s)	h_i (m.a.s.l.)	Comments
KFM24	48.8	1	0.1	–	−0.31	5.89E−08	−10.38	5.8E−09	–	*,**
KFM24	52.0	1	0.1	3.06E−08	−0.32	4.72E−07	−10.43	4.3E−08	0.4	
KFM24	72.1	1	0.1	2.58E−09	−0.24	1.22E−07	−10.42	1.2E−08	0.0	
KFM24	95.3	1	0.1	–	−0.17	6.67E−09	−10.32	6.5E−10	–	*
KFM24	95.9	1	0.1	–	−0.18	1.33E−08	−10.31	1.3E−09	–	
KFM24	119.7	1	0.1	–	−0.01	5.92E−08	−10.26	5.7E−09	–	
KFM24	126.7	1	0.1	1.03E−08	−0.04	3.08E−07	−10.22	2.9E−08	0.3	
KFM24	158.1	1	0.1	−5.28E−09	0.09	4.92E−07	−10.05	4.9E−08	0.0	
KFM24	169.5	1	0.1	–	0.15	5.11E−08	−10.03	5.0E−09	–	
KFM24	175.3	1	0.1	–	0.17	1.01E−07	−9.90	9.9E−09	–	*,**
KFM24	180.8	1	0.1	–	0.18	5.31E−07	−9.97	5.2E−08	–	
KFM24	185.0	1	0.1	−1.31E−08	0.23	3.19E−06	−9.95	3.1E−07	0.2	
KFM24	187.9	1	0.1	–	0.19	4.56E−08	−9.94	4.5E−09	–	*
KFM24	190.3	1	0.1	–	0.25	7.78E−09	−9.92	7.6E−10	–	*
KFM24	195.1	1	0.1	−4.19E−08	0.27	1.59E−06	−9.86	1.6E−07	0.0	
KFM24	195.6	1	0.1	–	0.28	2.78E−08	−9.86	2.7E−09	–	
KFM24	214.4	1	0.1	−7.22E−09	0.35	1.03E−07	−9.77	1.1E−08	−0.3	*
KFM24	232.4	1	0.1	−1.11E−08	0.44	9.33E−08	−9.68	1.0E−08	−0.6	*
KFM24	248.6	1	0.1	−5.00E−09	0.46	6.39E−08	−9.63	6.8E−09	−0.3	
KFM24	249.4	1	0.1	–	0.48	1.89E−08	−9.61	1.9E−09	–	
KFM24	249.7	1	0.1	–	0.48	1.14E−08	−9.62	1.1E−09	–	*
KFM24	251.0	1	0.1	–	0.53	3.61E−09	−9.60	3.5E−10	–	*
KFM24	261.1	1	0.1	–	0.52	9.36E−08	−9.52	9.2E−09	–	*,**
KFM24	284.4	1	0.1	–	0.69	6.94E−09	−9.39	6.8E−10	–	*,**
KFM24	297.4	1	0.1	–	0.77	6.11E−09	−9.31	6.0E−10	–	*,**
KFM24	304.8	1	0.1	–	0.81	6.11E−09	−9.27	6.0E−10	–	*,**
KFM24	306.5	1	0.1	–	0.83	7.78E−09	−9.18	7.7E−10	–	*
KFM24	370.3	1	0.1	–	1.45	1.50E−08	−8.66	1.5E−09	–	*,**
KFM24	387.8	1	0.1	–	1.60	3.89E−09	−8.46	3.8E−10	–	*,**
KFM24	389.8	1	0.1	–	1.62	1.33E−08	−8.30	1.3E−09	–	
KFM24	396.8	1	0.1	–	1.70	4.03E−08	−8.24	4.0E−09	–	
KFM24	398.9	1	0.1	4.42E−08	1.70	5.47E−07	−8.22	5.0E−08	2.6	
KFM24	412.7	1	0.1	1.72E−08	1.77	1.60E−07	−8.19	1.4E−08	3.0	
KFM24	414.5	1	0.1	–	1.76	1.42E−08	−8.16	1.4E−09	–	*

* Uncertain = The flow rate is less than 30 mL/h or the flow anomalies are overlapping or they are unclear because of noise.
** Flow 3 (Q_1) and Head 3 (h_{1FW}) is interpreted using the measurement of Flow 2 with pumping (L=5 m, dL=0.5 m).

Forsmark, borehole KFM24
Transmissivity and head of detected fractures

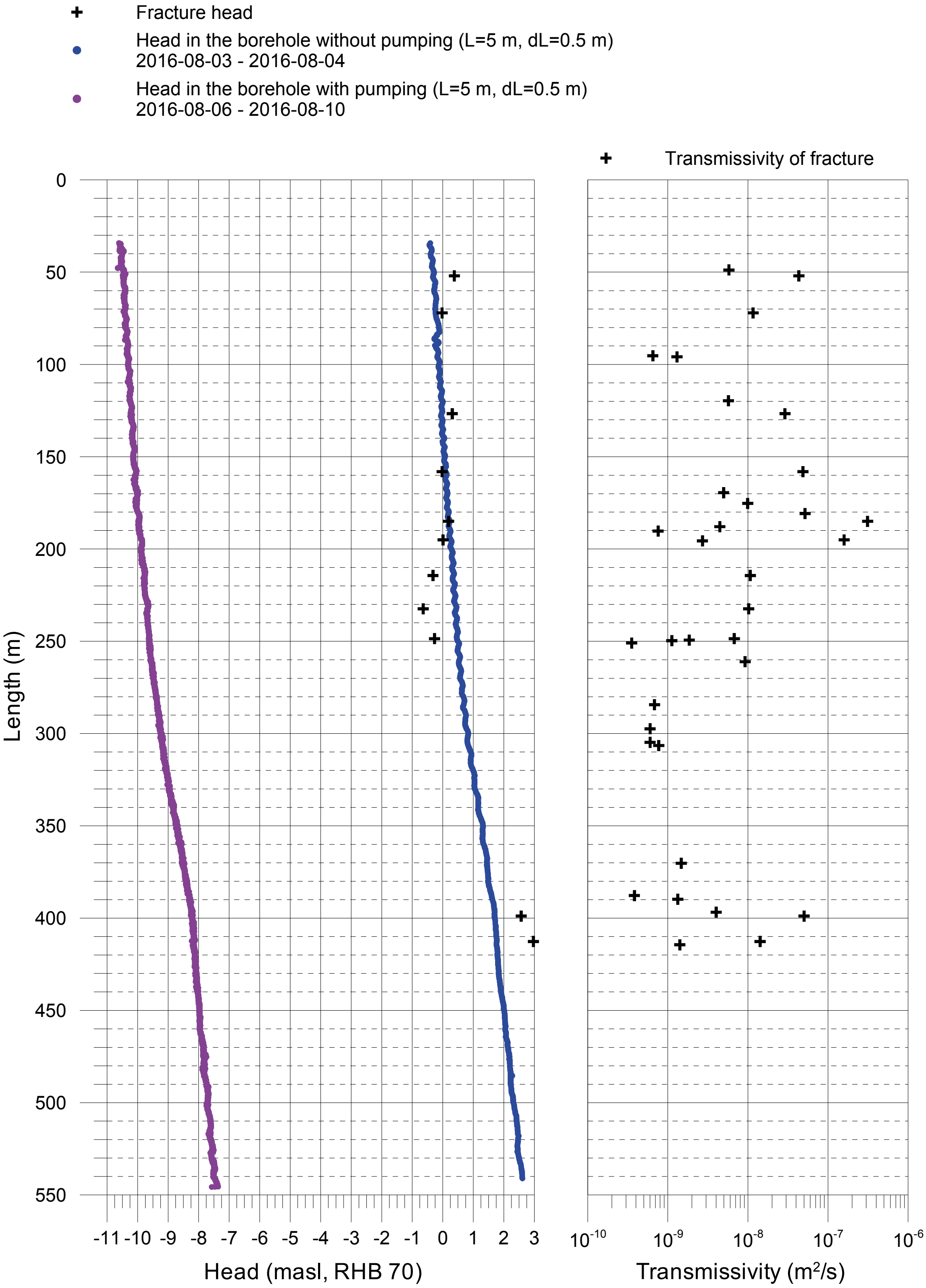

Forsmark, borehole KFM24
Comparison between section transmissivity and fracture transmissivity

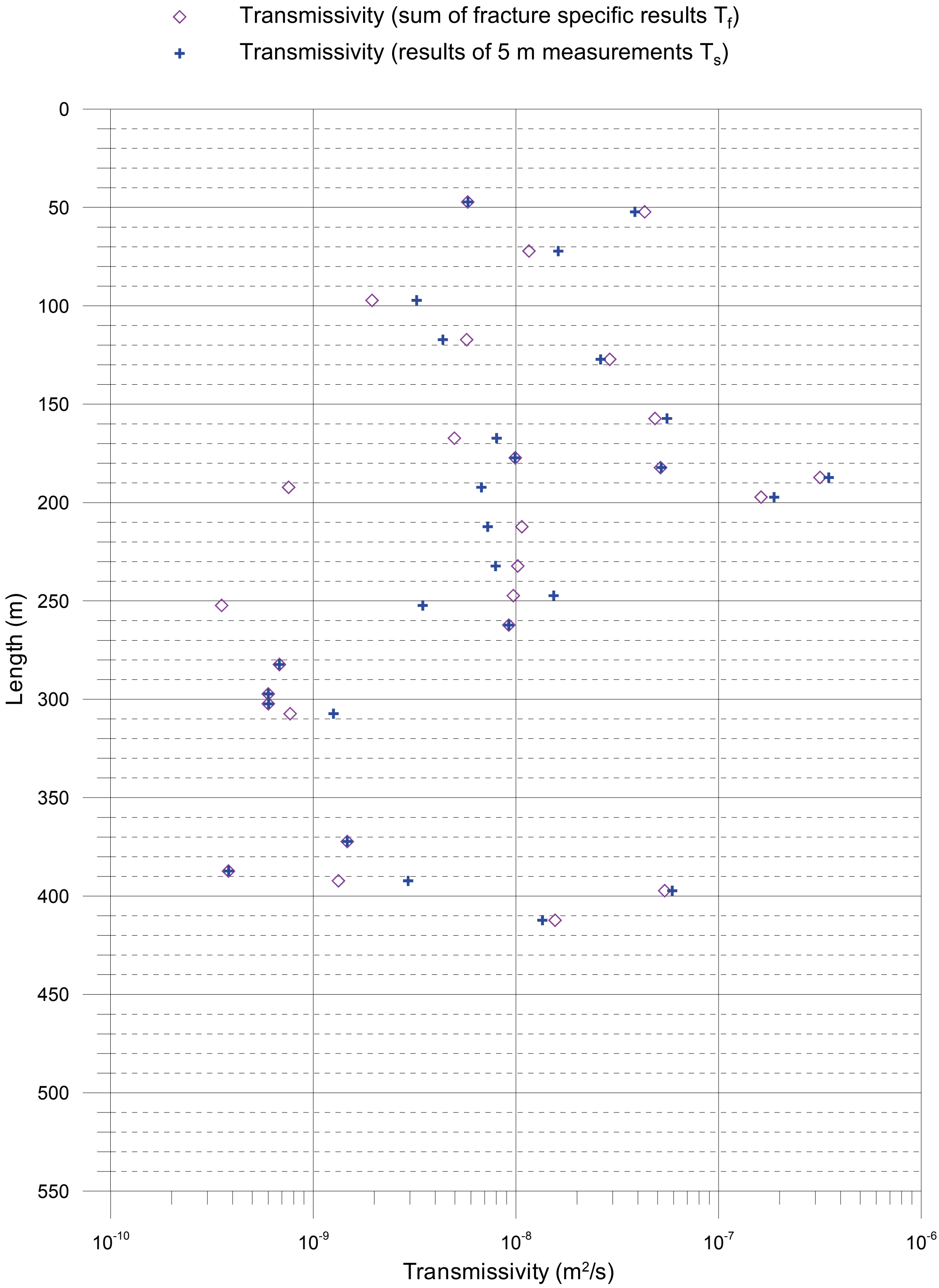

Forsmark, borehole KFM24
Head in the borehole during flow logging

Head(masl)= (Absolute pressure (Pa) - Airpressure (Pa) + Offset) /(1000 kg/m^3 * 9.80665 m/s^2) + Elevation (m)
Offset = Correction for absolute pressure sensor

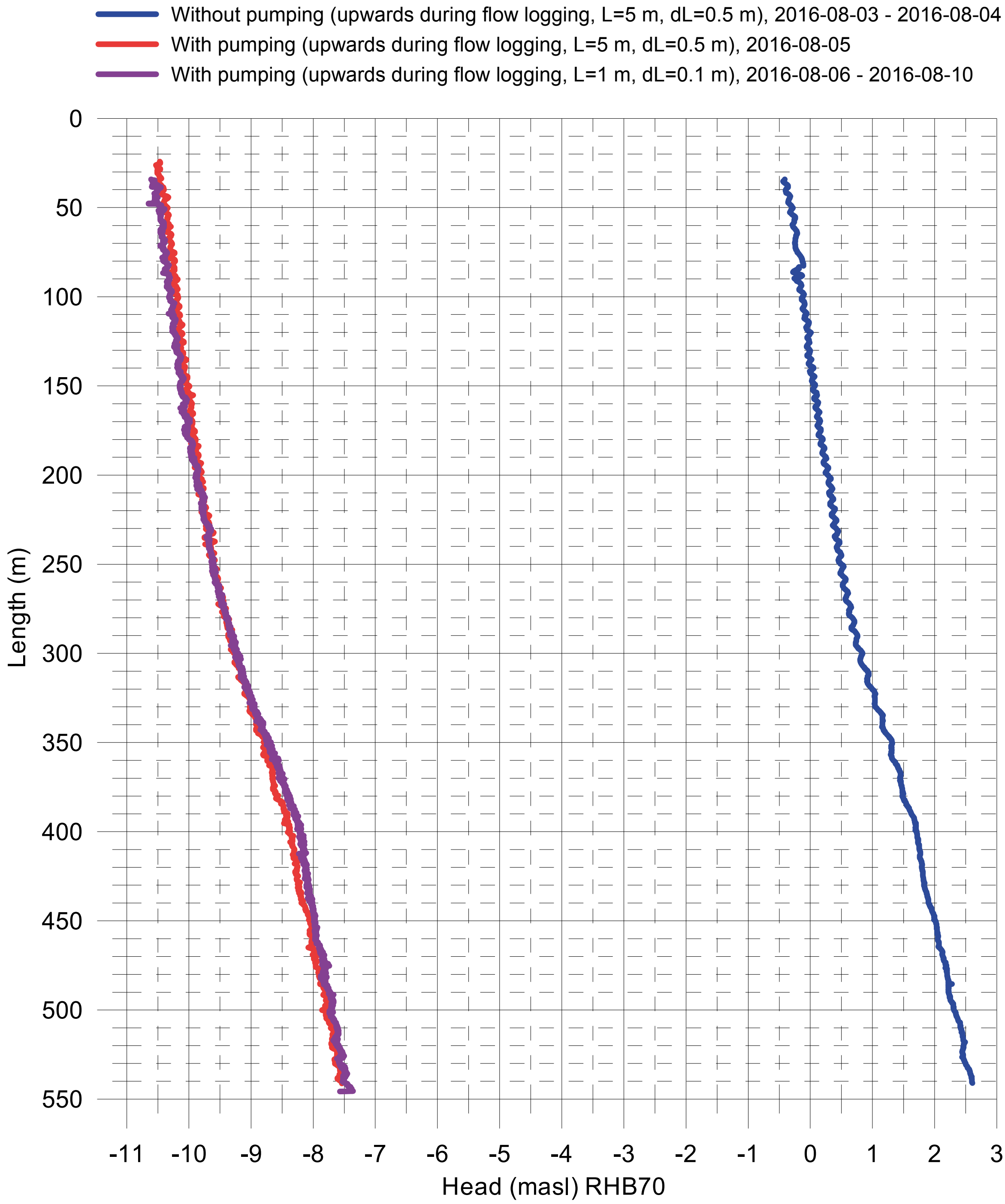

Forsmark, borehole KFM24
Air pressure, water level in the borehole and pumping rate during flow logging

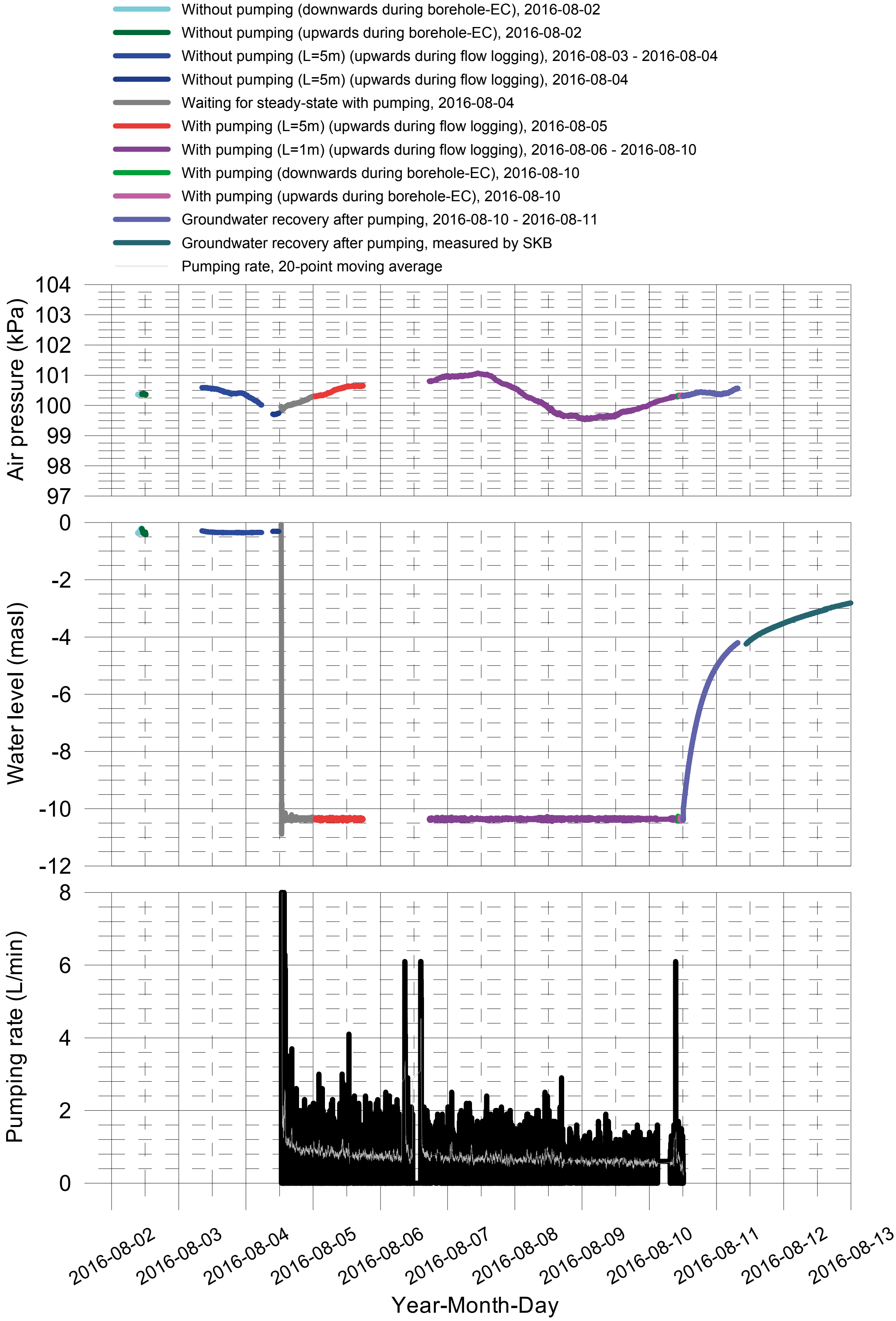

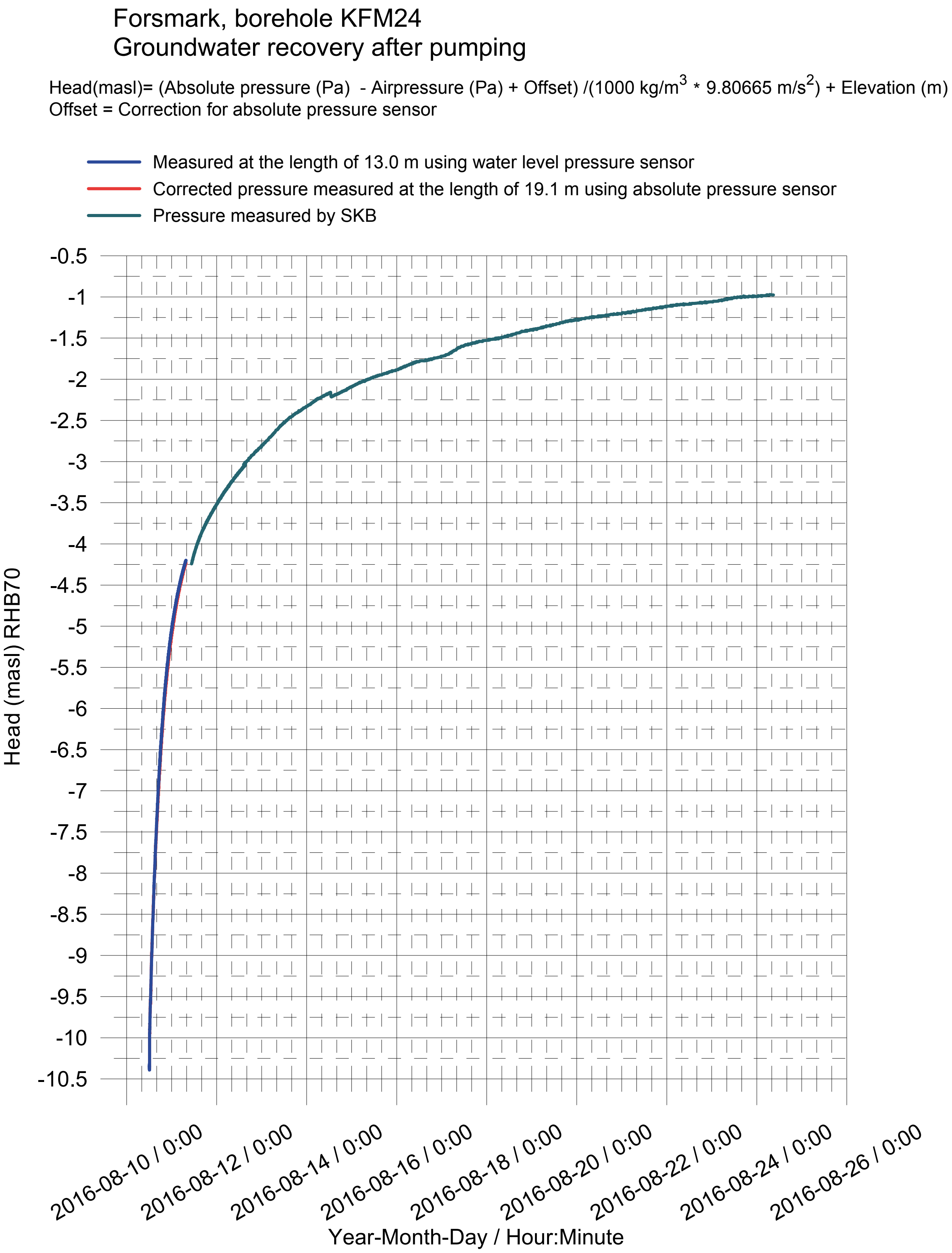

Forsmark, borehole KFM24
Groundwater recovery after pumping
Head(masl)= (Absolute pressure (Pa) - Airpressure (Pa) + Offset) /(1000 kg/m3 * 9.80665 m/s2) + Elevation (m)
Offset = Correction for absolute pressure sensor
Measured at the length of 13.0 m using water level pressure sensor
Corrected pressure measured at the length of 19.1 m using absolute pressure sensor
Pressure measured by SKB
Head (masl) RHB70
-0.5
-1
-1.5
-2
-2.5
-3
-3.5
-4
-4.5
-5
-5.5
-6
-6.5
-7
-7.5
-8
-8.5
-9
-9.5
-10
-10.5
2016-08-10 / 0:00
2016-08-12 / 0:00
2016-08-14 / 0:00
2016-08-16 / 0:00
2016-08-18 / 0:00
2016-08-20 / 0:00
2016-08-22 / 0:00
2016-08-24 / 0:00
2016-08-26 / 0:00
Year-Month-Day / Hour:Minute

Forsmark, borehole KFM24
Fracture-specific Flow, EC and Temperature results by date
Water level and Air pressure results by date

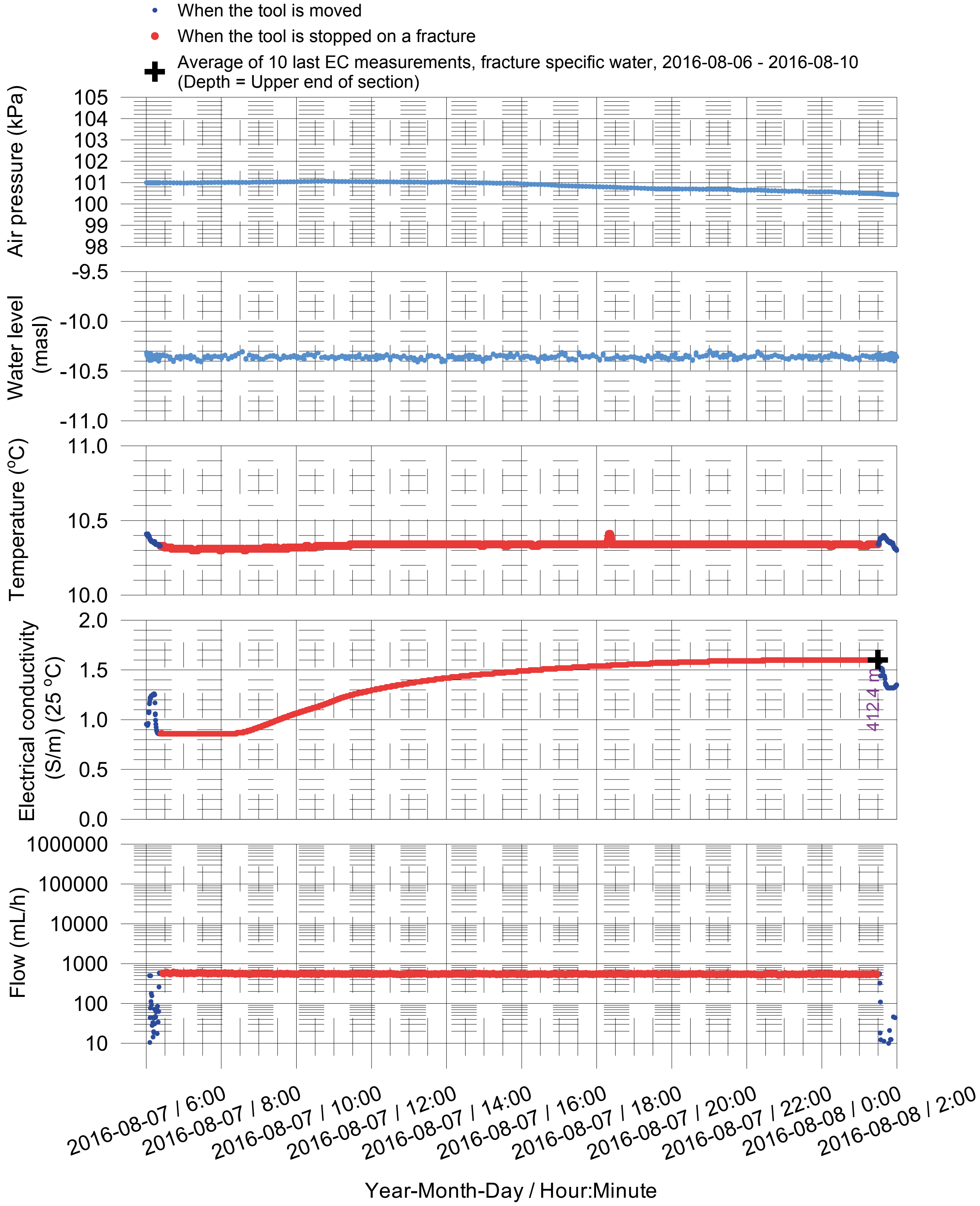

Forsmark, borehole KFM24
Fracture-specific Flow, EC and Temperature results by date
Water level and Air pressure results by date

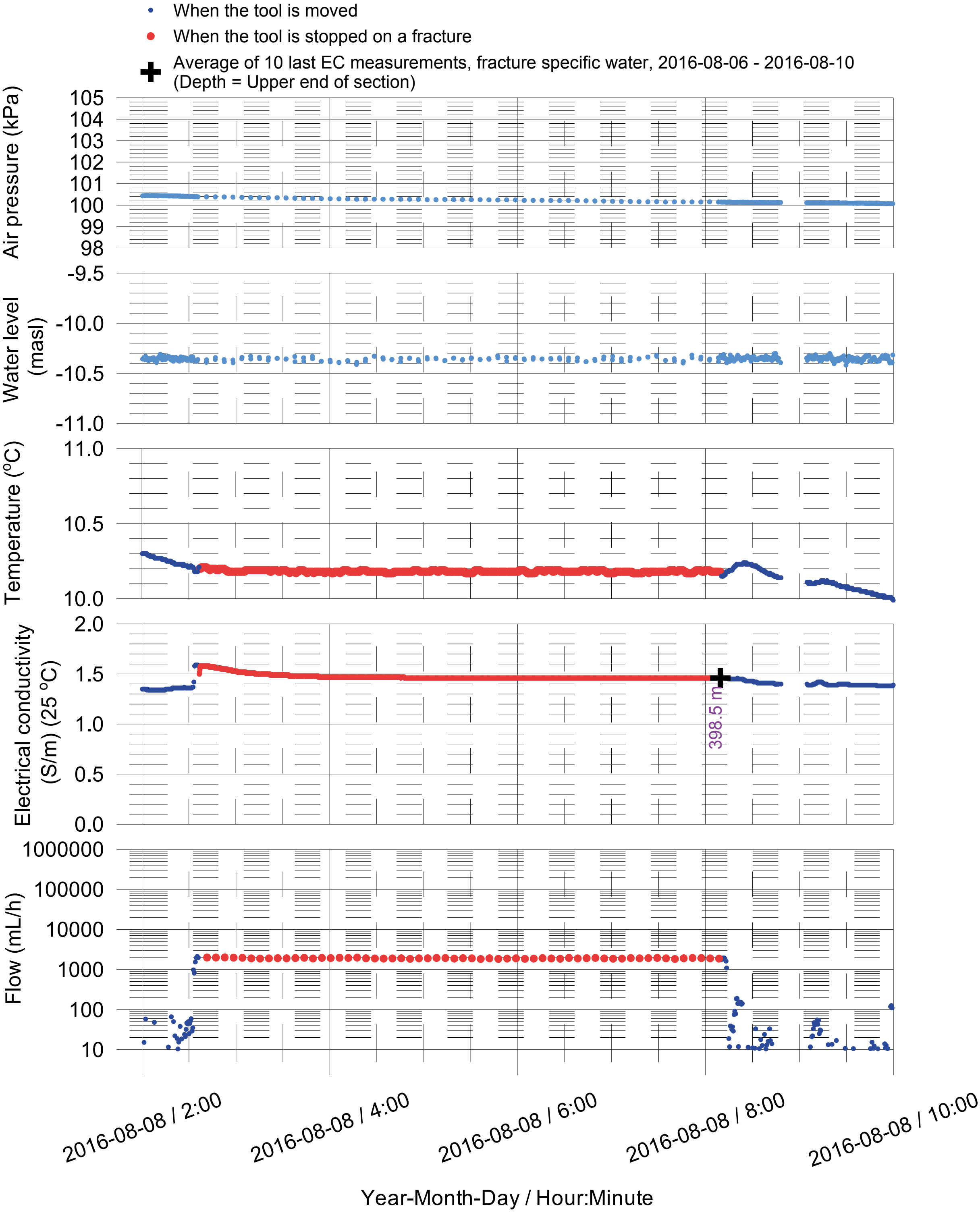

Forsmark, borehole KFM24
Fracture-specific Flow, EC and Temperature results by date
Water level and Air pressure results by date

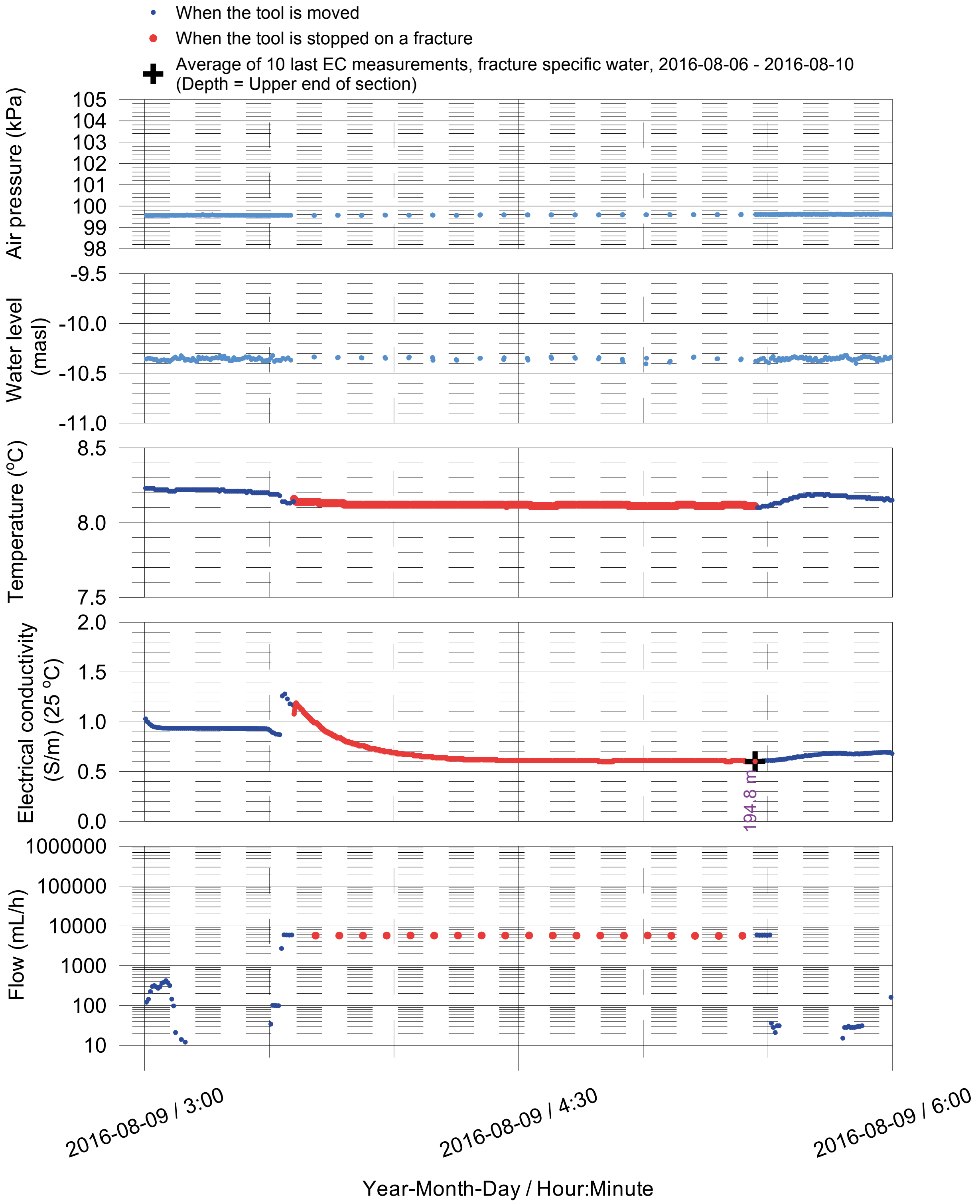

Forsmark, borehole KFM24
Fracture-specific Flow, EC and Temperature results by date
Water level and Air pressure results by date

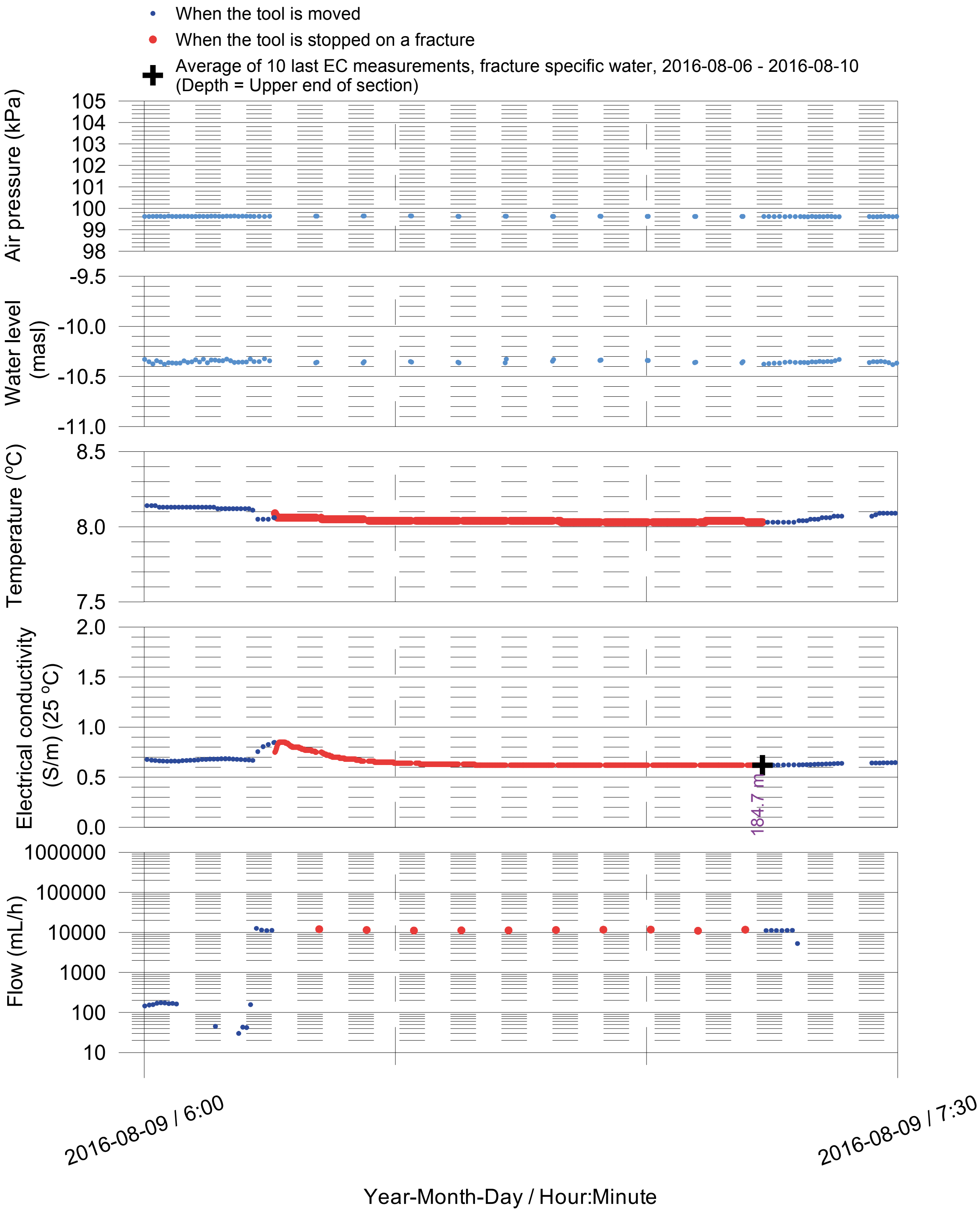

Forsmark, borehole KFM24
Fracture-specific Flow, EC and Temperature results by date
Water level and Air pressure results by date

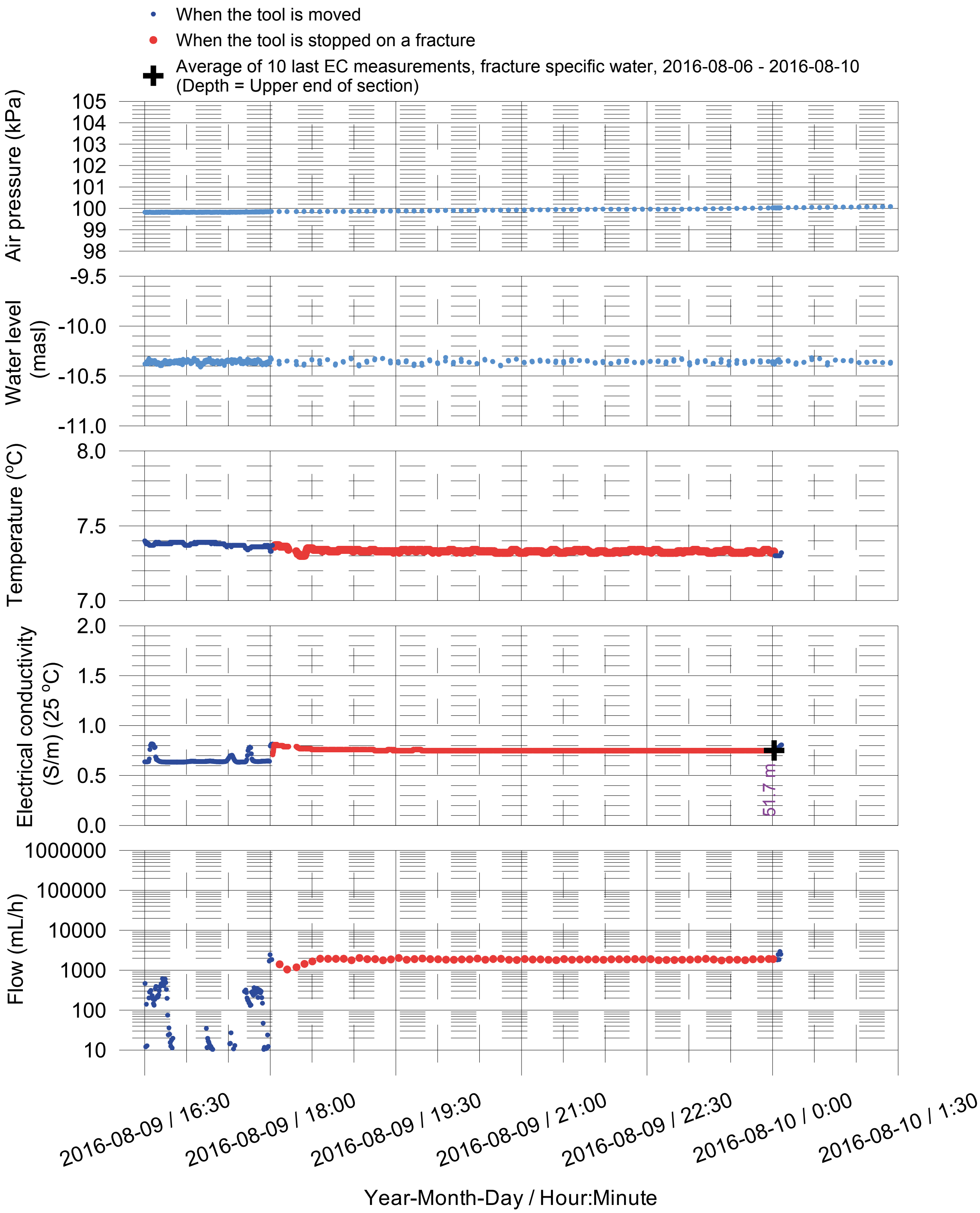

Arkitektkopia AB, Bromma, 2017

SKB is responsible for managing spent nuclear fuel and radioactive waste produced by the Swedish nuclear power plants such that man and the environment are protected in the near and distant future.

skb.se